MODIFICATION AND CHARACTERIZATION OF TECHNICAL BAMBOO FIBERS AND THEIR POLYPROPYLENE BASED COMPOSITES

A dissertation submitted for the degree of DOCTOR OF PHILOSOPHY

at

BANGLADESH UNIVERSITY OF ENGINEERING AND TECHNOLOGY

April 2014

by

Shamsun Nahar

Student No. 1009114003P

DEPARTMENT OF MATERIALS AND METALLURGICAL ENGINEERING

BANGLADESH UNIVERSITY OF ENGINEERING AND TECHNOLOGY

DHAKA, BANGLADESH

The thesis titled "**Modification and Characterization of Technical Bamboo Fibers and Their Polypropylene Based Composites**" submitted by Shamsun Nahar, Roll no:1009114003P, Session: October 2009, has been completed as satisfactory in partial fulfilment of the requirements for the degree of Doctor of Philosophy in Materials and Metallurgical Engineering on 29 April, 2014.

BOARD OF EXAMINERS

1._____ Dr. Mahbub Hasan Assistant Professor Department of MME, BUET, Dhaka	Chairman
2._____ Head Department of MME, BUET, Dhaka.	Member (Ex-officio)
3._____ Dr. Ahmed Sharif Associate Professor Department of MME, BUET, Dhaka.	Member
4._____ Dr. Kazi Md. Shorowordi Assistant Professor Department of MME, BUET, Dhaka.	Member
5._____ Dr. Md. Afsar Ali Professor Department of ME, BUET, Dhaka.	Member
6. _____ Dr. Dilip Kumar Saha Chief Scientific Officer Materials Science Division Bangladesh Atomic Energy Commission, Dhaka.	Member
7. _____ Dr. A.M. Sarwaruddin Chowdhury Professor Department of Applied Chemistry & Chemical Engineering University of Dhaka.	Member (External)

The thesis titled "**Modification and Characterization of Technical Bamboo Fibers and Their Polypropylene Based Composites**" submitted by Shamsun Nahar, Roll no:1009114003P, Session: October 2009, has been accepted as satisfactory in partial fulfilment of the requirements for the degree of Doctor of Philosophy in Materials and Metallurgical Engineering on 29 April, 2014.

BOARD OF EXAMINERS

1._____ Dr. Mahbub Hasan Assistant Professor Department of MME, BUET, Dhaka	Chairman
2._____ Head Department of MME, BUET, Dhaka.	Member (Ex-officio)
3._____ Dr. Ahmed Sharif Associate Professor Department of MME, BUET, Dhaka.	Member
4._____ Dr. Kazi Md. Shorowordi Assistant Professor Department of MME, BUET, Dhaka.	Member
5._____ Dr. Md. Afsar Ali Professor Department of ME, BUET, Dhaka.	Member
6. _____ Dr. Dilip Kumar Saha Chief Scientific Officer Materials Science Division Bangladesh Atomic Energy Commission, Dhaka.	Member
7. _____ Dr. A.M. Sarwaruddin Chowdhury Professor Department of Applied Chemistry & Chemical Engineering, University of Dhaka.	Member (External)

CANDIDATE'S DECLARATION

It is hereby declared that this thesis or any part of it has not been submitted elsewhere for the award of any degree or diploma.

Signature of the Candidate

_____

(Shamsun Nahar)

TABLE OF CONTENTS

List of Tables

List of Figures

Abbreviation

MFA- Microfibrill angle

BCS- Basic chromium sulfate

TGA- Thermogravimmetric analysis

XRD- X-ray diffraction

C.I.- Crystallinity index

D.C.- Degree of crystallinity

PP – Polypropylene

C.S.- Crystallite size

Acknowledgement

All praise is due to the almighty Allah; the most Gracious and the most Merciful.

First and foremost, I would like to express my utmost gratitude, profound regard and indebtness toward my supervisor Dr. Mahbub Hasan, Assistant Professor, Department of Materials and Metallurgical Engineering, Bangladesh University of Engineering and Technology (BUET), Dhaka, for his kindness and patience throughout the whole study. His thoughtful suggestion not only motivated me, but also encouraged at all stages of my research work finally made the successful thesis completion possible.

I would like to thank , Dr. Md. Mohar Ali, professor and Head, Dept. of MME, BUET and the teachers of MME Department, BUET, for their encouragement and guidance. I remember with gratefulness the kind help and inspiration of Dr. Dilip Kumar Saha, Chief Scientific Officer, Materials Science Division, Atomic Energy Centre, Dhaka.

I acknowledge with appreciation the co-operation of Mr. Yusuf Khan, Md Abdullah al Maksud, Ashiqur Rahman, Md. Harun-or Rashid and Md. Ahmed Ullah of BUET for their help at various stages of my research.

I am grateful to BUET for providing me financial support for conducting the research . I would like to express my deep gratitude to the Department of Materials and Metallurgical Engineering for providing facilities throughout the work.

I am also grateful to the members of my family.

Shamsun Nahar

Dhaka, 2014.

ABSTRACT

This research work attempted to propose a new technique for characterization of bamboo fiber as reinforcement in composite. Raw bamboo fiber was characterized by thermal, structural and mechanical testing. The tensile properties (tensile strength, strain to failure and Young's modulus) of raw bamboo fiber were studied by varying span length. FTIR spectroscopic analysis was done for observing the bonding in raw bamboo fiber. For determination of cellulose, hemicellulose, lignin, ash etc chemical analysis was conducted. TGA analysis was analysed for observing thermal stability. Degree of crystallinity, crystalline index and microfibril angle were measured using XRD peak analysis. Surface and cross-section of bamboo fiber were observed under SEM. For better mechanical properties raw fiber was modified physically and chemically. The raw bamboo fiber was treated physically with different doses of gamma radiation. In physically modified sample, degradation temperature was increased with increasing the radiation. But after obtaining the optimization, temperature was found to decrease. For chemical treatment waste chemical liquor from leather industry was used. Leather industry waste chemical liquor, containing mimosa, BCS and syntan, was used for fiber modification. Physical and chemical modifications have improved the mechanical, chemical and physical properties of fiber. FTIR spectroscopic analysis was done for treated sample and results showed the evidence of reaction with bamboo fiber and chemicals. In chemical analysis process, no significant change was observed. Crystallinity index and degree of crystallinity was found to improve with modifications. Fiber surface was found to be smooth and this was due to change of surface energy.

Among all modified samples doubly treated fiber, treated with basic chromium sulphate and $NaHCO_3$ (BCS+$NaHCO_3$), showed best results. BCS+$NaHCO_3$ treated fiber was selected as reinforcing agent for fabrication of composites with polypropylene matrix using hot press moulding machine under specific pressure and temperature. The effect of fiber content on the mechanical properties was studied by preparing the composite with different percentage of fiber loading. The tensile properties were found to improve in modified fiber than the raw fiber based

composite. Images of the fiber and fracture surfaces into the composites were taken to examine the failure mode and to investigate the interfacial adhesion between the fiber and matrix.

CHAPTER 1

INTRODUCTION

Renewable resources are of great importance in our modern society because of their positive effects on agriculture, environment and economy. Biopolymers being renewable raw materials, are gaining considerable importance because of the limited existing quantities of fossil supplies and the recent environment conservation regulations.

1.1 Overview

Cellulose rich biomass has acquired enormous significance as chemical feedstock, since it consists of cellulose, hemicelluloses and lignin, which are biopolymers containing many functional groups suitable to chemical derivatization. Cellulose is the most abundant polymer on earth, which also makes it the most common organic compound. Annual cellulose synthesis by plants is close to 10^{12} tons (Mangesh et al., 2012). Plants contain approximately 33% cellulose whereas wood and cotton contains around 50% and 90% cellulose respectively. Most of the cellulose is utilised as a raw material in paper production. This equates to approximately 10 million tons of pulp produced annually. From this, only four million tons are used for further chemical processing annually. It is quite clear from these values that only a very small fraction of cellulose is used for the production of commodity materials and chemicals (Mari, 2009). This fact was the starting point of the present research for understanding, designing, synthesising and finding new alternative applications for this well-known but well underused biomaterial. Cellulose is the most plentiful, natural, biodegradable and renewable raw material available for versatile applications. Cellulose consists of β-1,4 D- linked glucose chains, in which the glucose units are in 6-membered rings (i.e., pyranoses), joined by single oxygen atoms (acetal linkages) between the C-1 of one pyranose ring and the C-4 of the next ring of cellulose. Recently there is an ample interest in substituting cellulose in place of inorganic reinforces/fillers in polymer based composites. This is due to the virtue of cellulose being biodegradable reinforcing agent as well as its adaptability to be tailored for high performance applications in composites. This transformation is well sought in the wake of stringent environmental concerns. Cellulose based reinforced composites are strong, stiff and lightweight materials that consist of strong, stiff, but

commonly brittle fiber that are encapsulated in a softer, more ductile matrix material (Beckermann, 2007). The matrix distributes applied loads to the reinforced cellulose fiber within the composite, resulting in a material with improved mechanical properties compared to the un-reinforced matrix material. These bio-based composites have soaring demand by automotive industry, construction application, manufacturing household products and in the field of packaging (Ruhul et al., 2010; Mubarak et al., 2007).

Fibers with high cellulose content are found to have high crystallite content. These cellulose aggregates to make blocks and these are held by strong intra-molecular hydrogen bonds to form large molecules. This study combines the concepts of hydroxyl group modification of cellulose using chemical and nonchemical modification. The mechanical properties of natural fiber are associated with crystallinity of the fiber and the microfibril angle with respect to the main fiber axis. Sisal fiber content 67% cellulose and microfibril angle of $10\text{-}22^0$ having high tensile strength and modulus of elasticity of 530 MPa and 9-22 GPa respectively. On the other hand, coir fiber with a cellulose content 43% and microfibril angle of $30\text{-}49^0$ reported to have strength and modulus of elasticity of 106 MPa and 3GPa respectively (Sweety, 2011). The variation in cellulose and increased or decreased micro-fibril angle plays an important role in determining the mechanical properties of fiber reinforced composite.

Bangladesh being a tropical country, it is abundant with bamboo plant. A plenty of bamboo plant grows all over the country. The overall mechanical properties of bamboo are comparable to those of wood. Bamboo grows to its mature size in only 6–8 months, whereas wood takes about 10 years (Chen, 1998). Bamboo, a plant of the family Gramineae, is the longest grass in the world. It consists of a hollow culm or stem, with nodes or joints between segments of the stem, and oval leaves. Bamboo, similar to wood, is a natural organism composed to lignin, hemicelluloses, cellulose etc. (Jian, 2002). The culm, branches and leaves stay green throughout the bamboo's life, even during winter. The moso bamboo culm wall is mainly composed of parenchymatous ground tissue in which vascular bundles are embedded. The vascular bundles are composed of metaxylem vessels and sheaths of sclerenchyma fiber, surrounding light parenchymatous ground tissue. The sclerenchyma fibers are responsible for mechanical characteristics of bamboo and the parenchymatous tissue can pass loads and take the role of matrix (Zhuo et al., 2010). Moreover,

it is incredibly flexible; it will bend in strong winds, however it rarely breaks. It has a tensile strength superior to mild steel and a weight-to-strength ratio better than graphite. Bamboo is the strongest growing woody plant on earth. Bamboo is one of the cheapest lignocelluloses and abundantly available plant in the Asia (Sukla, 2012).

Bamboo fiber used as reinforcement and it is characterized and modified using different physical and chemical treatments. Thermoplastic polymer namely polypropylene used as the matrix material. It is a semi crystalline polymer. Its property and classification depend on its percentage of crystallinity. The melting temperature of polypropylene lies in the range of 160-170^0 C.

Chemical modification of bamboo fiber will conducted by using waste liquor releasing from leather industry. As a result, a new plan will be developed for managing waste liquor of leather industry. The reuse of waste liquor in composite manufacturing as well as reinforcement modification will be observed. These wastes are hazardous and toxic. By this research sound infrastructure, disposal of waste materials will be discussed. As a result leather industry waste will be minimized and able to recycle.

Several studies have been reported on the structure and anatomy of bamboo, bamboo dust as reinforcement, bamboo strips as reinforcement, bamboo block as reinforcement, effect of mercerization on the fine structure and mechanical properties of natural fibers, silane treatment on bamboo reinforced epoxy composite, increase in crystallinity of bamboo fiber with increase of alkali treatment etc. No study has reported bamboo as fiber and reuse of leather industry waste for modification of bamboo fiber.

As a developing country, new technologies have been proposed for bulk use of bamboo, as a raw material in the production of high value added and price competitive products. Currently, bamboo is being used for making traditional products such as handicraft, basketry and high-value added products of panels, parquets, furniture and construction materials. Among various diversified bamboo products, bamboo reinforced composites have high potential for wider use and applications. Bamboo fiber based composite can replace a variety of products including carbon and glass fiber composites. So bamboo fiber based composite can play an important role

to increase the economic stability and growth of our country. It can be used for doors, windows, furniture, ceiling tiles, partition boards, automotive interior parts, packaging moulding etc.

1.2 Objectives

The main objective of the study is to improve the mechanical properties of technical bamboo fiber using leather industry waste liquor for bamboo fiber reinforced polypropylene composites. This objective will be obtained by modification - physically and chemically and characterization of treated technical bamboo fiber. Tensile properties of raw and modified technical bamboo fiber will be characterized varying different fiber span length. The Young's modulus and strain to failure will be corrected by using newly developed equations in order to correlate with actual Young's modulus and strain to failure of bamboo fiber. Assessment of physical properties such as crystallinity, surface and cross-sectional change, density of raw and modified technical bamboo fiber will be obtained by XRD, SEM and pycnometer method. Wet chemical analysis will be done for determination of α-cellulose, hemicellulose, lignin, ash, hot water and cold water solubility of bamboo fiber. Physical, mechanical and chemical properties of technical bamboo fiber will be explained by FTIR process. After modification, best fiber will be selected for composite fabrication. Physico-mechanical and thermal properties of fabricated composites will be determined.

The research aim is to reduce the environmental pollution and to reuse the leather tannery waste liquor in the composite industry. Because Bangladesh is a developing country, urbanisation and industrialisation usually need balance by environmental objectives. This research will help to reduce environment pollution by adopting the following process such as safeguarding land by drainage and waste collection facilities, protecting water catchments. The other aim of the present thesis is to explore the possibilities of using Bangladesh bamboo fiber as reinforcement on thermoplastic matrix.

The thesis consists of five chapters. The second chapter of this thesis will present an analysis of the relevant literatures about natural fiber and natural fiber composites, especially bamboo fiber and their composites.

In the third chapter, experimental techniques are described which is used during the study. At first the technique used to perform single fiber tensile test will be explained. Next, a description of correction method using some newly developed equations is given (Subhankar et al., 2009). Several methods that were used to characterize the raw and modified bamboo fiber such as tensile test, wet chemical analysis, water absorption test, thermogravimetric analysis (TGA), Fourier transform infrared radiation (FTIR) spectroscopy, X-ray diffraction (XRD) and scanning electron microscope (SEM) are then described. In the fourth chapter, the experimental results are mentioned, discussed and analysed. Finally, in chapter five general conclusions and future works will be drawn into attention based on the obtained results.

CHAPTER 2

Literature Review

Animal or plants are the main sources of natural organic fiber. The majority of useful natural textile fibers are plant derived, with the exceptions of wool and silk. All plant fibers are composed of cellulose, whereas fibers of animal origin consist of proteins. Natural cellulose fibres tend to be stronger and stiffer than their animal counterparts and are therefore more suitable for use in composite materials.

2.1 Natural fiber

Generally synthetic fibers (glass, carbon, aramid, ceramic etc.) are used as the reinforcement in the composites. Among all synthetic fibers, glass fiber received much attention due to its low cost and better thermo-mechanical properties compared to other fibers. The problem of using synthetic fiber reinforced composites is that these composites are not biodegradable and are causing environmental pollution. For this reason, alternative reinforcement with natural fiber in composites has recently gained much attention because of having low cost and low density, biodegradability and recyclable nature. Therefore, scientists found natural fiber as a potential candidate for applications in consumer goods, low cost housing and automotive interior components and many others. Depending on the origin of the fiber, cellulose fiber can be classified into different categories. Sources and categories of natural fibers are mentioned in Table 2.1.

2.2 Comparison of natural cellulose fiber

For centuries, cellulose fibers have been used in the manufacture of various products such as rope, string, clothing, carpets and other decorative products. Wood fibers are cellulose that is mostly used in the world due to their extensive use in the pulp and paper industries. However, the use of other fiber types is increasing. The use of other fiber types is mentioned in Table 2.2.

Table 2.1 Sources and example of natural fiber (Gareth, 2007).

Source of fiber	Example
Grasses and reeds	These fibers are found in the stems of monocotyledonous plants such as bamboo and sugar cane.
Leaf fiber	These fibers run lengthwise through the leaves of most monocotyledonous plants such as sisal, henequen and abaca.
Blast fiber	These fibers are situated in the inner bark (phloem) of the stems of dicotyledonous plants. Common examples are jute, flax, hemp and kenaf.
Seed and fruit hairs	These are fiber that comes from seed hairs and flosses, which are primarily represented by cotton and coconut.
Wood fiber	These fiber are found in the xylem of angiosperm (hardwood) and gymnosperm (softwood) trees. Examples are pine, maple and spruce.

Table 2.2 Commercially important fiber sources (Gareth, 2007).

Fiber Source	Species	World Production (10^3 tonnes)	Origin
Wood	(>10,000 species)	1,750,000	Stem
Cotton lint	*Gossypium sp.*	18,450	Fruit
Bamboo	(>1250 species)	10,000	Stem
Jute	*Corchorus sp.*	2,300	Stem
Kenaf	*Hibiscus Cannabinus*	970	Stem
Flax	*LinumUsitatissimum*	830	Stem
Sisal	*Agave Sisilana*	378	Leaf
Coir	*CocosNucifera*	100	Fruit
Ramie	*Boehmeria Nivea*	100	Stem
Abaca	*Musa Textiles*	70	Leaf
Sunn hemp	*CrorolariaJuncea*	70	Stem
Roselle	*Hibiscus Sabdariffa*	250	Stem
Hemp	*Cannabis Sativa*	214	Stem

There are several physical properties that are important in selecting suitable cellulose fiber for use in composites. Fiber dimensions, defects, variability, crystallinity and structure are some of the most important properties that must be considered. Mechanical properties are even more important when selecting a suitable fiber for composite reinforcement. To produce a better composite material, it is important to utilise a higher strength reinforcing fiber.

However, fiber strength is not the only the contributing factor to composite strength, as good bonding between the fiber and matrix, good fiber orientation and good fiber dispersion are also required. The cost of the cellulose fiber is also a factor that could influence fiber selection. Fiber prices tend to fluctuate considerably and are dependent on a number of factors, such as supply and demand, quality and exchange rates. A comparison of the relative costs of a number of fiber can be seen in Table 2.3.The costs of bulk cellulose fiber are considerably lower than those of glass and carbon, but cellulose fiber require further processing to get them into a form where they can be used in composites. Despite this, cellulose fiber still appears to be a cheaper option when compared to synthetic fibers.

Table 2.3 Cost of natural plant fibers (Gareth, 2007).

Fiber Type Price	$US/Kg
Jute	0.3 - 0.7
Bamboo	0.5-1.0
Hemp	0.5 - 1.5
Flax	0.4 - 0.8
Sisal	0.4 - 1
Wood	0.2 - 0.4
Glass	1.5 – 3.2
Carbon	10 - 200

From the information of Table 2.4 it can be seen that bamboo, hemp and jute fibers are much stronger than the others, having the highest values for Young's modulus. These are the desirable attribute for fiber to be used as composite reinforcement. Although some synthetic fiber show more high values for Young's modulus, but they are not cost effective and are avoided in some sectors because of their non-biodegradability.

In this research paper bamboo has been chosen as reinforcement for composite material. Bamboo is a type of sustainable resource that is of fast growth rate, high mechanical strength and easy processing performance. It is distributed in tropic and subtropics of Asia, Africa and Latin America.

Table 2.4 Properties of natural fiber in relation to those of E-glass (Gareth, 2007).

	fiber									
Properties	E-glass	Hemp	Jute	Ramie	Coir	Sisal	Flax	Cotton	Kenaf	Bamboo
Density, g/cm^3	2.55	1.48	1.46	1.5	1.25	1.33	1.4	1.51	-	1.4
Tensile strength, (MPa)	2400	550-900	600-1100	500	220	600-700	800-1500	400	930	500-740
Young's modulus, (GPa)	69	50-70	10-30	44	6	38	60-80	12	-	30-50
Specific stiffness, (MN.m/kg)	27	34-47	7-21	29	5	29	43-57	8	-	-
Elongation at failure, (%)	3	1.6	1.8	2	15-25	2-3	1.2-1.6	3-10	-	2-5

For a long period, bamboo has been mainly used to build scaffold, guardrail, makeshift houses etc. in a raw state in building industry. In 1940s, bamboo plywood was developed, and the application of bamboo and wood developed rapidly to build girder, wall, pillar, rafter, bamboo mixed structure and interior ornament. According to different requirements, modern bamboo structure can be used in three occasions: low-price practical buildings, temporary structures like

building used in exhibition or rest, and high-class villa, tearoom etc. Bamboo, however, has the potential for much higher fiber yields that could result in lower costs with improvements in cultivation techniques (Srebrenkoska et al. 2009). Bamboo, compared to other fiber, also has the advantage of being extremely disease and pest resistant, and can be planted at high densities to prevent weeds from growing between the plants. Pesticides and herbicides are therefore not required in the cultivation of bamboo, and this provides a distinct advantage over other fiber in many countries where restrictions on herbicide use is prevalent.

2.3 Industrial bamboo fiber

Bamboos are the members of the grass family. Unlike ordinary grasses, most bamboos are arborescent (tree-like) and parential living for many decades. Their straight, erect, cylindrical stems are useful for wide variety of purpose. Bamboo mat-board (Bamboo-ply) is another bamboo-based industrial product, fast gaining popularity for its suitability for its much application. Bamboo's constitute is an important raw materials doe paper industry (Li et al. 2012). The shortage of housing in developing countries motivates the search for low cost materials that can be applied in the construction of affordable houses, especially in earthquake regions of the world. The understanding of the mechanical behaviour of bamboo has caught the attention of engineers, architects, biologists and material researchers due to bamboo's great potential to be used as a construction material. Bamboo presents advantages in relation to other construction materials for its lightness, high bending capacity and low cost, besides the fact that it requires simple and low cost processing techniques (John et al. 1999). The geometry of bamboo's longitudinal profile has a macroscopically functionally graded structure, which can withstand extreme wind loads. It has also been observed that the fiber distribution in the transverse cross-section at any particular height of a bamboo is dense in the outer periphery and sparse in the inner periphery, as a result, outer surface has higher strength than the inner surface. Bamboo is itself composite with cellulose fiber reinforcement and lignin matrix. The fiber strength is reported to be 600 MPa which is 12 times higher than the matrix strength. The Young's modulus of fiber is much higher (46 GPa) than that of the matrix (2GPa). Whereas the density of fiber is 1.16 and the density of matrix is 0.67 gm/cm^3. The average density of bamboo is 0.8 gm/cm^3 (Suwat et al., 2005).

2.3.1 Bamboo Plant Morphology

Bamboo is part of the giant grass family and is a fast growing annual plant. It can grow up to fifty to sixty metres in height and can reach between six and sixty millimetres in diameter depending on the plantation density. Bamboo plants have a well-developed primary root system with numerous branched secondary roots. A typical bamboo plant is shown in Figure 2.1.

Figure 2.1 A typical Bamboo plant.

The cross-sectional structure of a bamboo stalk can be seen in Figure 2.2. The bamboo culm, cylindrical and hollow, is divided at intervals by nodes. The culm is comprised of exodermis (bark which is heavily overlaid with a waxy covering called cutin to prevent loss of water from the culms), parenchyma cells, vascular bundles and endodermis (inner surface layer). The vascular bundle is made up of vessels (transporting water), sieve tubes (transporting nutrition) and thick-walled fiber. The amount and the distribution of the fiber, having comparable

mechanical strength with steel, determine the overall strength of bamboo culms (Suwat et al., 2005).

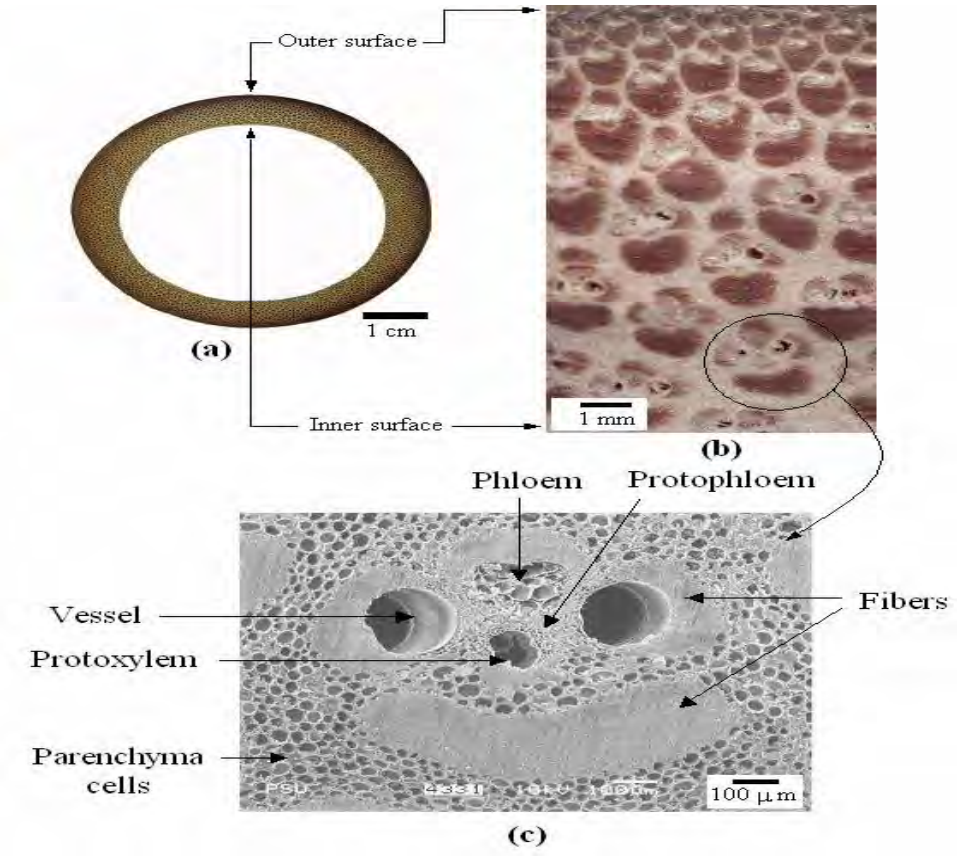

Figure 2.2 Microstructure of bamboo (a) Photograph showing culm circular cross-section, (b) Optical micrograph showing distribution of vascular bundles from the outer to the inner surface, and (c) SEM micrograph showing parenchyma cells and vascular bundle which consists of vessels, phloem and fiber (Leise et al. 1992).

The fiber contributes 60-70% by weight of the total culm tissue. The number of vascular bundles per mm^2 is closely related to Young's modulus, the fiber length to elastic bending stress. So far, fiber length is hardly considered when selecting a bamboo species for a given purpose except pulping, but from practical experience such relations may already be utilized. Across the culm wall the fiber length often increases from the periphery towards the middle and decreases towards the inner part. Along the culm from base to top no remarkable pattern for the fiber length exists except a slight reduction, whereas a great variation is evident within one internode of up to 100% and more. The shortest fibers are always near the nodes, the largest are in the

middle. Thus the nodal part has a reduced strength due to its shorter fiber and marks the breaking point for the standing culm. In service, however, bamboo breaks hardly at the nodes because of a higher fiber portion due to reduced parenchyma and increased lignifications (Liese et al. 1992).

2.3.2 Bamboo fiber morphology

Lignocellulosic fiber can actually be considered as composites themselves as they consist of helically wound cellulose microfibrils in an amorphous matrix of lignin and hemicellulose. Each fiber consists of many microfibrils that run along the length of the fiber (Figure 2.3).

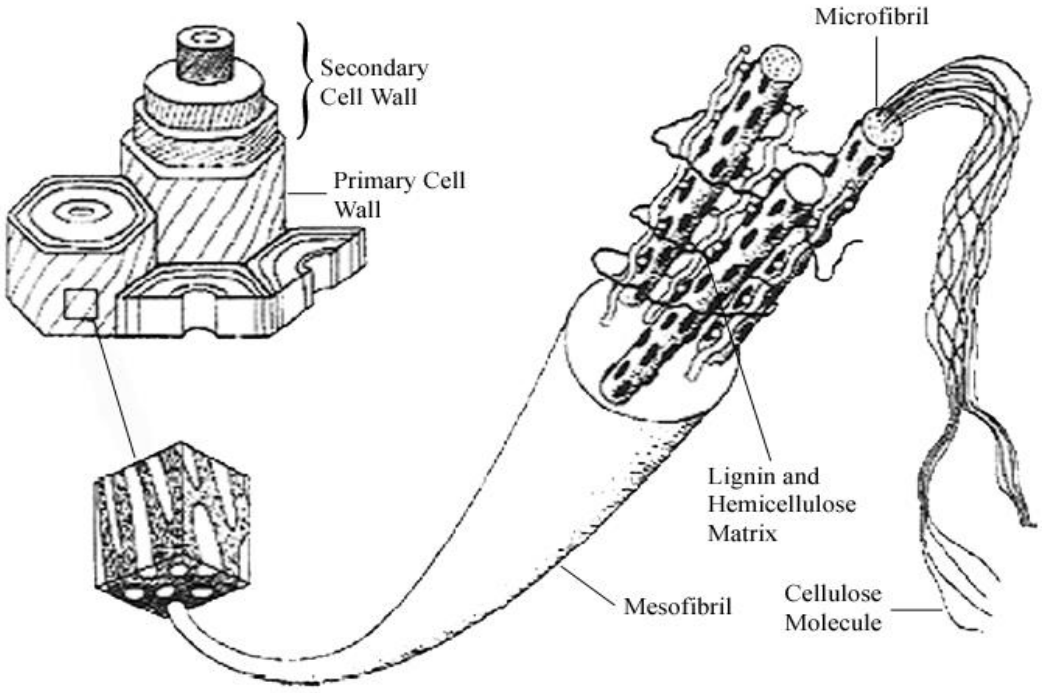

Figure 2.3 Fiber with primary and secondary walls. Cellulose molecules aggregated to form microfibrils, which in turn compose mesofibrils (Gareth, 2007).

The lamellation consists of alternating broad and narrow layers with different fibrillar orientation. In broader lamellae, fibrils are oriented at a smaller angle to the fiber axis whereas the narrow ones show mostly a transverse orientation. The narrow lamellae exhibit higher lignin content than the broader ones. The polylamellate wall structures of the fiber lead to an extremely high tensile strength. The polylamellate structures do not exist in the cell wall of the fiber of the

normal wood. Based on its anatomical properties, ultra structure and plant fracture mechanism bamboo establishes itself as a superior natural fiber among other known natural fiber (like jute, coir, sisal, straw, banana, etc.) Amongst these various lingo-cellulosic fiber, bamboo has 60% cellulose with a considerably higher percentage of lignin (~32%), its microfibrillar angle being relatively small (2^0–10^0). These facts about bamboo support its high tensile strength (Liese et al. 1992).

2.3.3 Factors affecting fiber properties

The mechanical properties of single fiber are strongly influenced by many factors, particularly chemical composition and internal fiber structure, which differ between different parts of a plant as well as different plants. The most efficient cellulose fibers are those with high cellulose content coupled with a low microfibril angle in the range of 2-10^0 to the fiber axis. Other factors that may affect the fiber properties are maturity, separating processes, microscopic and molecular defects such as pits and nodes, soil type and weather conditions under which they were grown. The highly oriented crystalline structure of cellulose makes the fiber stiff and strong in tension, but also sensitive towards kink band formation under compressive loading. The presence of kink bands significantly reduces fiber strength in compression and in tension.

2.4 Bamboo fiber constituents

The chemical composition of bamboo varies according to the variety, the area of production and the maturation of the plant. Bamboo fiber are mainly composed of cellulose, hemicelluloses, lignin and pectins, although the quantities of each are different in exodermis and endodermis. Exodermis fiber contains higher cellulose contents and is therefore stronger than endodermis. Endodermis fiber also contains high levels of lignin, which is undesirable for fiber that is to be used in composite material (Han et al., 2007).

2.4.1 Cellulose

Cellulose, the most abundant biopolymer resource in the world, is widely considered as a nearly inexhaustible raw material with fascinating structures and properties. Cellulose consists of

β 1,4 D linked glucose chains, in which the glucose units are in 6-membered rings (i.e., pyranoses), joined by single oxygen atoms (acetal linkages) between the C-1 of one pyranose ring and the C-4 of the next ring (Figure 2.4). Four different polymorphs of cellulose are known, including cellulose I, II, III, and IV. Cellulose I and II are the most studied forms of cellulose. In living plants, cellulose I is the most widespread crystalline form, which consists of an assembly succession of crystallites and disordered amorphous regions. The natural crystal is made up of metastable cellulose I with all cellulose strands in a highly ordered parallel arrangement. Two coexisting crystal phases, cellulose Iα and cellulose Iβ are contained in cellulose I. Phase Iα has a triclinic unit cell containing one chain, whereas cellulose Iβ is represented by a monoclinic unit cell containing two parallel chains. Chemically, cellulose II has higher chemical reactivity than cellulose I and can be made into excellent cellophane, so it is regarded as one of the most useful fiber and has broad applications in chemical industry. The crystal structure of cellulose I in native cellulose can be converted to that of cellulose II (by mercerization.). During the process of mercerization, entire fibers are converted into a swollen state and the assembly and orientation of microfibrils are completely disrupted. The original parallel-chain crystal structure of cellulose I changes to anti-parallel chains of cellulose II. The dominant hydrogen bond is O2-H---O6 in cellulose I, whereas it is O2-H---O6, O6-H---O6 and O2-H---O2 in cellulose II. Since cellulose II involves chain folding, its structure is more difficult to unravel and the reverse transformation from cellulose II to cellulose I does not occur (Yiying et al., 2007 and Fan et al., 2011). The molecular structure, arrangement and crystallite structure of cellulose are shown in Figures 2.5 and 2.6 respectively.

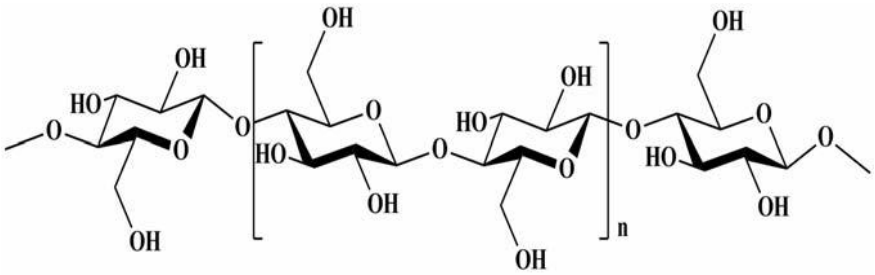

Figure 2.4 Chemical structure of cellulose (Gareth et al. 2007).

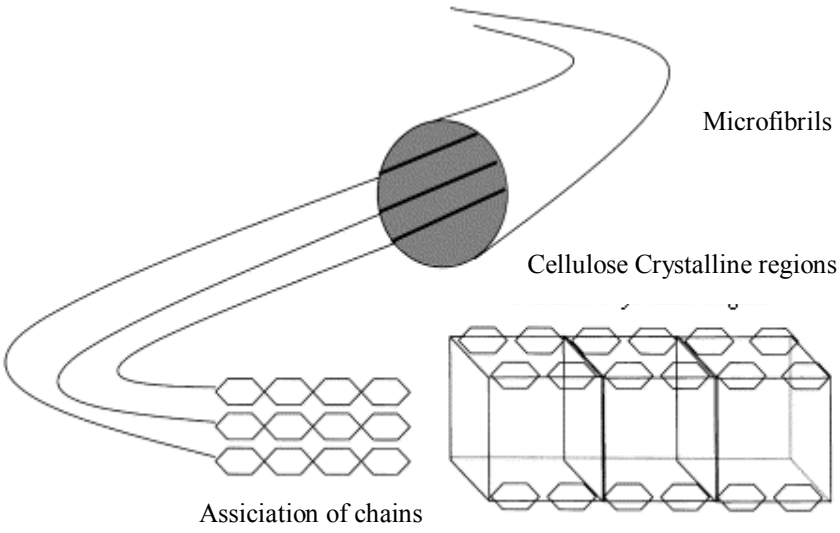

Figure 2.5 The molecular structure and arrangement of cellulose (Gareth et al. 2007).

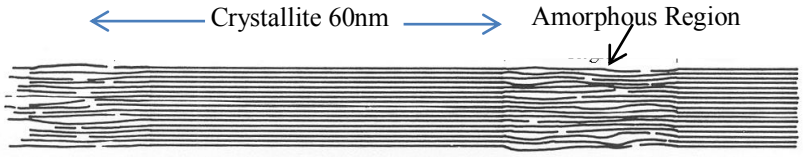

Figure 2.6 Schematic representation of the crystallite structure of cellulose (Gareth et al. 2007).

The rigidity and strength of cellulose and lignocellulose based materials is a result of hydrogen bonding, both between chains and within chains. The amorphous cellulose regions have fewer inter-chain hydrogen bonds, thus exposing reactive inter-chain hydroxyl groups (OH) for bonding with water molecules. Amorphous cellulose can therefore be considered hydrophilic due to its tendency to bond with water. Crystalline cellulose on the other hand is closely packed, and very few accessible inter-chain OH groups are available for bonding with water. As a result, crystalline cellulose is far less hydrophilic than amorphous cellulose. Crystalline microfibrils consist of tightly packed cellulose chains with accessible hydroxyl groups present on the surface

of the structure (Figure 2.7). Only the very strongest acids and alkalis can penetrate and modify the crystalline lattice of cellulose.

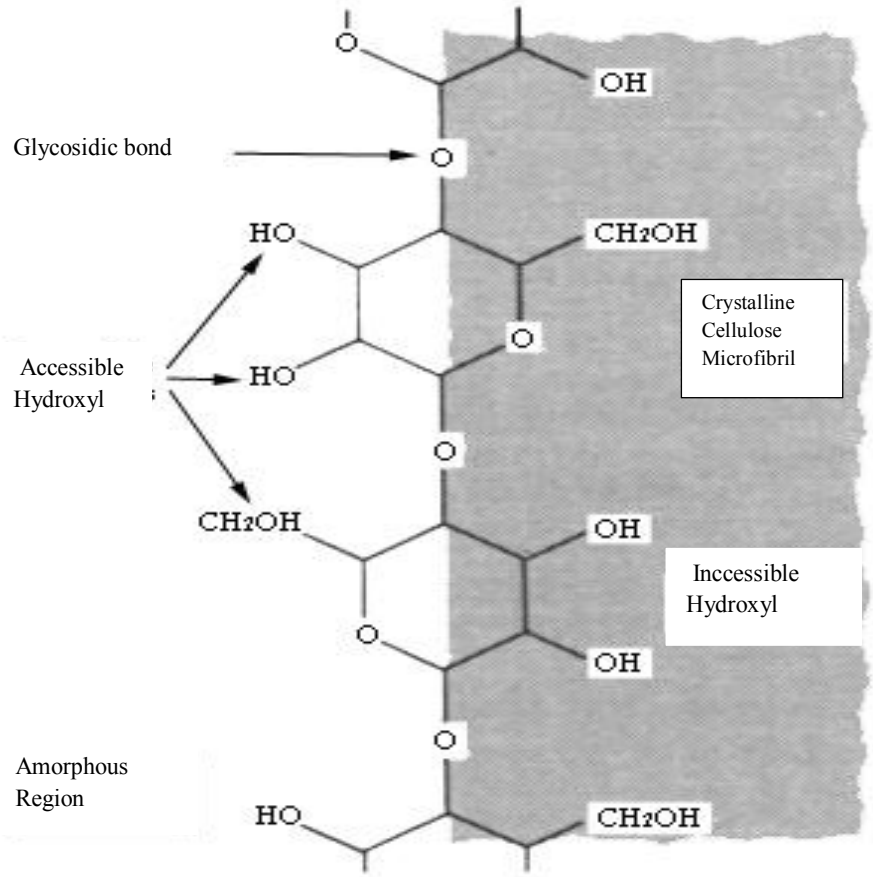

Figure 2.7 Schematic representation of the microfibril surface (Gareth et al. 2007).

2.4.2 Lignin

Lignin is a complex chemical compound most commonly derived from woody plant and an integral part of secondary cell wall or plants. It is one of the most abundant organic polymers of earth exceeding by cellulose. As a biopolymer lignin is unusual because of its heterogeneity and lack of defined primary structure. Its commonly noted function is the support through the strengthening of wood in trees. Lignin fills the spaces in the cell wall between cellulose, hemicelluloses and pectin components. It is covalently linked to hemicelluloses and therefore,

cross linking different plant polysaccharides confirming mechanical strength in the cell wall and extension the plant as a whole. The cross linking of polysaccharides by lignin is an obstacle for water absorption to the cell wall. Thus, Lignin makes it possible for the plant vascular tissue to conduct water efficiently (Trujillo, 2010). Schematic representation of lignin is shown in Figure 2.8.

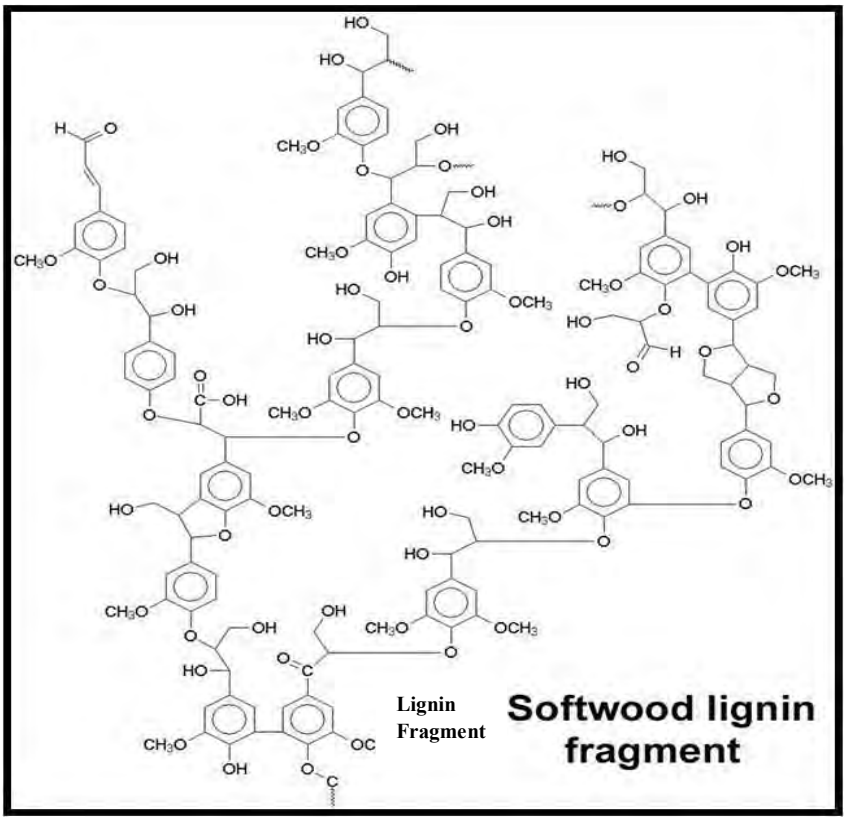

Figure 2.8 Schematic representation of lignin (www.en.wikipedia.org.wiki/lignin).

2.4.3 Hemicellulose

Hemicellulose is highly variables across cell types and plant species. It is a branching macromolecule constructed of 5 and 6 carbon sugars. They are generally insoluble in pH -7 water but soluble in basic solutions. Hemicellulose limits the stretchiness of the cell wall by linking adjacent microfibrils and preventing them from sliding against each other for unlimited distances. Xylose, mannose and glactose form the hemicelluloses backbone; arabinose, glucuronic acid and galactose form the side chains (Mubarak et al, 2006). Schematic

representation of the crystallite structure of cellulose, hemicelluloses, pectin is shown in Figure 2.9.

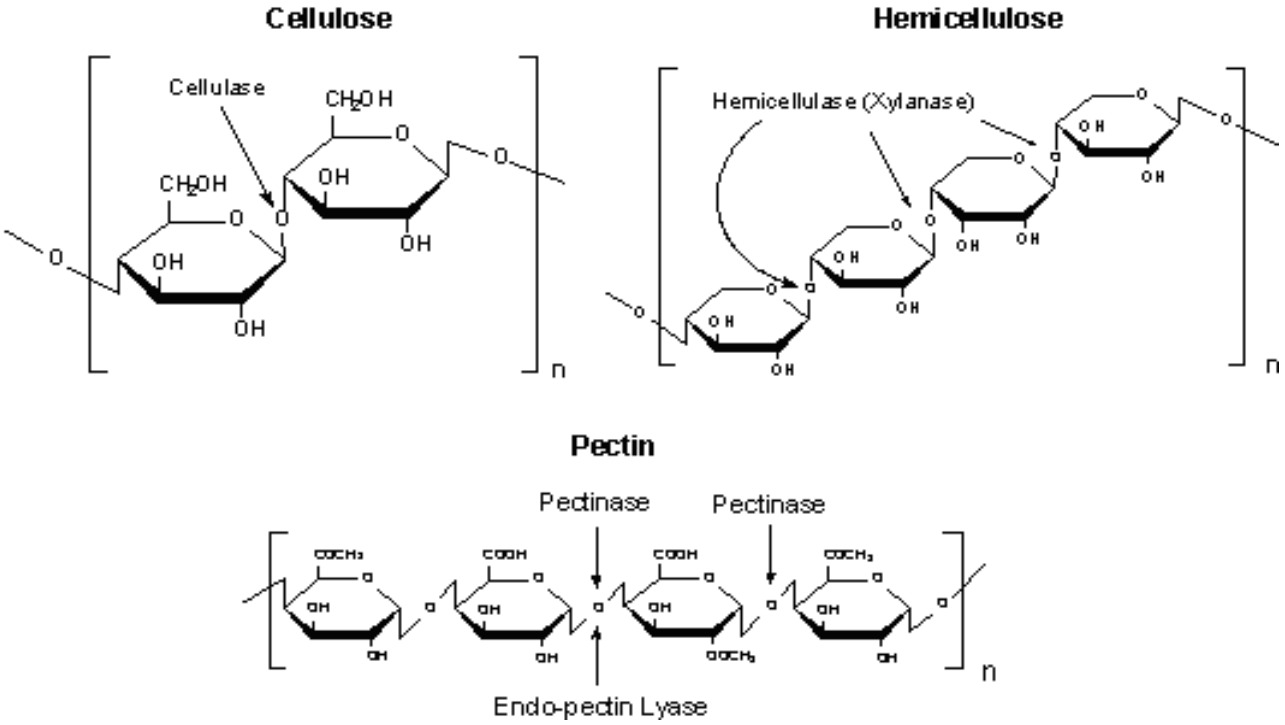

Figure 2.9 Schematic representation of the crystallite structure of cellulose, hemicelluloses, pectin (www.lib.tkk.fi/Diss/2005/isbn9512276909).

A summary of the cell wall polymers responsible for the properties of cellulose fiber can be seen in Figure 2.10.

Biological Degradation
Hemicelluloses
Accessible Cellulose
Non-Crystalline Cellulose

Moisture Sorption
Hemicelluloses
Accessible Cellulose
Non-Crystalline Cellulose
Lignin
Crystalline Cellulose

Ultraviolet Degradation
Lignin
Hemicelluloses
Accessible Cellulose
Non-Crystalline Cellulose
Crystalline Cellulose

Thermal Degradation
Hemicelluloses
Cellulose
Lignin

Strength
Crystalline Cellulose
Amorphous Constituents
Lignin

Figure 2.10 Cell wall polymers responsible for the properties of lignocellulosic in order of importance (El-Zaher, 2001).

2.5 Literature review on bamboo fiber

Bamboo fiber is a technical fiber. Technical fiber is a fiber which is constructed of connected elementary fiber (Nele, 2010). **A** fiber bundle is a bundle in which every fiber is isomorphic, in some coherent way, to a technical fiber (sometimes also called typical fiber) (Ncatlab, 2014; Wikipedia, 2014). Fiber bundles are held together in matrix, hemicellulose/ lignin in technical fiber. Technical fiber are separated from the xylem material (woody core) and sometimes also from epidermis. But the fiber bundles are collected from the phloem and support the conductive cells of the phloem and provide strength to stem.

Tuhidul et al. (2009) researched on jute fabric-reinforced poly (caprolactone) biocomposites (30–70% jute), which were fabricated by compression molding. Tensile strength, tensile modulus, bending strength, bending modulus and impact strength of the non-irradiated composites (50% jute) were found to be 65 MPa, 0.75 GPa, 75 MPa, 4.2 GPa and 6.8 kJ/m^2, respectively. The composites were irradiated with gamma radiation at different doses (50–1000 krad) at a dose rate of 232 krad/hr and mechanical properties were investigated. The irradiated composites containing 50% jute showed improved physico-mechanical properties. The degradation properties of the composites were observed. The morphology was evaluated by scanning electron microscope.

Ruhul et al. (2009) worked on jute yarn reinforced polypropylene (PP) composites and were prepared by compression molding. To prepare the composites, jute yarns were treated with 1–5% aqueous starch solution (w/w) varying different soaking time (1–5 mins). The yarn content in the composite was about 50% by weight. Starch treated jute composites showed higher mechanical properties than that of the untreated jute composites. Composites prepared with 3% starch treated yarns (for 3 mins soaking time) demonstrated tensile strength 52 MPa, tensile modulus 700 MPa, bending strength 50 MPa and bending modulus 1406 MPa. Optimized composite was then treated with gamma radiation (Co-60) at a dose of 500 krad and found further improvement of the mechanical properties. Water uptake of the composites at room temperature (25^0C) was measured and it was found that starch treated samples showed higher water uptake properties than the raw sample. After 500 hours of simulating weathering testing, optimized composites retained its 75% TS and 93% TM was calculated.

Zaman et al. (2010) studied on jute fabrics reinforced polyethylene (PE), polypropylene (PP) and mixture of PP+PE matrices based composites (50 wt% fiber) and this composite were prepared by compression molding. It was found that the mixture of 80% PP + 20% PE hybrid matrices based jute fabrics reinforced composites performed the best results. Gamma radiation (250–1000 krad) was applied on PP, PE and jute fabrics then composites were fabricated. The mechanical properties of the irradiated composites (500 krad) were found to increase significantly compared to that of the non-irradiated composites. Electrical properties like dielectric constant, loss tangent and conductivity with temperature variation of the composites were studied.

Haydar et al. (2009) worked on jute fabrics (hessian cloth) reinforced polypropylene (PP) matrix composites, which were fabricated by compression molding. Jute fabrics and matrices were irradiated with gamma and UV radiation at different doses. Mechanical properties of irradiated jute fabrics and matrices based composites were found to increase significantly. Optimized jute fabrics were treated with starch solution of different concentrations for different soaking time. Composite made of 0.5% (for UV) and 0.3% (for gamma) starch treated jute fabrics (5 min soaking time) showed the best mechanical properties. Scanning electron microscopic analysis of untreated and treated composites was also performed in their study.

Mubarak et al. (2006) researched on plywood surface using UV and Gamma radiation. In order to further improve the physical properties, plywood surface was pretreated with UV and Gamma radiation at different radiation intensities before photocuring. After pretreatment with radiation the plywood surface was coated with different prepared formulations containing epoxy acrylate (EA-1020) as an oligomer, difunctional monomers such as tripropylene glycol diacrylate (TPGDA), 2-hexadioldiacrylate (HDDA), Ethylene Glycol dimethacrylate (EGDMA) and trifunctional monomer trimethylpropentriacrylate (TMPTA) with photoinitiator Darocur 1664. Thin polymer films were prepared on glass plate with formulated solutions and cured under UV radiation. Pendulum hardness (PH) and gel content of the film were studied for selecting the formulations as top coat and as base coat. The polished plywood surface was coated with selected formulation and cured under UV radiation. Various rheological properties of UV cured

plywood surface such as pendulum hardness, scratch hardness, microgloss, adhesion strength, percentage chipped off area and abrasion resistance were studied.

Haydaruzzaman et al. (2010) worked on hessian cloth (jute fabrics) reinforced polypropylene (PP) composites, which were prepared by compression molding. The mechanical properties were later evaluated. Jute fabrics and PP sheets were treated with UV radiation at different intensities and then composites were fabricated. It was found that mechanical properties of the irradiated jute and irradiated PP-based composites were found to increase significantly compared to that of the untreated counterparts. Irradiated jute fabrics were also treated with aqueous starch solution (1–5%, w/w) for 2–10 min. Composites made of 3% starch-treated jute fabrics (5 min soaking time) and irradiated PP showed the best mechanical properties. Tensile strength, bending strength, tensile modulus, bending modulus and impact strength of the composites were found to be improved compared to the untreated composites. Water uptake, thermal degradation and dielectric properties of the resulting composites were also performed.

Haydar et al. (2010) studied on jute fabrics reinforced thermoset composites that prepared with different formulations using urethane acrylate oligomer, methanol, and benzyl peroxide. Jute fabrics were soaked in the prepared formulations and fiber content in the composites was optimized with the extent of mechanical properties. Among all the resulting composites, 55 wt% jute content at oligomer: methanol: benzyl peroxide 75:24.5:0.5 (w/w/w) ratios showed the best mechanical properties. The optimized jute fabrics were cured under UV radiation at different intensities and their mechanical properties were measured. Jute fabrics were treated with potassium permanganate ($KMnO_4$) solution of different concentrations (0.01, 0.02, 0.03, and 0.05 wt %) for different soaking times (1-5 min) before the composite fabrication. Optimized jute fabrics (jute fabrics treated with 0.02 wt% $KMnO_4$ for 2 min soaking time) were soaked in the optimized formulation and cured under UV radiation at different intensities and measured their mechanical properties. Scanning electron microscopic investigation showed that surface modification improves fiber/matrix adhesion. Water uptake and soil degradation test of the treated and untreated composite samples were also performed.

Tamikazu Kume (2006) used nuclear technology such as gamma-rays, electron beams and ion beams irradiation, which is widely used for the sterilization and modification of bio-resources. Radiation has been effectively used in various agricultural fields such as food irradiation, sterile insect technique, sterilization of substrate, degradation and crosslinking of natural polymers, mutation breeding, radioisotopes, etc. contributing for human being to supply foods and sustainable environment.

El-Zaher (2001) estimated crystalline and amorphous regions and was very interested in absorptivity of pigments, humidity, and chemical reactions. In addition, the performance behavior of textile materials depending on the complex interaction of their basic mechanical properties, such as tensile, bending, and shear were also characteristics. Therefore, the work delt with the study of the variation of crystallinity and amorphosity of dralon fabric exposed to ultraviolet (UV) light irradiation for periods ranging from 0 to 120 h using the X-ray diffraction (XRD) technique. The radiation-induced changes in the optical properties of the fabric, which in turn reflect the damaged sites in the irradiated fabric, were also evaluated using spectrophotometric analysis and the obtained results are discussed in relation to the mechanical properties of dralon fabric, such as tensile strength and percentage elongation at break. The results indicated changes in crystallinity, tensile strength and elongation percentage at break, besides variations in optical properties of dralon fabric after exposure to UV light. These changes may be attributed to the variation caused in the macro and micromolecular structure of the fabric network due to UV irradiation.

Mokhtar et al. (2002) worked on the graft copolymerization of N-phenylmaleimide and its p-hydroxy derivative onto cotton fabric using gamma radiation was studied. The effects of monomer concentration, dose rate and irradiation time have been investigated. The surface topology, the x-ray diffraction and the thermal stability of the modified fabric also were studied. In addition, the dyeing characteristics of the grafted fabrics when dyed with basic dyes together with the color fastness of these dyes towards UV radiation were also investigated.

Alam et al. (2003) worked on polymerization of acrylamide performed by gamma ray irradiation at various radiation doses with the help of a Co-60 source. It was used to produce the samples

from aqueous solutions of acrylamide monomer in single distilled water having the concentrations of 20, 30 and 40% (w/w). Solubility test, differential scanning calorimetry and infrared spectroscopy demonstrate that the properties of the samples prepared by irradiation were quite different from that of a monomer. The degree of polymer conversion was found to depend on doses and concentrations, where maximum conversion reaches at doses of 0.18, 0.16, and 0.10 KGy for 20, 30, and 40% concentrations, respectively. Viscosity and molecular weight (MW) of irradiated samples increased with both the doses and concentrations showing the value of MW < 108; which strongly indicates the polymer formation. The amount of gel content that represents the cross-linked portions in the irradiated samples is found to be negligible, suggesting the formation mainly of polyacrylamide.

Hasan et al. (2003) prepared jute yarns with pretreated by alkali (5% NaOH) and were grafted with two types of monomer such as 3-(trimethoxysilyl)-propylmethacrylate (silane) and acrylamide (AA) under ultraviolet (UV) radiation. The monomer concentrations were 30% in methanol (MeOH) and irradiation times were 30 min and 60 min for silane and AA respectively. The alkali treated silane-grafted jute yarn produced enhanced tensile strength (TS) (265%), elongation at break (Eb) (350%) with 27% polymer loading (PL) and alkali-treated AA-grafted jute yarn produced enhanced TS (210%), Eb (270%) with 23% PL than that of virgin fiber. Again, the surface of jute yarns were pretreated by alkali along with UV and gamma radiation with different intensities and grafted with silane and acrylamide to further improve the tensile properties of the jute yarn. The jute yarns were pretreated with alkali and UV radiation and grafted with silane showed the best properties such as TS (360%), EB (380%) and 31% PL. Simulated weathering test and water uptake of untreated and treated jute yarns were studied. The alkali, UV-pretreated silanized jute yarns showed lesser water uptake as well as less weight loss and mechanical properties as compared with treated samples.

Shehrzade et al. (2003) treated jute yarns were with ionizing gamma radiation to improve the physico-mechanical properties. To optimize the grafting conditions, jute yarns were soaked for different soaking times (3, 5, 10, and 30 min) in1,6-hexanediol diacrylate (HDDA), methanol (MeOH) solutions of different HDDA (1–10%) concentration along with photoinitiator Darocur-1664 (3%) and were cured under UV lamp at different UV radiation intensities. Concentrations

of monomer, soaking time and UV radiation intensities were optimized with extent of mechanical properties; 5% HDDA, 5% min soaking time performed the best tensile strength (TS) (67%), modulus (108%), and polymer loading (PL) (11%). Virgin jute samples were pretreated with gamma radiation for different doses (25–1000 krad) at 600krad/hr supplied from Co-60 gamma source. Tensile strength, elongations at break (Eb) and modulus, and PLs of these gamma-pretreated samples were observed. Pretreatment with gamma radiation enhanced tensile strength and modulus that were 67.7% and 48% respectively, whereas elongation was increased up to 56% compared to that of virgin yarn. It is observed that only gamma-pretreated samples exhibit higher tensile strength. When gamma-pretreated samples were grafted with HDDA and cured with UV, the tensile properties decreased but PL increased.

Hasan et al. (2005) grafted cellulose (Whatman 41 filter paper) under in situ UV radiation with organosilicone monomer 3-(trimethoxysilyl)-propylmethacrylate (silane) at optimized system (30% silane and 30-min irradiation) and obtained enhanced mechanical properties like tensile strength factor (TS-140%) and elongation at break (Eb-200%) with 25% polymer loading. To improve the mechanical properties, cellulose was pretreated under UV and gamma radiation at different radiation intensities and was grafted with 30% silane under in situ UV radiation. Although the gamma pretreated grafted sample showed higher polymer loading (PL 31%), the UV-pretreated grafted sample showed better enhancement of mechanical properties (PL 33%, TS 250%, and Eb 274%). For further improvement, cellulose was pretreated by alkali (5% NaOH) along with UV and gamma radiation with different intensities and grafted with silane under UV radiation. Among the treatments, the alkali UV-irradiated grafted sample showed the best performance (TS-260% and Eb-280%) with 37% polymer loading at 10th UV pass. Water uptake of treated and untreated samples was studied and less water uptake was observed by the treated samples, which corroborates the finding that silane might be deposited or reacted on cellulose backbone of pure cellulose.

Basfar et al. (2010) developed several formulations with polypropylene (PP) in combination with antioxidants, calcium stearate, hindered amine light stabilizers (HALS) and ultraviolet light absorber (UVA) for making woven jumbo bags, which will be capable of carrying a load of two tons of materials in outdoor conditions. Thin films of these formulations were extruded followed

by stretching to improve mechanical properties. Both stretched and un-stretched PP films were subjected to severe accelerated weathering by ultraviolet (UV) radiation for various periods and it was observed that un-stretched films reached 50% retention of tensile strength (TS) within 500 hours of exposure, while stretched films (tapes) did not reach 50% TS retention even after 10,500 hours of the exposure indicating an improved UV stability of the stretched films of PP.

Athawale et al. (1999) worked on graft copolymer in molecules with one or more species of block connected to the main chain as a side chain(s). These side chains have constitutional or configurationally features that differ from those in the main chain. In the graft copolymer, the distinguishing feature of the side chains is constitutional, that is, the side chains comprise units derived from at least one species of the monomer different from those which supply the units of the main chain. The simplest case of a graft copolymer can be represented as: poly (A)-*graft* poly (B), where the monomer named first (A in this case) supplies the backbone (main-chain) units, while that named second (B) is in the side chain. An approach to chemically bonded natural-synthetic copolymer compositions is through graft polymerization. Grafting has been utilized as an important technique for modifying the chemical and physical properties of the polymer. Graft copolymers are assuming increasing importance because of their tremendous industrial potential. Some of the graft copolymers with high commercial utility are (*a*) acrylonitrile-butadiene-styrene (ABS) (a graft copolymer obtained by grafting polyacrylonitrile and polystyrene onto polybutadiene); (*b*) alkali-treated cellulose-*graft*-polyacrylonitrile and starch-*graft*-polyacrylonitrile, which are used as "super absorbents" in diapers, sanitary napkins, and the like; and (*c*) high-impact polystyrene (i.e., polystyrene-*graft*-polystyrene) copolymer.

Li et al. (2007) filled Poly (trimethylene terephthalate) with nano-$CaCO_3$ and ultra-fine talc that was prepared by melt blending using a co-rotating twin screw extruder. The effect of these two inorganic filler on the crystallization and melting behavior, mechanical properties and rheological behavior of PTT were characterized. The DSC results indicated that both nano-$CaCO_3$ and ultra-fine talc exhibited heterogeneous nucleation effect on the crystallization of PTT and more significant nucleation effect were observed in PTT/ nano-$CaCO_3$ composite due to the smaller size and better dispersion of nano-$CaCO_3$ in PTT matrix. Mechanical properties study suggested that the incorporation of nano-$CaCO_3$ and ultra-fine talc greatly improved the tensile

and flexural properties of PTT. Ultra-fine talc tends to lower the impact properties, while nano-$CaCO_3$ tends to increase the impact strength of the PTT/nano-$CaCO_3$ composite. When 2 wt% of nano-$CaCO_3$ was added, the impact strength increased by one time. Rheological behavior study indicated nano-$CaCO_3$ exhibited plasticization effect on PTT melt and decreased the viscosity of PTT, while ultra-fine talc increased the viscosity of PTT due to the hindrance of the layer structure of talc.

Among different polyethylene cross-linking methods, such as peroxide, irradiation, and silane cross-linking, silane-based methods are the most suitable methods for producing cable insulation and hot water pipe materials due to process simplicity and superior properties of its product. Electrical, thermal and mechanical properties of silane-grafted water-cross-linked polyethylene were investigated by Barzin et al (2007). The effects of silane grafting and gel content on volume resistivity, tensile properties and melting behavior of low density polyethylene (LDPE) were studied. Results indicated that volume resistivity increased with increasing gel content. Stress at break increased with increasing grafting level and gel content. Elongation at break increased with grafting and decreased with gel content. High temperature tensile properties showed that cross-linked polyethylene (XLPE) is more stable than LDPE at high temperature. In differential scanning calorimetry (DSC) analysis a broad endothermic peak appeared for XLPE due to phase separation. Melting point and crystalline percentage decreased with increased grafting level and gel content. Incorporation of carbon black into XLPE reduced the volume resistivity and degree of crystallization.

Cai et al. (2007) successfully prepared Poly (styrene-acrylonitrile) (SAN)/clay nano-composites by melt intercalation method. The hexadecyltriphenylphosphonium bromide (P16) and cetylpyridium chloride (CPC) were used to modify the montmorillonite (MMT). The structure and thermal stability property of the organic modified MMT were respectively characterized by Fourier transfer infrared (FT-IR) spectra, X-ray diffraction (XRD) and thermogravimetric analysis (TGA). The results indicate that the cationic surfactants intercalate into the gallery of MMT and the organic-modified MMT by P16 and CPC had higher thermal stability than hexadecyltri methyl ammonium bromide (C16) modified MMT. The influences of the different organic modified MMT on the structure and properties of the SAN/clay nanocomposites were

investigated by XRD, transmission electronic microscopy (TEM), high-resolution electron microscopy (HREM), TGA and dynamic mechanical analysis (DMA), respectively. The results indicated that the SAN cannot intercalate into the interlayers of the pristine MMT and resulted in micro-composites. However, the dispersion of the organic-modified MMT in the SAN is rather facile and the SAN nano-composites revealed an intermediate morphology, an intercalated structure with some exfoliation and the presence of small tactoids. The thermal stability and the char residue at 700^0C of the SAN/clay nano-composites remarkably enhanced compared with pure SAN. DMA measurements show that the silicate clays improved the storage modulus and glass transition temperature (Tg) of the SAN matrix in the nano-composites.

Khan et al. (2007) grafted the sisal fiber (Agavaesisalana) with methacrylonitrile (MAN) under UV radiation in order to modify its mechanical and degradable properties. A number of MAN solutions of different concentrations in methanol (MeOH) along with photoinitiatorDarocur-2959 were prepared. The soaking time, radiation dose and monomer concentration were optimized. Sisal fiber soaked for 60 min in 50%MAN and irradiated at 8th UV pass achieved highest values of tensile properties like tensile strength (TS- 140.2 MPa) and elongation at break factor (Ef- 8) with 8% polymer loading (PL). To further improve the properties of sisal fiber, a number of additives (1%) such as urea (U), polyvinylpyrrolidone (PNVP), tripropelene glycol diacrylate (TPGDA), hexanedioldiacrylate (HDDA), trimethyl propane triacrylate (TMPTA), ethylene glycol dimethacrylate (EGDMA) were used in the 50% MAN formulation to graft at the optimized condition. Among the additives used, urea has significantly influenced the PL (9%), TS (190 MPa), and Ef (9) values of the treated sisal fiber. Water uptake and accelerated weathering test were also performed.

Huq et al. (2010) studied the effect of LLDPE incorporation in the jute fiber-reinforced PET composites (50% fiber by wt). The effect of LLDPE incorporation into PET was investigated by measuring the mechanical properties of the LLDPE blended jute fiber-reinforced PET composites. LLDPE was blended (20-80% by wt) with PET and the thin films were made by compression molding. Water uptake of the composites was also investigated. Degradation of all the composites was carried out in soil medium.

Samia et al. (2011) studied coir fiber which derived from the husk of the coconut (*Cocosnucifera*). Coir has one of the highest concentrations of lignin, which makes it stronger. They investigated that in recent years, wide range of research has been carried out on fiber reinforced polymer composites. The aim of the research was to characterize brown single coir fiber for manufacturing polymer composites reinforced with characterized fiber. Adhesion between the fiber and polymer is one of factors affecting the strength of manufactured composites. In order to increase the adhesion, the coir fiber was chemically treated separately in single stage with $Cr_2(SO4)_3.12(H_2O)$ and double stages (with $CrSO_4$ and $NaHCO_3$). Both the raw and treated fibers were characterized by tensile testing, Fourier transform infrared (FTIR) spectroscopic analysis, scanning electron microscopic analysis. Tensile properties of chemically treated coir fiber was found higher than raw coir fiber, while the double stage treated coir fiber had better mechanical properties compared to the single stage treated coir fiber. Scanning electron micrographs showed rougher surface in case of the raw coir fiber. The surface was found clean and smooth in case of the treated coir fiber. Thus the performance of coir fiber composites in industrial application can be improved by chemical treatment.

Atanassov et al. (2010) researched on the thermo oxidative degradation kinetics of tetrafluoroethylene- ethylene copolymer (TFE-E) and its composites filled with 10 mass% black rice husks ash (BRHA), white rice husks ash (WRHA) or Aerosil A200 Degussa (AR) in air was studied using the Coats-Redfern calculation procedure. The thermo-oxidative degradation of these composites occurs in two stages and their most probable kinetic mechanisms were established, as well as the values of the activation energy E, frequency factor A in the Arrhenius equation and the changes of Gibbs free energy ΔG, enthalpy ΔH and entropy ΔS for the formation of the activated complex from the reagents, respectively. The thermo-oxidative degradation of the samples studied was accompanied by kinetic compensation effect. The lifetime values were calculated at different temperatures to conclude that the use of BRHA as filler reduced lifetime to the highest extent.

Mubarak et al. (2010) prepared composites of jute fabric and gelatin by solution casting or solution-impregnation technique. Jute content in the composite was optimized on the basis of their mechanical properties. Composite containing 50% jute showed best mechanical properties

in terms of tensile strength (TS), tensile modulus (TM), bending strength (BS), bending modulus (BM) and impact strength (IS). Incorporation of urea into the composite showed better improvement in the mechanical properties than the untreated composites. Scanning electron micrographs of the urea treated composites showed better adhesion between gelatin matrix and jute fabrics.

Xiong et al. (2010) modified with the TiO_2 nanoparticles by di-block copolymers, poly(methyl methacrylate)-b-polystyrene (PMMA-b-PS), via reversible addition-fragmentation chain transfer (RAFT) polymerization, and the epoxy nano-composites containing different TiO_2 and with different contents were prepared. Subsequently, the effects of TiO_2 content on the mechanical and thermal properties of nano-composites were investigated. The results indicated that after grafting copolymers onto TiO_2, the dispersion of TiO_2 and interaction with epoxy matrix could be significantly increased. Therefore, the mechanical properties of the nano-composites were improved greatly. When the TiO_2-PMMA-b-PS content was 1 wt%, the impact strength and flexural strength reached their best and increased up to 96% and 43% respectively. Furthermore, the thermal stability of the nano-composites was also distinctly improved.

2.6 Literature review on FTIR

Infrared spectroscopy is among the most widely utilized techniques for determination of molecular structures and identification of compounds in biological samples. The absorbed energy of infrared radiation results in stretch and deformation vibrations of specific molecular bonds (C-H, O-H, N-H etc.), which are characteristic for the chemical composition of the particular sample. The FTIR spectra of plant tissues, therefore, represent a fingerprint of the major organic constituents, such as carbohydrates, proteins, lipids, lignin, and other aromatic or other abundant compounds. Wood has been studied by FTIR for a long time. Technological advances have been achieved by the introduction of FTIR-attenuated total reflection (ATR) spectroscopy, which requires no further sample pre-treatment and. Thus, it is suitable as a high throughput method. FTIR spectra have been used to characterize the chemistry of wood, the influence of fungi on wood and for the detection of fungi in wood (Rumana et al., 2008). Infrared spectroscopy was applied to distinguish tree species as well. FTIR spectra have been also used to characterize the

chemistry of bamboo. There were peaks representing bamboo, which shifted due to the influence of chemical treatment (Gunter et al. 2009; Abd et al. 1992; Zhuo et al. 2010; Mahuya et al. 2006). Smith studied microcrystalline cellulose with FTIR (Smith 2001). A typical spectrum of bamboo fiber is given in Fig 4.13. FTIR determines the functional groups, molecular structure, rigidness of compounds. In the IR spectrum different kinds of functional groups absorbed the radiation and for that different types of peaks are observed. A particular wavelength is responsible for a particular compound and this is totally responsible on the structure and the nature of the compound. There are two types of vibration are observed in the IR radiation; i) Stretching vibration and ii) Bending vibration. In the stretching vibration distance between the bonded atoms are decreased and increased but they lies in the same plane. Stretching vibration can be two types i) Symmetric stretching ii) Asymmetric stretching. Wave number of asymmetric stretching usually is in the higher wave number than the symmetric stretching. In bending vibration molecules vibrated with respect to their axis. Bending vibration can be of two types; i) Scissoring vibration and ii) Rocking vibration. The tendency in scissoring vibration is to come the molecules more closely, whereas rocking tends to change their position in the same direction. For that the wave number in scissoring is much higher than rocking. Relation between vibration is given below

$$V_{assy} \rightarrow V_{sym} \rightarrow V_{bend}$$

Wave number depends on following factors

i) Different vibrations of bonds
ii) Coupled vibrations of bonds
iii) Fermi resonance
iv) Inductive effects
v) Hybridization effect
vi) Mesomeric effect
vii) Hydrogen bonding effect
viii) Effect of ring size

Different vibrations of bonds

Dipole moment changes wave number in the same sample in same bonding. In methyl radical (-

CH_3) C-H symmetric vibration at 2872 cm^{-1}, asymmetric vibration at 2872 cm^{-1}, bending vibration at (720-1450) cm^{-1}. Wave number depends on different vibrations.

Effect of coupled vibration

In any compound C-H bond shows only one wave number in the spectrum i.e symmetric vibration. But if any C-H is bonded with another C-H bond they showed two wave numbers symmetric and asymmetric. This is called coupled vibration.

Inductive effect

Any molecule closer to functional if changes their position then the IR active molecule can change their wave number. The change of wave number due to the presence of new substitute in the functional group is called the inductive effect. There are two types of inductive effect; i) Positive inductive effect – where H atom of functional is replaced by donor atoms, as a result IR absorption band will found in lower wave number and ii) Negative inductive effect – where presence of electron donor acceptor reduces the bond length. As a result IR absorption band will found in higher wave number.

Hybridization

Presence of s orbital is higher, which makes the bond length higher in the molecule. As a result, IR absorption band is found in lower wave number.

Resonance Effect

Bond length increases when resonance effect is observed. As a result, IR absorption band is found in lower wave number.

Hydrogen binding effect

There are two types of hydrogen bonding in any molecules i) Intramolecular hydrogen bonding ii) Intermolecular hydrogen bonding. For hydrogen bonding IR spectrum found to in lower wave number. IR spectrum region is 4000-650 cm^{-1}. This wave number can be divided in two main region;

i) Functional group region and

ii) Finger print vibration region.

2.7 Literature review on modification

Gamma radiation

Natural fibers are renewable, cheap and easily available materials, which can be obtained from agricultural and forest corps. Those can be used for domestic and industrial application. Now natural fibers are used in textiles, insulating materials, pulp and increasingly as reinforcements in polymer matrix based eco-friendly composite. Moreover, due to increasing environmental and health concerns, emphasis is being placed on the synthesis of polymeric materials that are biodegradable and pose the least threat to the environment. For that reason natural fibers are used as reinforcement in bio-composite and have a number of advantages, including biodegradability, low cost, easy availability, low density, non-abrasive nature (Amar Shing et al., 2010, M. A. Haque et al., 2010). Natural fiber consists of 1,4-β D glycoside linkage, which readily absorbs moisture from environment. Bamboo contains 67% holocellulose, in which 60% α-cellulose, 16% hemicelluloses and 24% lignin. A hydro-d-glucose is the main elementary unit of cellulose macromolecules, which contain three hydroxyl groups per glucose rings. These hydroxyl groups (-OH) form intra-molecular hydrogen bonds with other glucose rings as well as with -OH groups from the moisture. Therefore, hydroxyl groups in the cellulose structure account for its hydrophilic character, which is a drawback of this natural fiber and their moisture content, can reach up to 12.33%. In order to develop composites with better mechanical properties and environmental performance, it is necessary to impart hydrophobicity to the fiber. Hydrophobicity of natural fiber and hydrophobicity nature of polymer matrix contributes poor mechanical properties of composites. Moisture absorption can result in swelling of fiber and concerns on the dimension stability of the fiber composite cannot be ignored. To overcome this problem, many attempt such as physical and chemical treatments, lead to change in the surface structure and surface energy change of the fiber. Adequate adhesion between the interfaces can be achieved by better wetting and chemical bonding between the natural fiber and polymer matrix. Many researchers have done to improve the properties by physical treatment

(Visco et al. 2010; Haydaruzzaman et al. 2010). For that reason gamma radiation (physical treatment) was applied on bamboo fiber. Gamma radiation at different doses (25-100 KGy) improved the strength of the bamboo fiber.

Gamma radiation is very strong type of ionizing radiation source and has significance effect on polymeric materials. High energy radiation effect on organic polymers produces ionization and excitation. The polymer undergo cleavage or scission i.e., the polymer molecules may be broken into smaller fragments or may be cross-linking happened depending on the radiation dose and nature of polymer molecules. When organic bamboo fiber is radiated, free radicals are produced. Subsequent rupture of chemical bonds yield fragment of the large polymer molecules. As a result free molecules rupture the chemical bond. Chemical bonds yield fragments of the large polymer molecules. The free radicals thus produced may react to change the chemical structure of the polymer and alter the physical properties of the molecules. It also may undergo cross-linking i.e., the molecules may be linked together into large molecules. When bamboo fiber was irradiated by gamma radiation, then tensile strength and Young's modulus were increased with radiation doses and decreased after attaining a maximum value at a certain dose. The increases of mechanical properties with increasing gamma radiation doses were may be due to the inter cross-linked between the neighbouring cellulose molecules that occurs under gamma exposure. As the pre-treatment doses of gamma radiation were increased, mechanical properties were decreased, which might be associated due to the ionizing radiation degradation of cellulose backbone at higher gamma dose. During degradation, there would be loss in strength due to primary bond breakage in the cellulose constituent and therefore, be related to changes taking places in the middle lamella, which reduce the ultimate cell strength (Hydaruzzaman et al., 2009).

Bamboo fiber is a cellulosic structure with a chain of homo-polysacchride consisting of identical monomeric units of β-D-glucopyranose as shown in Figure 2.11

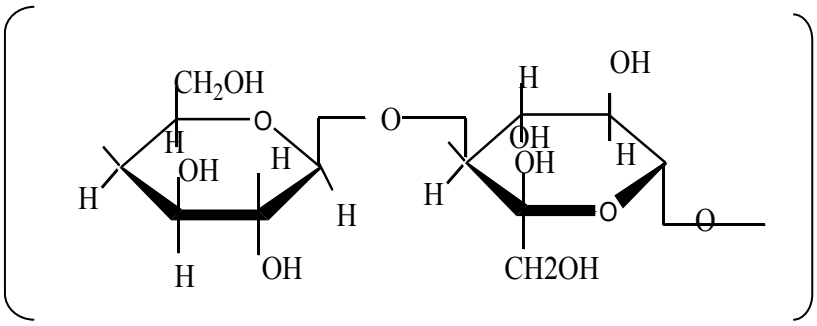

Figure 2.11 Monomeric units of β-D-glucopyranose of bamboo fiber (Anna et al. 2012).

The chains are cemented together by lignin and hemicelluloses i.e. lignin act as matrix to bind the technical bamboo fiber. In addition to those, the structure contains other minor constituents such as wax and fats, inorganic salts and pigments. When bamboo fiber samples are subjected to high energy radiation (gamma), radicals are produced into the cellulose chains by hydrogen and hydroxyl abstraction, as explained in Figure 2.12 (1). Gamma radiation also ruptures some carbon-carbon bonds and produces radicals (Figure 2.12 (2)). Chain scissions may also take place to form other radicals Figure 2.12 (3).

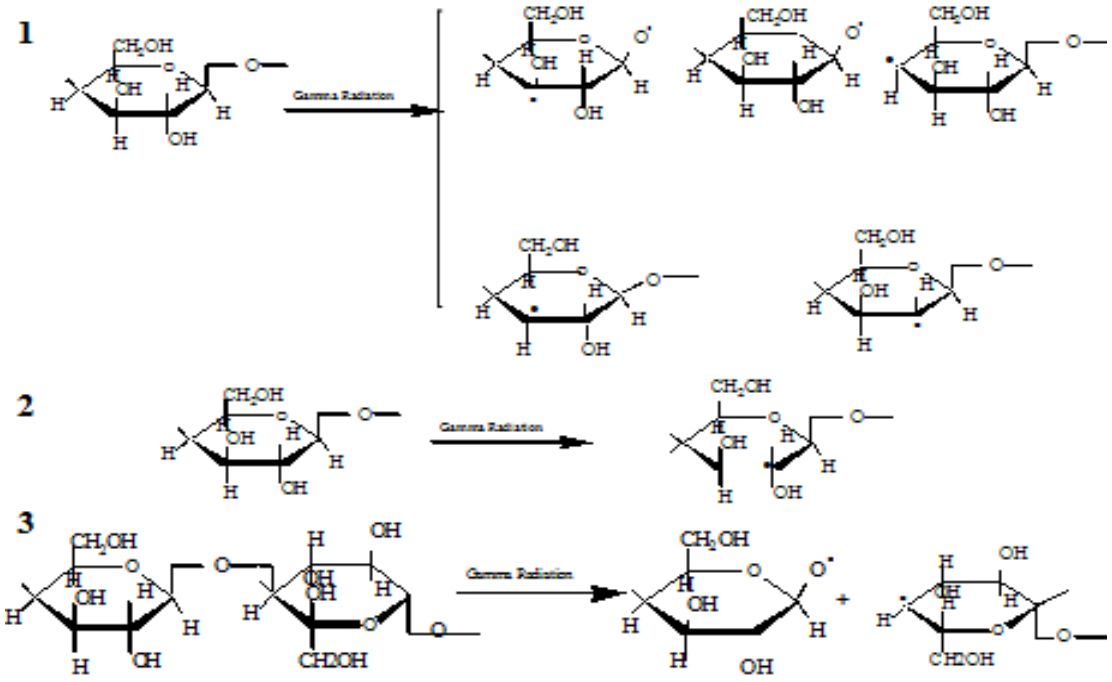

Figure 2.12 Modes of free radical generation into irradiated bamboo fiber. Radicals are formed after C-H, C-O or C-C bond cleavages: (1) hydrogen and hydroxyl abstraction (2) cycle opening (3) chain scission.

Gamma radiation was used as ionizing radiation processor. Gamma radiation is one of the three types of natural radioactivity and denoted by γ. Gamma rays are electromagnetic radiation. Gamma rays are photons, just like light, except of much higher energy, typically from several keV to several MeV. X-Rays and gamma rays are the same thing; the difference is how they were produced. Like all forms of electromagnetic radiation, the gamma ray has no mass and no charge. Gamma rays are ionizing radiation and are thus biologically hazardous. They are classically produced by the decay from high energy states of atomic nuclei (gamma decay). Gamma rays interact with material by colliding with the electrons in the shells of atoms. They lose their energy slowly in material, being able to travel significant distances before stopping. Depending on their initial energy, gamma rays can travel from 1 to hundreds of meters in air and can easily go right through people (Han et al. 2008; Beckermann 2007).

Gamma radiation offers unique advantages for preparing cross linking. This process has led to ever increasing applications of radiation technique in polymerization, such as using gamma radiation in cellulose fiber. The polymerization in fiber in the aqueous media (deuterium oxide) was done in the absence of additional chemical environment (Alam et al. 2003). To make natural fiber competitor with synthetic fiber, development and improvement in physical properties radiation was induced (Shehrzade et al. 2003). Some researchers have found that cellulose and the common cellulose esters and that ether undergo ionizing radiation processing. This offers unique advantages for preparing polyacrylamide and this has led to ever increasing applications of this technique in polymerization. Ionizing radiation such as gamma radiation is known to deposit energy in solid cellulose by Compton scattering and the rapid localization of energy within molecules produce trapped macrocellulosic radicals. The radicals thus generated are responsible for changing the physical, chemical and biological properties of cellulose fiber (Khan et al. 2006). Figure 2.13 shows the capacity of gamma radiation of penetration.

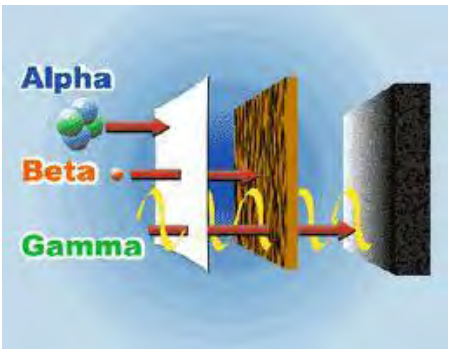

Figure 2.13 Symmetric representation of gamma radiation (Haydar et al. 2010).

Mimosa and Mimosa + $NaHCO_3$

Mimosa is a tannin (also known as vegetable tannin, natural organic tannins or sometimes tannoid, i.e. a type of biomolecule, as opposed to modern synthetic tannin) is an astringent, bitter plant polyphenolic compound that binds to and precipitates cellulose and various other organic compounds including amino acids and alkaloids (en.silvateam.com/Products-Services/Leather /.../Mimosa-extracts*)*.

The term tannin (from *tanna*, an old high German word for oak or fir tree, as in Tannenbaum) refers to the use of wood tannins from oak in tanning animal hides into leather; hence the words "tan" and "tanning" for the treatment of leather. However, the term "tannin" by extension is widely applied to any large polyphonolic compound containing sufficient hydroxyls and other suitable groups (such as carboxyls) to form strong complexes with cellulose and other macromolecules (www.mimosa-sa.com/frame.htm).

The tannin compounds are widely distributed in many species of plants, where they play a role in protection from predation, and perhaps also as pesticides, and in plant growth regulation.

Tannins have molecular weights ranging from 500 to over 3,000 (gallic acid esters) and up to 20,000 (proanthocyanidins). Tannins are incompatible with alkalis, gelatin, heavy metals, iron, lime water, metallic salts, strong oxidizing agents and zinc sulfate, since they form complexes and precipitate in aqueous solution (www.kaisersheepskin.com/apps/webstore/products/show/2693051). Tannins are mainly physically located in the vacuoles or surface wax of plants. These storage sites keep tannins active against plant predators, but also keep some tannins from affecting plant metabolism while the plant tissue is alive; it is only after cell breakdown and

death that the tannins are active in metabolic effects. Tannins are classified as ergastic substances, i.e., non-protoplasm materials found in cells.

Tannins are found in leaf, bud, seed, root and stem tissues. An example of the location of the tannins in stem tissue is that they are often found in the growth areas of trees, such as the secondary phloem and xylem and the layer between the cortex and epidermis. Tannins may help regulate the growth of these tissues (www.kaisersheepskin.com/apps/webstore/products/show/2693051).

Vegetable tannins are classified according to their chemical structure:

(i) Pyrogallol or hydrolysable tannins, such as Chestnut and Myrabolam extract.

(ii) Catechol or condensed tannins, such as Mimosa (or Wattle) and Quebracho extract.

Mimosa is a condensed tannis with a more stable structure in which nuclei connected through C-C links. Chemical structure and external colour are shown in Figures 2.14 and 2.15 respectively.

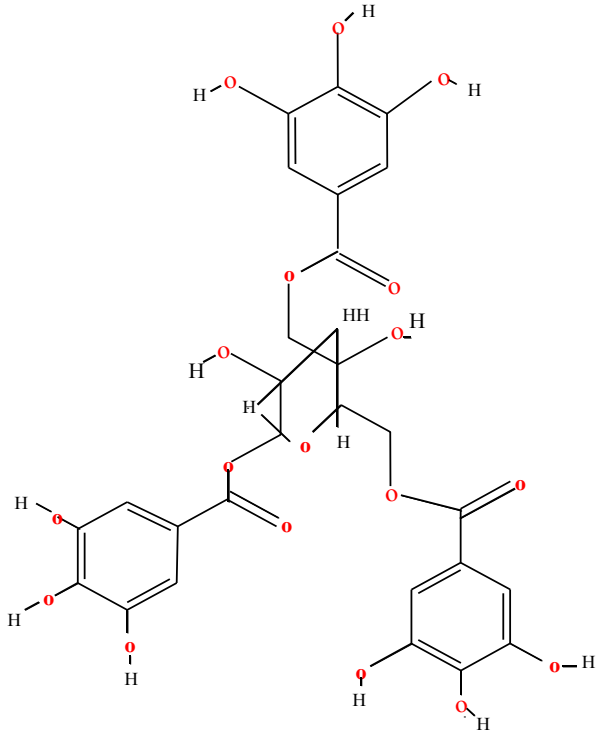

Figure 2.14 Chemical structure of mimosa (Covington,2011).

Figure 2.15 Mimosa powder (Mixture of compound).

Renewable resources have positive effects on environment and economy in our modern society. Biopolymers being renewable raw material, are gaining considerable importance recently. Biomass like cellulose has acquired enormous significance as chemical feedstock because it consists of cellulose, hemicellulose and lignin. These are biopolymers, which contains many functional groups suitable to chemical derivatizaton. Technical bamboo fiber, a lignocellulosic material, is an abundant natural resource in some parts of the world. Bamboo fiber has about double Lewis acid component in its structure. Moreover, as there are several voids in the cross-section of bamboo, it has a higher moisture absorption capacity (Mangesh et al., 2012). Mimosa was used to modify the physical and chemical properties of bamboo fiber. Mimosa is a polyphenol water soluble plant compounds etched from shredded wood bark, leaves and roots. It has the capacity to penetrate into the biological fiber. Chemically, mimosa is a polyphenol named 3,4-dihydroxy-2[[(3,4,5-trihydroxybenzoyl) oxa] oxan-2-yl]methol 3,4,5 trihydroxy benzonzte with molecular weight 36346866 g/mol having chemical formula $C_{27}H_{24}O_{18}$. In mimosa there are 11 H-bond donor which have been shown in Figure 2.14. Mimosa can scavenge carcinogenic and mutagenic oxygen free radical which will be bonded with hydroxyl of cellulosic fiber. As a result cellulose can be able to stabilise against putrefaction, rendering it resistance to biochemical degradation. The resulting fiber may have a final modification and content of as much as 30 to 70% by weight with respect to the cellulose content. For this reason very slow penetration of these large molecules the saturation of fiber with these large amounts of mimosa. Carboxylic groups present in the bamboo cellulose relates with the hydroxyl groups of mimosa at pH values between 3 and 6.Carboxyl groups of on the surface of cellulose react

rapidly with fresh mimosa causing a constriction of the cellulose. This effect is the astringency caused by mimosa solution. The principle attraction between the cellulose and mimosa is based on hydrogen bonding and dipole interactions. The free energy of the transfer of the mimosa in cellulose into a bound phase in aqueous solution is increasing more negative as the mutual interaction increase (Athawale et al., 1999). Mimosa is a higher molecular weight molecule. Higher molecular weight means bigger molecules, leading to slower penetration, causing more surface reaction. In common with every other reaction, the first step of the mimosa tanning reaction is the transfer from the solution environment into the substrate environment.

The thermodynamics of the equilibrium are determined by the solvating power of the solvent on the solute, when greater affinity between the solvent and a solute results in a tendency for the solute to remain in the solvent.

Basic chromium sulfate and basic chromium sulfate + $NaHCO_3$

Chemical formula of Basic chromium Sulfate is $Cr(OH)SO_4$. This salt can act as complex ligands. The use of chromium (III) salt is currently the commonest method for tanning in leather. But in this research paper basic chromium sulfate was used to tan the cellulose fiber. In this tanning process of cellulose infusion and fixing of the chromium (III) species were conducted as consecutive procedure. The availability of ioni ed carboxyl varies from pH 2. . . This is the reactivity range of carboxylic group of cellulose and since the metal salt only reacts with ionized carboxyl. This basic chromium salt acts as complex ligands. Chromium is a $3d^4 4s^2$ element, so chromium (III) compounds have the electronic configuration $3d^3$, forming octahedral compound. Chemical Structure of complex ligand of basic chromium sulphate is shown in Figure 2.16.

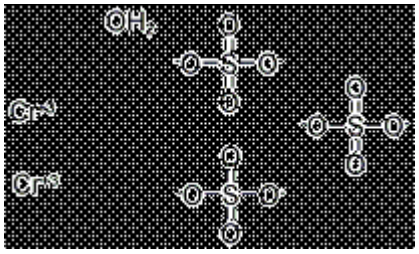

Figure 2.16 Chemical structure of complexing ligand of basic chromium sulfate (www.wikipeida.tanis.com).

The hydroxyl-species of basic chromium sulfate is unstable dimerses, by creating bridging hydroxyl compounds, because oxygen forms bond via lone pair. This process is called olation. It is rapid but not intermediate reaction. Colour and the appearance of basic chromium sulphate are given in Figure 2.17.

Figure 2.17 Picture of basic chromium sulfate powder.

The following processes happen during BCS treatment:

1. In BCS treatment the water exchange is an associative reaction. For the complication BCS has given the implications of the stability of Cr (III).
2. The dimer complex, constructed from the two hydroxyl bridges, was assumed to be the preferred form of the chromium dimer.
3. The stability of the transition metal complexes depends on the kinetic stability because chromium forms complexes with carboxylates with is kinetically more stable.
3. As the mechanism of exchange between ligands into octahedral complexes depend on the stability of the intermediate crystal field. The crystal field activation energy is very high for chromium complexes. For that complexes are kinetically stable (Covington 2011).

Athawale worked on graft copolymer in molecules with one or more species of block connected to the main chain as a side chain(s); these side chains have constitutional or configurationally features that differ from those in the main chain (Athawale, 2007). In the graft copolymer, the distinguishing feature of the side chains is constitutional, that is, the side chains comprise units derived from at least one species of the monomer different from those which supply the units of the main chain. The simplest case of a graft copolymer can be represented as: poly(A)-*graft*poly

(B), where the monomer named first (A in this case) supplies the backbone (main-chain) units, while that named second (B) is in the side chain. An approach to chemically bonded natural-synthetic copolymer compositions is through graft polymerization. Grafting has been utilized as an important technique for modifying the chemical and physical properties of the polymer. Graft copolymers are assuming increasing importance because of their tremendous industrial potential. Some of the graft copolymers with high commercial utility are (*a*) acrylonitrile-butadiene-styrene (ABS) (a graft copolymer obtained by grafting polyacrylonitrile and polystyrene onto polybutadiene); (*b*) alkali-treated cellulose-*graft*-polyacrylonitrile and starch-*graft*-polyacrylonitrile, which are used as "super absorbents" in diapers, sanitary napkins, and the like; and (*c*) high-impact polystyrene (i.e., polystyrene-*graft*-polystyrene) copolymer (Lin et al., 2007).

The basis of the chrome tanning reaction is the matching of the reactivity of the chromium(III) salt with the reactivity of cellulose. The availability of carboxyl varies over the pH range 2-6. This is the reactivity range of cellulose, since metal salt only reacts with ionized carboxyl. This can be modeled in the following way, using empirical formulae:

$$Cr^{+3} \overset{OH^-}{\leftrightharpoons} [Cr(OH)]^{2+} \overset{OH^-}{\leftrightharpoons} [Cr(OH)_2]^{+} \overset{OH^-}{\leftrightharpoons} Cr(OH)_3$$

From the above equation, it is seen that the ultimate basic compound has the empirical formula $[Cr(OH)_2]^+$, rather than the $Cr(OH)_3$ that might be expected from the valence. Chromium is a $3d^4 4s^2$ element, so chromium (III) compounds have the electronic configuration $3d^3$ forming octahedral compounds. The hexa-aquoa ion is acidic, ionizing as a weak acid or may be made basic by adding alkali with sodium bi-carbonate.

Syntan and Syntan + $NaHCO_3$

Syntan is an aromatic polyacids, which possess affinity to carboxyl of cellulose. They combine with cellulose irreversibly. Syntan are most important organic polyacids with tanning potency. It is also misnomer and has no resemblance with natural vegetable tannins. Chemically they are generally condensation products of phenolsulfonic acids and formaldehyde.

Syntan has the power of dispersing insoluble materials and speed up the tanning process, functions as pH adjustors, bleaching agents and as inactivates as cationic groups of cellulose. The function of the sulfonic acid group is to affect the necessary degree of solubility of syntan in water and to charge cellulose negatively enabling the syntan to gain access to the cellulose through attraction. Structure of syntan is mentioned in Figure 2.18.

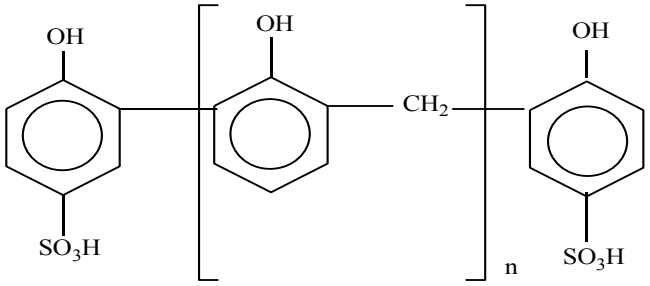

Figure 2.18 Structure of syntan (Covington, 2011).

Abbreviation for synthetic tannins is syntan. It covers substances, which are manufactured to replace the natural vegetable extracts partially or completely, to accelerate production and to make it cheaper. Introduction of new functional groups, which do not occur in vegetable tannins such as sulfonic groups opened new prospects for tanning. Syntans are frequently used in tanning. Sizes of 800 or less, which correspond to 2-4 aromatic rings, are of practical importance. Bonds between aromatic rings in syntans are essential for their properties. For example extension of a molecule by a CH_2 member weakens tanning ability of syntan. Replacement of such a bridge by a sulfonyl group, one increases tanning and improves resistance to light. Resistance to light is also improved by a $-SO_2-NH-$ sulfonamide sequence. Bonding groups can be put in the following order of increasing light resistance:

$-CH_2-<-CHR-<-CH_2NH-CO-NHCH_2-<-CR_2-<-CO_2-<-SO_2-NH-$

Apart from the bridges connecting aromatic rings, the amount, kind and position of functional groups built into these rings are significant. Only hydroxyls, sulfo groups and amino groups have been applied.

Thus factors characterizing a syntan are:

1) number and kind of rings in the molecule

2) number and kind of functional groups
3) molecular weight

Syntans produced in industry generally are not chemical individual, chemical species, generally one speaks of an average of the properties mentioned.

Hydroxyls: Hydroxyls attached to aromatic rings, have phenolic character; it is desirable to introduce them into the molecule in greatest possible amount. Regular distribution of hydroxyls is advantageous since maximum possible conjugated bonds can be formed. It is known that derivatives of α-napthol are better tanning agents than those of β-napthol. Presence of other substituents in the ring influences reactivity. R (alkyl) substituents decrease tanning ability of syntans, sulfo and carboxylic groups in ortho and para position improve the tanning ability, whereas they decrease this ability in meta position. As rule hydroxylic groups do not occur in syntan side chains.

Sulfonic group: Sulfonic group as a substituent on the aromatic ring, it is strongly dissociated, and gives acidic character to the compound. It affects the tanning ability negatively but increases its water solubility. As a rule compound which has one sulfonic group per 3 to 4 rings are applied.

Amino groups: Amino groups occur sometimes in syntans, may act as hydrophiles, however their action is limited to acidic medium only. If the amino groups are the only functional groups they participate in the binding of cellulose. They probably form H-bonds with oxygen from the carboxylic group. The solubility of syntans containing only amino groups decreases with the acidity of the solution, whereas under the same conditions its ability to bind to cellulose increases (Pradeep et al. 2010; Khan et al. 2009, Samia et al. 2010, Sanjay et al. 2009). Structure of syntan and structure of bond formation with syntan and substrate are shown in Figures 2.19 and 2.20 respectively.

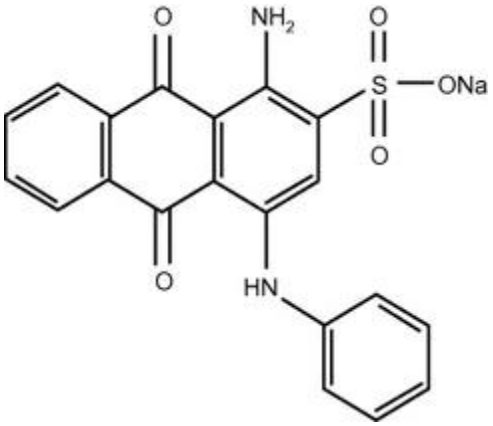

Figure 2.19 Chemical structure of syntan (www. bio.miami.edu).

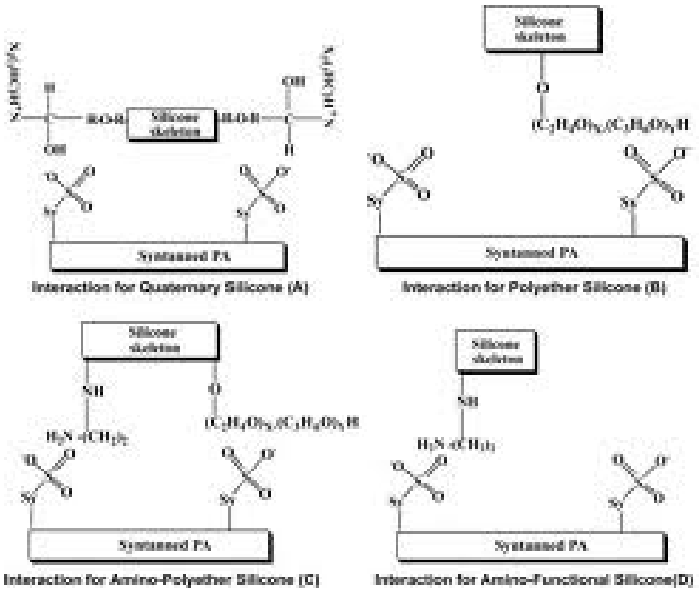

Figure 2.20 Structure of bond formation with syntan and substrate (www.lib.tkk.fi/Diss/2005/ isbn9512276909).

2.8 Literature review on thermal study

Thermogravimetry offers precise control of heating conditions, such as variable temperature range and accurate heating rate. This analysis needs only a small quantity of sample. It is also possible to quantify the amount of moisture and volatiles present in the composites, which have a deteriorating, effect on the material properties. The thermogravimetric data provides number of

stages of thermal breakdown, weight loss of the material in each stage, threshold temperature etc. Both TG and DTG (differential thermogravimetric) curves provide information about the nature and conditions of degradation of the material. The effects of crystallinity, orientation and crosslinking on the pyrolytic behaviour of cellulose fiber can be obtained from thermogravimmetry. It is observed that the thermal breakdown of cellulose proceeds essentially through two types of reactions. At low temperature between (120^0C and 250°C), a gradual degradation occurs, which includes depolymerization, hydrolysis, oxidation, dehydration and decarboxylation. At higher temperature, rapid volatilization occurs accompanied by the formation of levoglucosan and a charred product. Decomposition leads to loss in fiber strength and a marked reduction in degree of polymerization. Initial molecular weight decrease is severe and occurs via rupture of chains at the crystalline/amorphous interface.

The major constituents of bamboo fiber are cellulose, hemicellulose, pectins, lignin etc. Of these, cellulose is the main fraction reporting 68% of the fiber followed by hemicellulose and pectins. The differences in the proportions of cellulose, hemicellulose and pectins in bamboo fiber contribute to the thermal characteristics of the sample. Figure 2.21 shows the structure of cellulose backbone present in the fiber.

Bamboo, like other natural fiber, is hygroscopic and exhibits a tendency to be equilibrium with the relative humidity with the surrounding atmosphere, either by taking of moisture from, or giving out moisture to the atmosphere. They are very prone to swell/warp and shrink when exposed to hot and moist weather condition respectively. However, for application like composite, this aspect is detrimental so far as dimension stability is concerned. Natural fiber absorbs moisture as the cell wall polymer contains hydroxyl or other oxygenated group that attack moisture through H-bonding (Mahuya et al 2008; Shunliu et al. 2009).

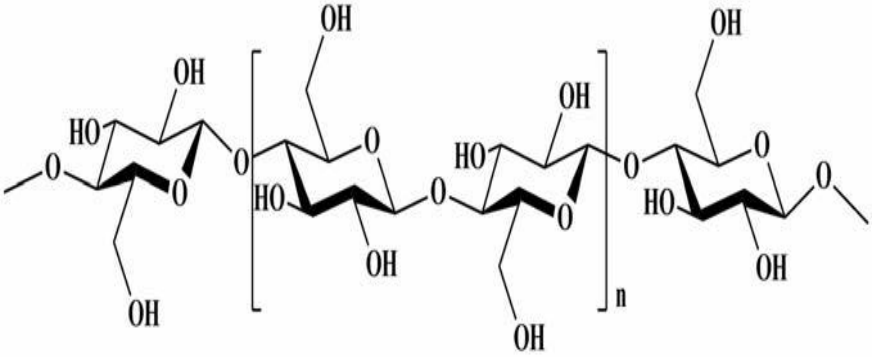

Figure 2.21 Cellulose chain with 1-4 β glycosidic linkage between adjacent monomers (Gareth et al. 2007).

2.9 Matrix

2.9.1 Polypropylene

Polypropylene (PP) is a thermoplastic polymer. It is one of the most extensively used polymers in both developed and developing countries. Polypropylene is available with different reinforcing agents or fillers, such as talc, mica or calcium carbonate; chopped or continuous strand fiber. Many additives have been developed to enhance the thermal stability of polypropylene to minimize degradation during processing. One of the most important requirements of the polypropylene used in the manufacture of the composite is that it should be relatively pure and free of residual catalyst (Alves et al. 2005). PP provides most of the advantages with regards to economic (price), ecological (recycling behavior) and technical requirements (higher thermal stability).

2.9.2 Molecular Structure of Polypropylene

In isotactic PP, each monomer unit in the chain arranged in a regular head-to-tail assembly without any branching. Furthermore, the configuration of each methyl group is the same. Occasionally, some imperfect monomer insertion gives the type of fault shown in Figure 2.16. An extreme example of clamfests is a tactic PP, with complete loss of streric raw. In syndiotactic configuration, methyl groups are alternatively on either side of the carbon chain.

The unique structure of bamboo culm determines its perfect mechanical characteristics. The culm is characterized by nodes. The internodes have a culm wall surrounding a large cavity, called lacuna. In the internodes, the cells are strongly axially oriented. The moso bamboo culm wall is mainly composed of parenchymatous ground tissue in which vascular bundles are embedded. The vascular bundles are composed of metaxylem vessels and sheaths of sclerenchyma fiber which appear dark in contrast to the surrounding light parenchymatous ground tissue. The sclerenchyma fiber are the main component determining the mechanical characteristics of bamboo and the parenchymatous tissue can pass loads and take the role of a composite matrix. Therefore, in view of macro-mechanical behaviour, bamboo is a typical unidirectional fiber reinforced bio-composite. Its mechanical properties depend on the mechanical characteristics of its components, as well as on its microstructure characteristics, such as the volume fraction and the distribution of sclerenchyma fiber and the interface properties of bamboo components (Zhuo et al. 2010).

Normally, sclerenchyma fiber have high strength and low modulus of elasticity (MOE), while parenchymatous ground tissue has low strength and high MOE and high capability of deformation. Therefore, in view of mechanical behaviour, the bamboo can be simplified as a composite of parallel connection model composed of two elements, i.e., fiber and parenchymatous ground tissue, as shown in Figure 4.5 as simplified model (Zhuo et al. 2010). As the bamboo fiber is composed of schelenchyma cell for that fibers pass load to the parenchymatious cell. Parenchymatious cell deformed more than the schelenchyma cell. For that reason bamboo fiber has shown better Young's modulus.

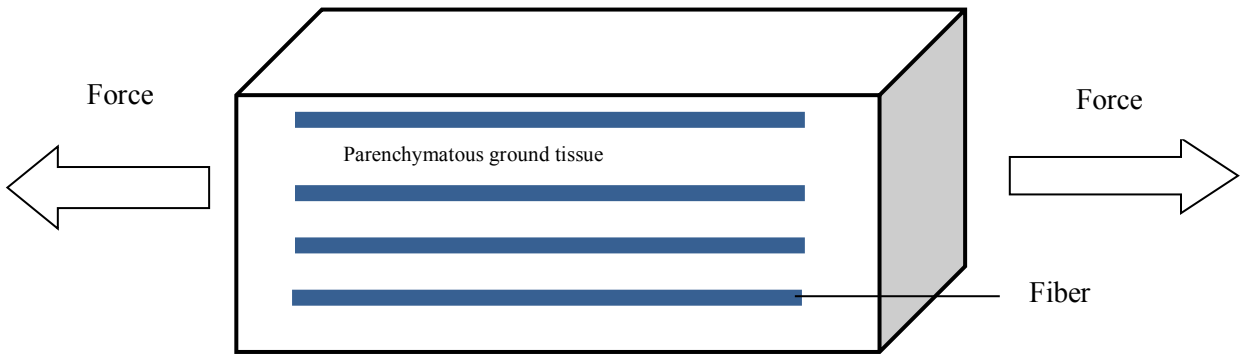

Figure 4.5 Schematic representation of a simplified parallel connection model of bamboo fiber and parenchymatous ground tissue (Zhuo et al. 2010).

The corrected and uncorrected Young's of bamboo fiber is shown Figure 4.6. From the Figure, it can be observed that in the uncorrected curve, the Young's modulus increased with an increase in span length. In this experiment the average uncorrected extrapolated Young's modulus value found is 33.79 GPa. Alpha values (machine displacement) were calculated for all tested fiber, which are shown in the Figure 4.7. Line values from the curve of Figure 4.7 are used for correction.

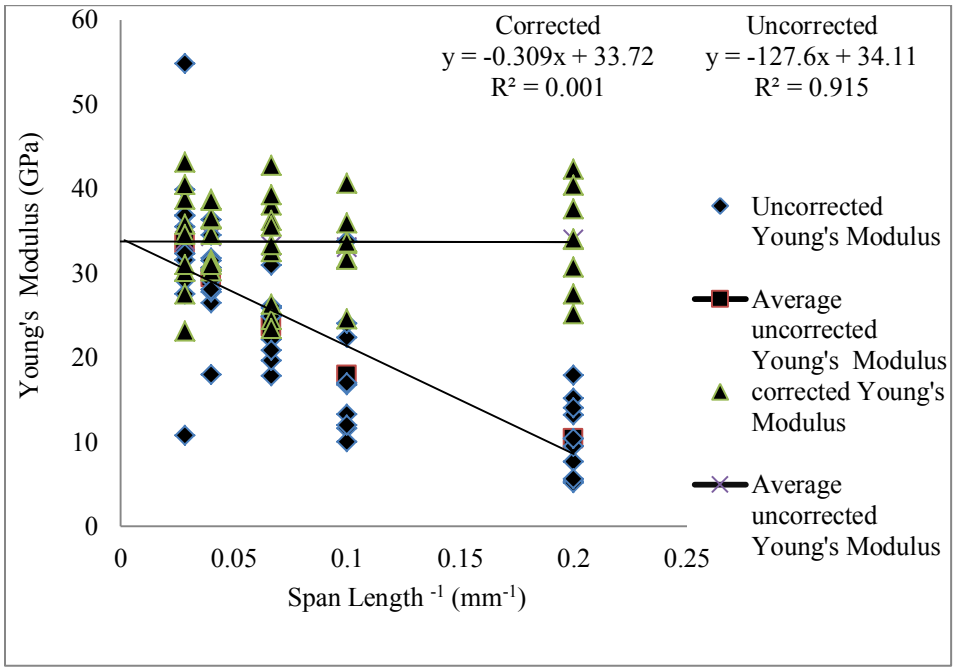

Figure 4.6 Uncorrected and corrected Young's modulus for bamboo fiber in function of span length^{-1}.

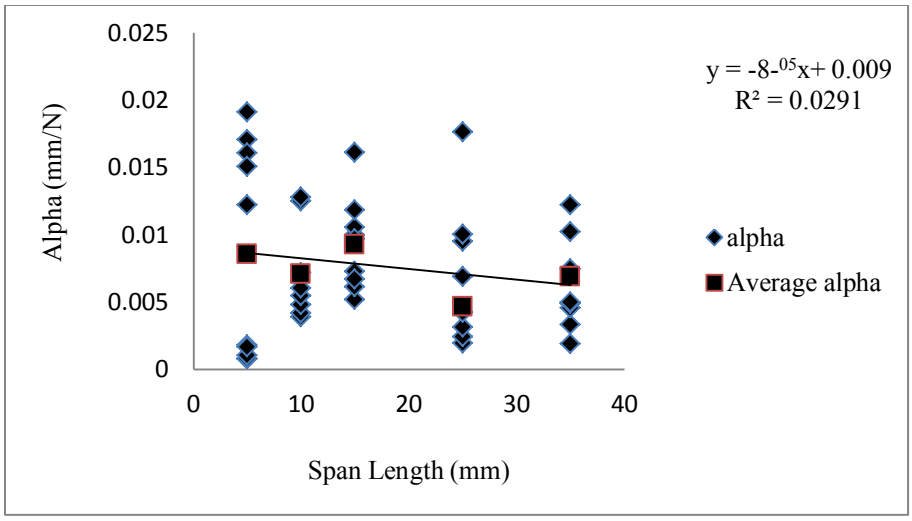

Figure 4.7 Line values of alpha in function of span length for bamboo fiber.

It observed from Fig 4.7 that alpha values also depend on the span length. Alpha values are decreasing with increasing the span length of bamboo fiber. Corrected Young's modulus and strain to failure were calculated by measuring alpha (α_i) values using the following newly developed equations (Subhankar 2010);

$$\Delta L_{total} = \Delta L_{fiber} + \Delta L_{grip} \quad (4.1)$$

Machine displacement (α_i) is calculated by using the following newly developed equations;

$$\alpha_i = \frac{\Delta L_{total}}{F} - \frac{\Delta L_0}{E_0 \times Ai} \quad (4.2)$$

Where,

$$\frac{\Delta L_{total}}{F} = \frac{\varepsilon \times L_0}{\sigma \times A_i} = \frac{1}{E} \times \frac{L_0}{A_i} \quad (4.3)$$

α_i is the machine displacement for each fiber, L_o is the original span length, E_o is the extrapolated Young's modulus, A_i is the cross-sectional area for each fiber, E is the Young's modulus for each fiber, ε is the strain, σ is the stress and F is the force.

Corrected strain to failure was calculated by using the equation 4.4. Young's modulus was calculated from the slope of corrected strain-stress curve.

$$\frac{\Delta L_{fiber}}{L_0}_{(Corrected)} = \frac{\Delta L_{total}}{L_0} - \frac{\Delta L_{grip}}{L_0} \quad (4.4)$$

Where

$$\frac{\Delta L_{grip}}{L_0}_{(Corrected)} = \frac{\alpha_i \times \sigma \times A_i}{L_0} \quad (4.5)$$

α_i is the line value of α_i (average value was taken from every span length). Subsequently the linear trend line was plotted and equation was obtained.

Bamboo fiber has better tensile strength and Young's modulus. This is mainly due to the fiber in bamboo is embedded in parenchymatous ground tissue, which can pass loads and distribute the stresses loaded on vascular bundle.

Analysis of strain to failure of raw fiber

Strain to failure was found to decrease with increase in span length, which is mentioned in Table 4.1. Figure 4.8 shows the tress- strain curves for uncorrected and corrected bamboo fiber. The cross sectional morphology of bamboo fiber is shown in Figure 4.2. It is observed that the bamboo fiber has a lot of lumens or porosity. Better tensile strength observed in the bamboo fiber may be due to the porosity and fiber is possessing better strain to failure.

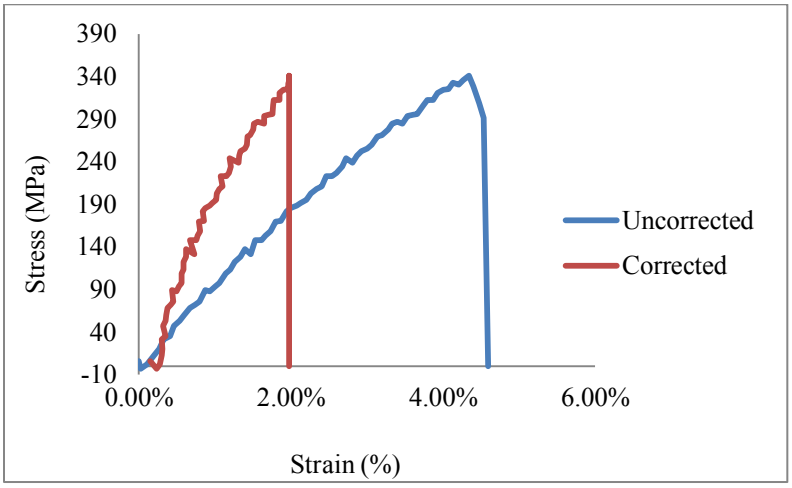

Figure 4.8 Stress- strain curves for uncorrected and corrected bamboo fiber.

4.1.2 Chemical analysis

Wet chemical analysis was conducted for bamboo culm. For chemical analysis T 207, T 222 om-98, T 412 om-94, T 429 cm-84, T 211 cm-99 method was used for determination of composition. Results from wet chemical analysis are given in Table 4.2. During chemical analysis, alpha cellulose was found to be 50.23±.18% indicating that homopolysacsride consist of β-D-glucopyranose linked together by β-1,4 linkage. Each cellulose monomer contained three hydroxyl groups that were able to form hydrogen bond for crystalline packing governing the tensile properties of cellulose of bamboo. Li worked on *Phyllostachys pubescens* bamboo and found 5.14% hot water solubility, 22.11% lignin, 70.84% holocellulose, 47.30% α-cellulose, 1.94% ash (Xiaobo, 2004). Ghoshal et al. worked on bamboo fiber and found 60% cellulose and 32% lignin (Ghoshal et al., 2011).

Table 4.2 Chemical analysis result from bamboo culm.

Sample	Hot Water Soluble %	Moisture%	Lignin %	Holocellulose %	α-cellulose %	Hemicellulose%	Ash%
Bamboo	5.07±0.06	12.33±0.56	23.91±0.58	67.08±0.17	50.23±0.18	16.85±0.09	1.38±0.05

4.1.3 Thermal analysis

Thermal decomposition of each sample took place in between a programmed temperature range of 10 to 550^{o}C. Most natural fiber loses their strength at about 160^{0}C. Thermal analysis of cellulose fiber was carried out and the effects of crystallinity, orientation and crosslinking on the pyrolytic behaviour of cellulose were observed. Thermal characteristics and properties of bamboo fiber are shown in Figure 4.9 and Table 4.3.

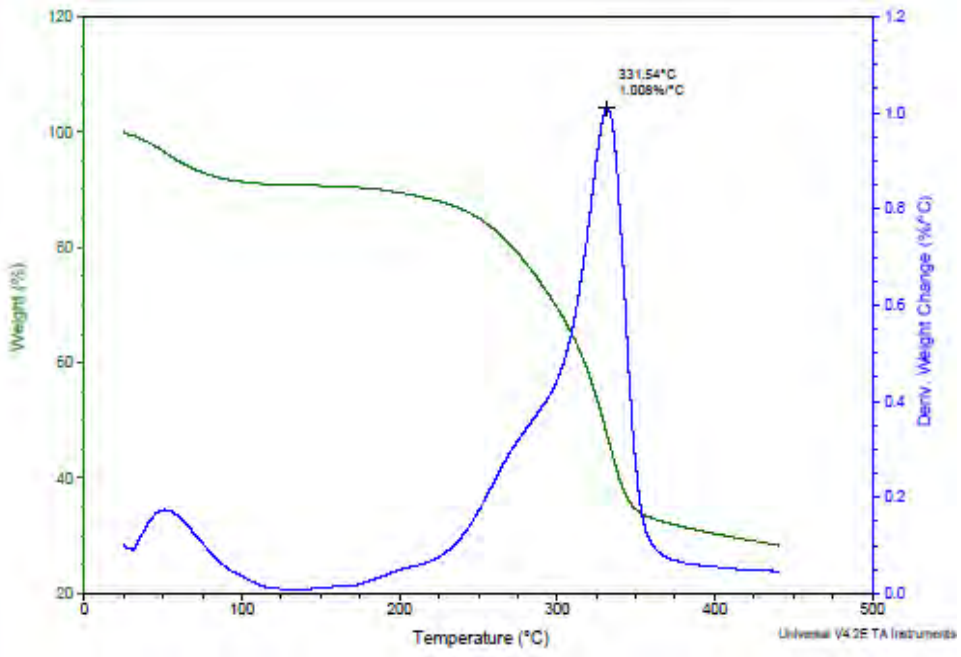

Figure 4.9 Thermogramme curve for bamboo fiber showing derivative weight change temperature at 331^{0}C.

Table 4.3 TGA analysis from bamboo culm.

Sample	Wt. change between 50-150^{0}C (%)	Wt. change between 150-300^{0}C (%)	Wt. change between 300-450^{0}C (%)	Derivative wt. change temp (%/^{0}C)	Residual wt. (%)	10%wt. loss temp (^{0}C)	50% wt. loss temp (^{0}C)
Bamboo	9.31	30.77	71.66	331.54	28.34	188.15	329.15

Bamboo itself behaves as a natural composite. The major source of thermal stability in cellulose of bamboo is due to hydrogen bonding, which allows thermal energy to be distributed over many bonds. Between 75 to 175^{0}C dehydration as well as degradation of lignin occurred and most of the cellulose was decomposed at a temperature of 350°C. Table 4.3 indicates that at temperature between 50-150^{0}C, 9.31% weight was lost. It indicated that at this temperature range only

dehydration took place. Dehydration of cellulose takes place in the amorphous region. The second peak at about 325^0C. 30.77% weight change between 150-300^0C indicates thermal degradation for depolymerisation of hemicellulose and the cleavage of glucosidic linkages of cellulose. The rate of thermal degradation between outer and inner layers of the cellulose fibrils in fiber particles present in samples may be significantly different. Consequently, complete pyrolysis took place in a relatively wider temperature band showing a broad decomposition peaks in 331^0C. In this temperature rage degradation of lignin and hemicellulose was taking place. At 300-450^0C, a major weight change is observed, which is 71.66%. In this temperature range, pyrolysis of 1,4 β linkage occurred. Table 4.3 is also indicating that 50% weight loss temperature is 329^0C. It is revealing that H- bond and 1,4 β linkage bond are very strong. For that cleavage of cellulose polymer change required more energy in thermal analysis.

4.1.4 XRD analysis

The methods of measuring the degree of crystallinity by X-ray diffraction techniques are based on the fact that the total coherent scattering intensity from assemblage of N atoms is independent of their state or aggregation. This is a direct consequence of the law of conservation of energy.
A natural fiber can be partially crystalline and partially amorphous. Partially crystalline polymers are customarily called crystalline polymers. Crystallinity index and the degree of crystallinity is important parameter for crystalline polymers (Fan et al. 2010; Akpalu et al. 2010). The physical and mechanical properties of polymers are profoundly dependent on the crystallinity index degree of crystallinity. It is well known that the degree of crystallinity can be determined by a variety of physical methods, for example, X-ray diffraction, calorimetry, density measurements, infrared spectroscopy (IR) and nuclear magnetic resonance (NMR). Determination of degree of crystallinity by X-ray diffraction has been claimed to be inherently superior to other methods (Zhishen et al. 1995; Chostian et al. 2010).

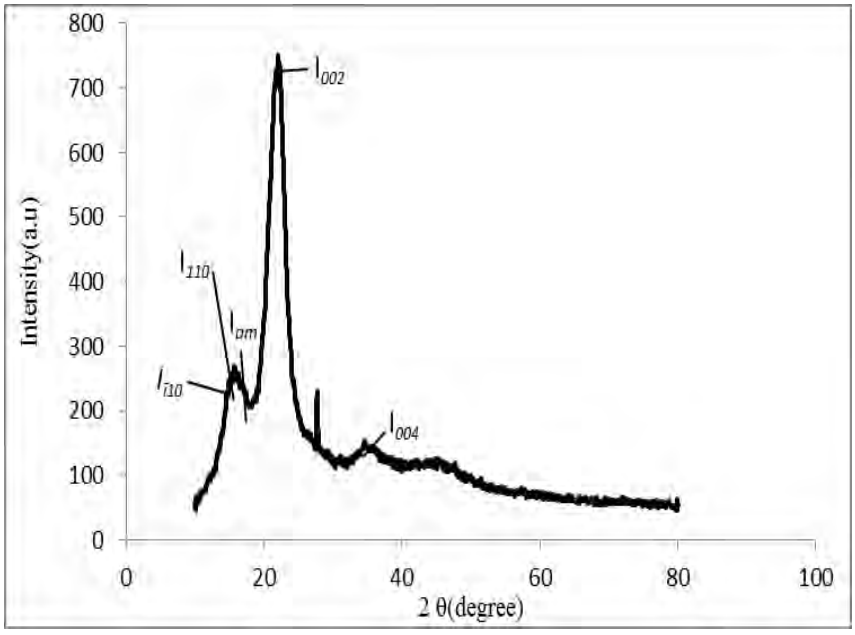

Figure 4.10 XRD study of raw bamboo fiber.

4.1.4.1 Crystallinity index (CI)

Percentage of crystallinity index (% CI) expresses the relative degree of crystallinity. The equation used to calculate the % CI was modified by Segal et al., in the following form:

$$\text{CI}\% = \frac{(I_{002} - Iam)}{I_{002}} \tag{4.6}$$

Where I_{002} is the maximum intensity (in arbitrary units) of the *002* lattice diffraction and I_{am} is the intensity of diffraction in the same as $2\Theta \sim 18^0$. During determination of % crystallinity index (% CI) of raw bamboo fiber from Figure 4.11 using Equation 4.06, the value has found 69.75%. Mahuya et al. found % of crystallinity in bamboo strip of 45.57% and in bamboo dust of 43.54% (Mahuya et al. 2012). Leolovich found 60-62% in natural soft and hard wood, 68-69% in cotton, 65-66% in flax (Liolovich 2008).

4.1.4.2 Degree of crystallinity

Total intensity of X-ray scattered by a given material is independent of the state of order, theory predicts it. This suggests that if one could partition the scattering into scattering arising from the

crystalline component and scattering arising from the amorphous component; it would be possible to measure the mass fraction of crystalline material, i.e., the degree of crystallinity (D. C). Ruland, in 1961, proposed a method for achieving this partitioning using equation 4.7. More commonly, approximately, calibrated methods of measuring crystallinity, Wc, are employed where

$$Wc = Ic / (Ic + k\ Ia) \quad (4.7)$$

Where K= 0.884 and the range of intensities is 10– 32^0 in 2Θ.

Degree of crystallinity for raw bamboo fiber is found to be 74.86%. Mahuya found 67.51% and 66.7% for bamboo strip and bamboo dust respectively (Mahuya 2012).

4.1.4.3 Microfibril Angle (MFA) *e*stimation obtained from XRD Method

Microfibril angle can also be estimated through X-ray diffraction measurement. The measurements were taken by using the diffraction intensity of bamboo samples. As shown in Figure 4.11, the angle T was obtained from the diffraction intensity around (002) arc and the angle can be calculated using an equation 4.08 proposed by previous workers, e.g. Cave (1966) and Cave's (1966) using and Yamamoto's (1993) using formula as follows:

$$MFA=0.6\ T \quad (4.8)$$

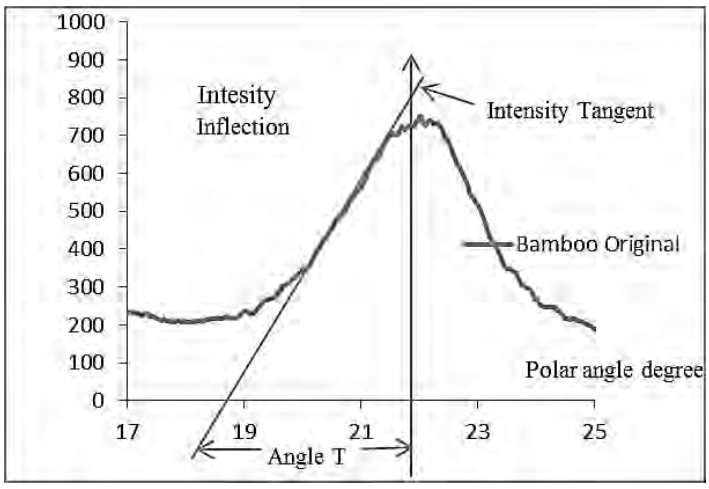

Figure 4.11 Measurement procedure of angle T from a (002) arc diffraction.

X-ray diffraction can provide a lot of information on bamboo ultrastructure. The relation between angle T and MFA was very good in order to estimate the secondary wall of bamboo. In this experiment MFA for bamboo fiber was found to be 3.90^0 (Table 4.4).

4.1.4.4 Crystallite size (C.S.) estimation obtained from XRD method

Measurements of crystallite size were made with the reflection technique using an X-ray diffractometer. Crystallite size was measured using equation 4.9. The crystallite size in the direction perpendicular to the 002 crystal using the Scherrer equation

$$L = 0.9\frac{\lambda}{HCos\theta} \tag{4.9}$$

Table 4.4 XRD result from raw bamboo culm.

Sample No	MFA	C.S (nm)	C.I %	D.C%
Original	3.90	2.44	69.75	74.86%

4.1.5 FTIR Analysis

FTIR spectrum of bamboo fiber is shown in Figures 4.12 to 4.16. Functional group region is 4000-1550 cm^{-1} and functional vibrate in this region with a definite wave number (Hazrat Ali 2013). Finger print vibration region is 1500-400 cm^{-1} and functional vibrate in this region with a definite wave number. Table 4.5 shows the main infrared transition of bamboo fiber.

Crystallinity Index

Intensities of some bands in IR spectra have been found to be sensitive to variations of cellulose crystallinity and have been used to evaluate degree of crystallinity (D.C.) of cellulose. The ratios of peaks at 1423 cm-1 and 896 cm^{-1}, 1368 cm^{-1} and 2887 cm^{-1} and 1368 cm^{-1} and 662 cm^{-1} are normally used to measure D.C. In this study, the ratio of 1368 cm^{-1} and 2887 cm^{-1} is above 1,

which seems to be unsuitable for evaluation, while the ratios of 1423 to 896 cm^{-1} and 1368 to 662 cm^{-1} are 74.86% and 49.3% respectively. The value calculated by using Segal empirical method is 75.6%, indicating that the ratio of 1423 to 896 cm^{-1} is more suitable for D.C. evaluation.

Infrared spectrum of bamboo fiber is displayed in Figure 4.12. The typical functional groups and the IR signal with the possible sources are listed in Table 4.05 for a reference. Figure 4.13 shows a weak absorbance around 1743 cm^{-1} in the FTIR spectrum of bamboo fiber, which might be attributed to the presence of the carboxylic ester (C=O) in pectin and waxes. Figure 4.13 is also showing the finger print region of bamboo fiber spectrum. Figure 4.14 is showing 1800-1600 cm^{-1} region of FTIR spectra. Figure 4.15 is showing 2400-2100 cm^{-1} region of FTIR spectra. Figure 4.16 is showing 4000-2400cm^{-1} region of FTIR spectra. In Figure 4.16 O3-H----O5 intramolecular H-bond and free O6-H & O2-H for weakly absorbed water are showing.

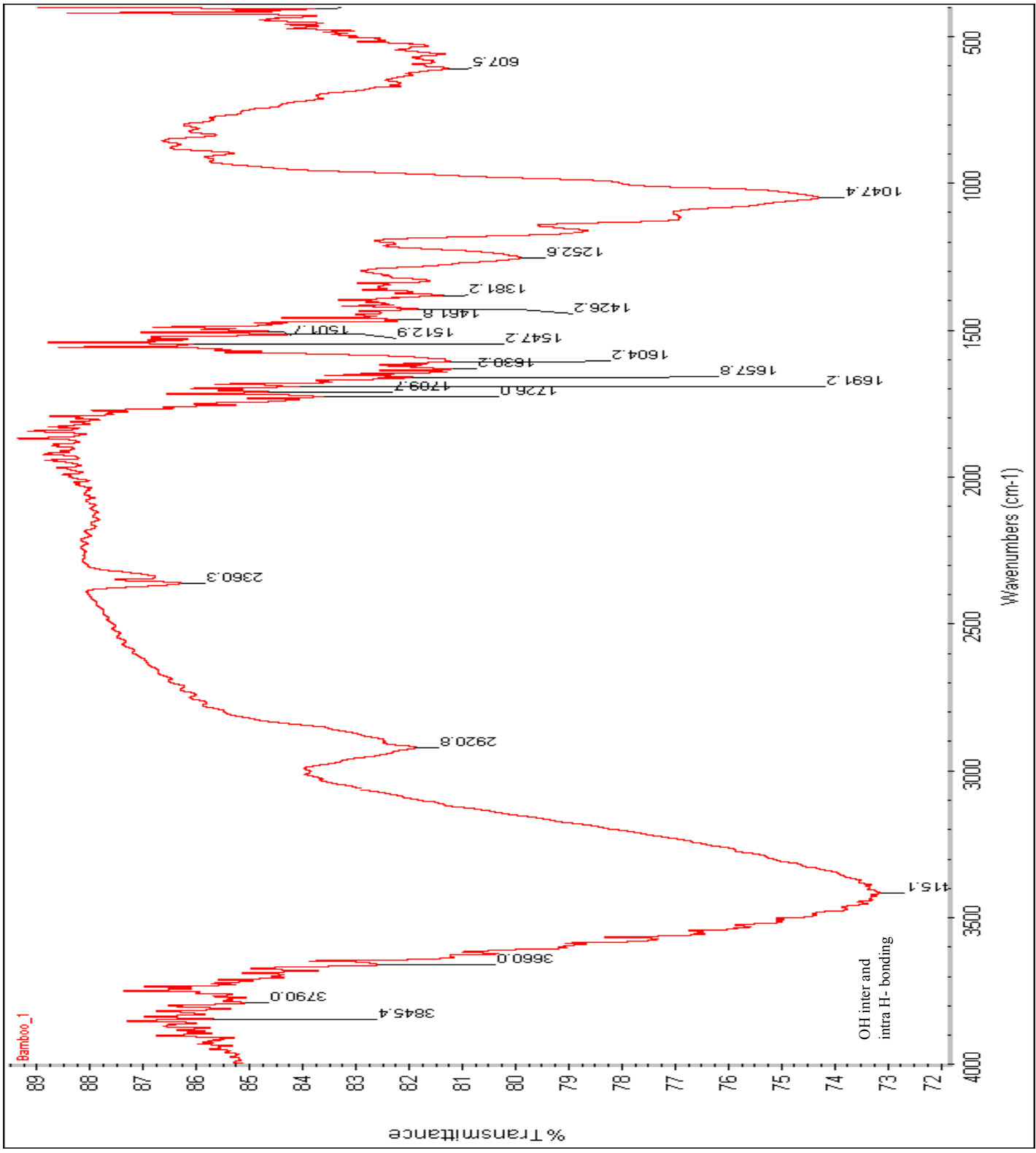

Figure 4.12 FTIR spectra of raw bamboo fiber indicating different functional group.

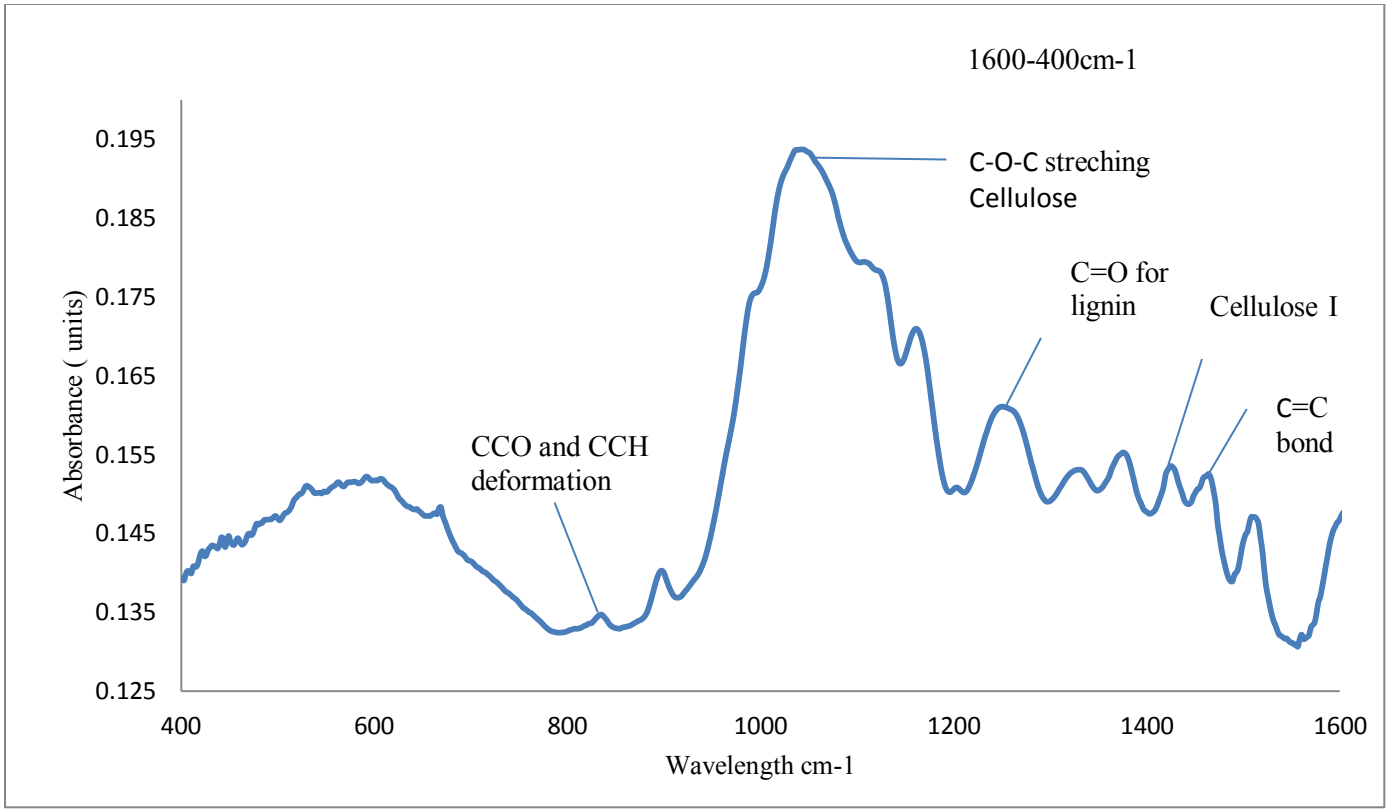

Figure 4.13 Finger print region of FTIR spectra of raw bamboo fiber.

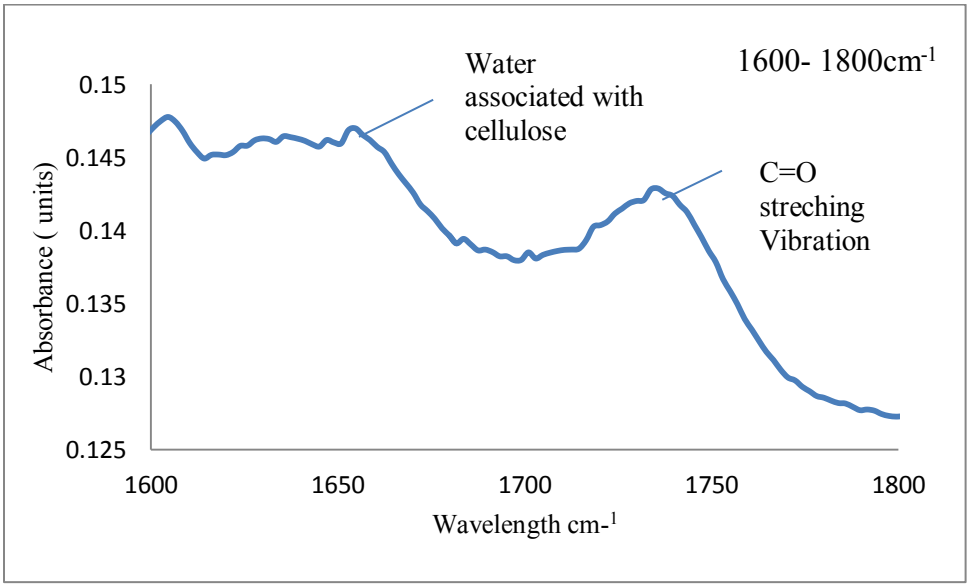

Figure 4.14 1800-1600 cm^{-1} region of FTIR spectra of raw bamboo fiber.

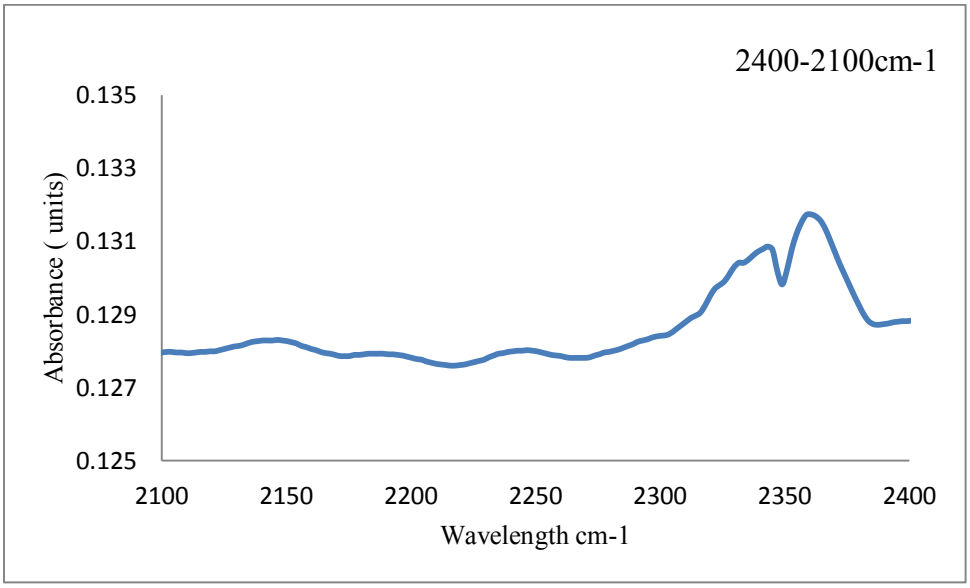

Figure 4.15 2400-2100 cm^{-1} region of FTIR spectra of raw bamboo fiber .

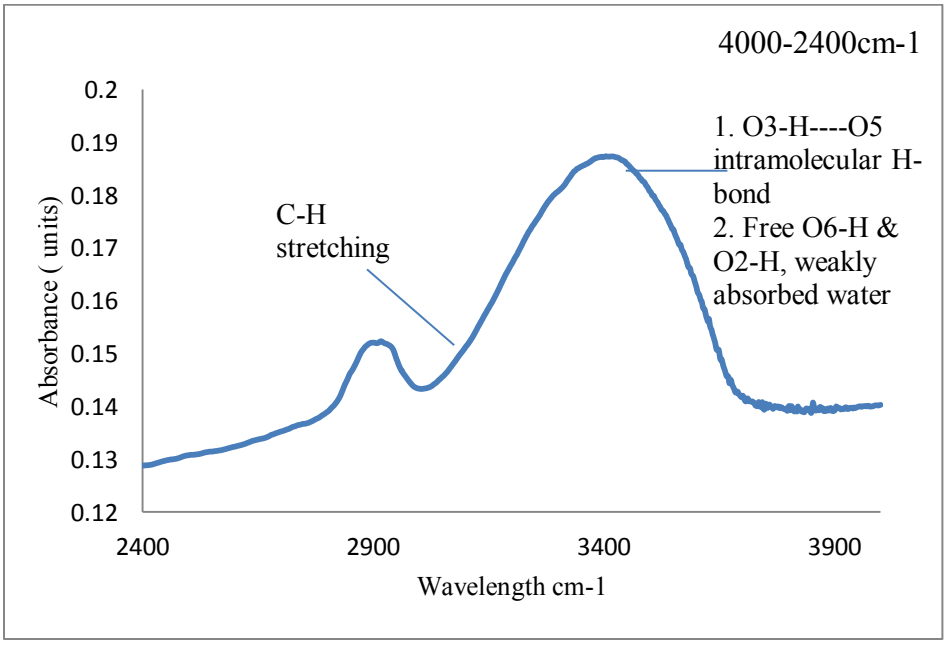

Figure 4.16 4000- 2400 cm^{-1} region of FTIR spectra of raw bamboo fiber.

Table 4.5 Main infrared transition for bamboo fiber.

Wave number (cm-1)	Band origin	Short comments
3,336	OH stretching	Cellulose, Hemicellulose
2,887	C–H symmetrical stretching	Cellulose, Hemicellulose
1,729	C=O stretching vibration	Pectin, Waxes
1,623	OH bending of absorbed water	Water
1,524	N–H deformation	Secondary amide (upward direction)
1,510	Aromatic skeletal vibration plus C=O stretch	S > G; Upward direction ,G condensed>G etherified
1,506	C=C aromatic symmetrical stretching	Lignin
1,505	Same as peak 1,510	Downward direction
1,496	C=S stretching –N–C=S	(downward direction)
1,485	C=S stretching –N–C=S	(upward direction)
1,286	Amide III Protein	(upward direction)
1,270	Guaiacyl ring	Breathing Present in both factors, downand upward direction in first and second factor loading respectively.
1,251	C–O stretching CH_3COOR	acetic ester (upward direction)
1,246	C=O and G ring stretching	Lignin
1,227	C–C plus C–O plus C=O stretch; G condensed > G etherified	Downward direction
1,202	C-O-C symmetric stretching	Cellulose, Hemicellulose
1,197	C–O–C, C–O	Dominated by ring vibration of carbohydrates
1,496	C=S stretching –N–C=S	(downward direction)
1,485	C=S stretching –N–C=S	(upward direction)
1,270	Guaiacyl ring breathing Present in both factors.	Downward and up ward direction in first and second factor loading
1,238	C–O stretching	Downward direction
1,208	C–N stretching vibration	Aliphatic amine(upwards direction)
1,155	C-O-C asymmetrical stretching	Cellulose, Hemicellulose
1048, 1,019, 995	C-C, C-OH, C-H ring and side group vibrations	Cellulose, Hemicellulose
896	COC,CCO and CCH deformation and stretching	Cellulose
662	C-OH out-of-plane bending	Cellulose
490	Asymmetrical vibration of O=C-C=O	Cellulose

4.1.6 Water absorption test

Water uptake tests of the bamboo fiber (about 500 mg) were performed in de-ionized water at room temperature (25^0C) upto 120 minutes. Bamboo fiber samples were placed in static glass beakers containing 100 ml of deionized water. At set time points, samples were taken out and dried for 6 hours at 105^oC and then reweighed.

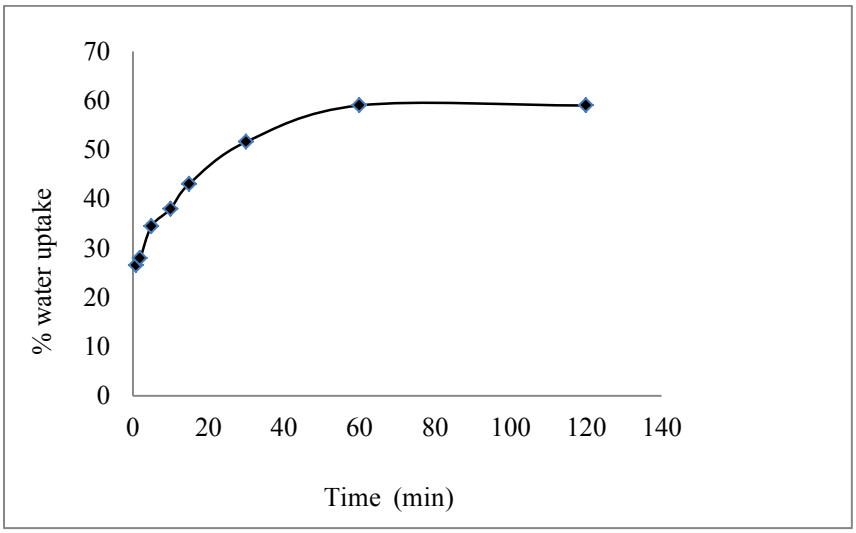

Figure 4.17 Variation of water uptake (%) by raw bamboo fiber with time in aqueous media at room temperature (25^0C).

Water uptake was measured by soaking the samples of bamboo fiber in a static glass beaker contained deionized water at room temperature (25^0C) for 120 min. The results are presented in Figure 4.17. It was found that bamboo absorbed water in a typical manner that is, initially there was very rapid gain of water and then the absorption became slower and static with time. For example, after 1 minute of immersion in water, jute absorbed 26.50% of water, but 37.98% and 59.01% of mass was gained after 10 and 60 min, respectively (Ruhul et al. 2009). In bamboo fiber after 1 minute of immersion in water, it absorbed 19% of water, but 78% and 93% of mass was gained after 10 and 60 minutes respectively. Basically bamboo and jute absorbs most of water after 10 minute of immersion in water. Bamboo and jute is mainly built up of cellulose, which is a hydrophilic glucan polymer. The elementary unit of bamboo is anhydro-d-glucose, which contains three hydroxyl (–OH) groups. Due to the presence of pendant hydroxyl and polar

groups in various constituents of fiber, moisture absorption of fiber is very high. These hydroxyl groups in the cellulose structure account for the strong hydrophilic nature of bamboo and jute and as a result, within an hour, bamboo and jute absorbs such a huge amount of water. Lignin decreases the permeability and degradability of walls and is important in determining the mechanical behaviour of predominantly non-living tissues such as wood. For that reason water uptake was become static.

4.1.7 Biodegradation test

The amount of weight loss in water of bamboo fiber was increasing with time which is mentioned in Figure 4.8. At the initial stage the rate of degradation was very slow. After cleavage-induced in crystallization, the rate of degradation was increased sharply in fiber sample. This is may be due to the lignification. Structure of bamboo is made of alternate crystalline and amorphous phases. A single chain may enter multiple crystal and amorphous domains. The crystalline phase is primarily composed of chain segments in ordered conformation, whereas the amorphous phase contains chain ends, entangled chains and segments in some disordered conformation. During degradation, it has been reported that the hydrolysis process consists of two major mechanisms. In the first mechanism, water molecules diffuse into the amorphous region, resulting in scission of some disordered chains. The densely ordered crystalline phase, which is more difficult for water to penetrate, stays largely unaffected. As water molecules react with the amorphous chain segments, these cleaved disordered chains can disentangle as their mobility is significantly improved. The additional degree of freedom facilitates the formation of new crystalline regions and increases the overall crystallinity. This phenomenon is termed ‘cleavage-induced crystallization’. As a result, the crystallinity will reach a maximum, which marks the initiation of the second mechanism (Mahuya et al. 2009).

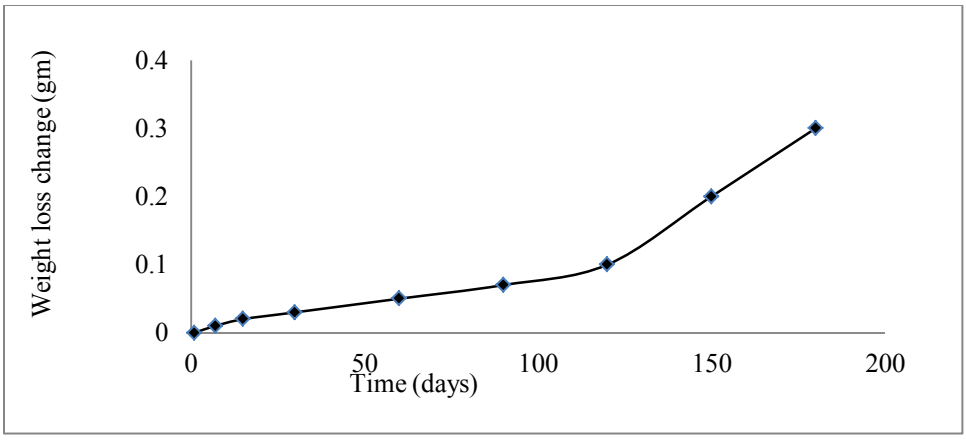

Figure 4.18 Variation biodegradability test in terms of weight loss by raw bamboo fiber with time in aqueous media at room temperature (25^0C).

Water molecules can slowly attack the crystalline phase resulting in chain segments small enough to be water soluble and susceptible to metabolism. It is conceivable that the weight loss of amorphous phase during degradation can also contribute to the increase in crystallinity observed in the early stages of degradation (Bruce et al. 2002). Phenolic polymer lignin incorporated a three dimensional space between cell wall microfibrils is termed lignification. After the cleavage in three dimension network the degradation rate increased.

4.1.8 Soil degradation test

In the soil degradation test at first the degradation rate was very slow. After 30 days rate became very fast because of presence of microorganism. As bamboo fiber is biodegradable for that it degraded very easily in the soil. Figure 4.19 shows weight loss by soil degradation test by soil buried process.

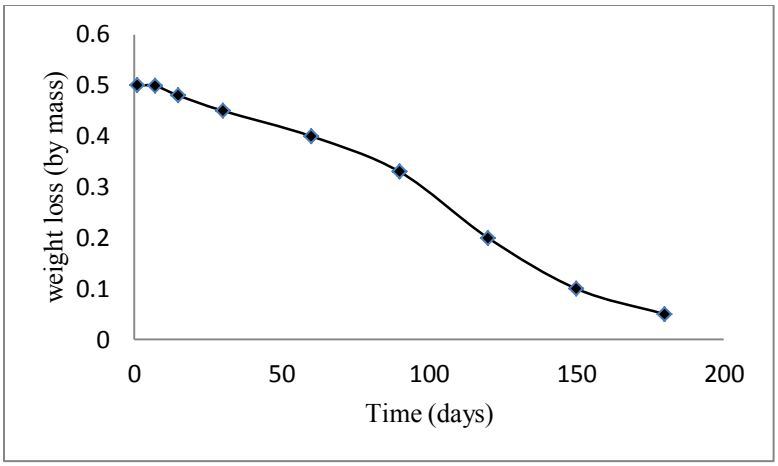

Fig 4.19 Weight losses in soil degradation test by soil buried of raw bamboo fiber.

4.1.9 Optical microscopic test

The bamboo fiber treated with copper (II) nitrate solutions to observe the orientation of meso fiber. The orientation of meso fiber can be detected under light microscope. However, it was found that the orientations of MFA in the samples treated with the Cu solution were much more distinctive. This may result in more accurate measurements of MFA. An example of microfibril orientations in S2 layer in bamboo observed under light microscope at 100 times magnification is given in Fig 4.20. It was found that, microfibrils in S2 layer layer have a Z-helical orientation; while in S1 layer have S-helical orientation. The average MFA in S2 inner layer is 3.98±0.10° for bamboo fiber, which is smaller than 2.65° measured for hemp previously by Dasong (Dasong et al 2010). This may be due partly to the different bamboo fiber from different geographical sources.

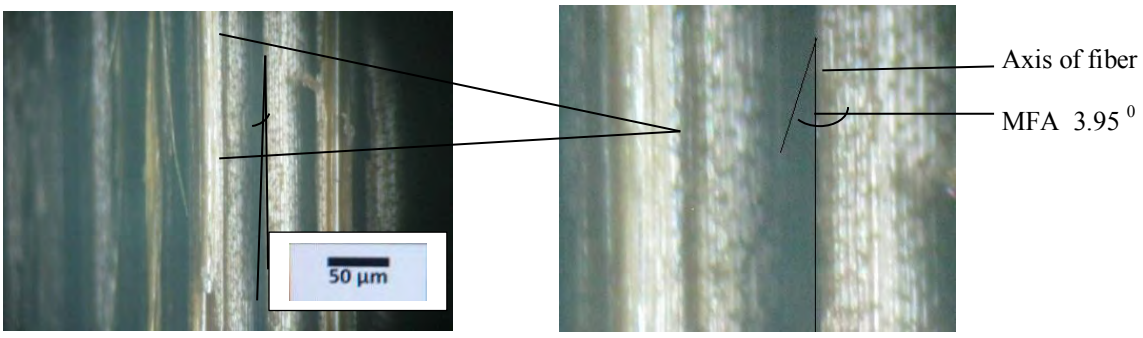

Figure 4.20 Microfibril angle of raw bamboo fiber: MFA in S2 layer.

The average MFA in the outer part of S2 layer ranges from 2° to 10° which is in agreement with the results of previous worker (Prodeep et al. 2010). MFA measured from the XRD and Optical microscope was found to very similar. The result of MFA has given in Table 4.6.

Table 4.6 MFA measurement from XRD and optical microscope.

Sample name	Microfibril angle (MFA deg)	MFA (XRD)
Bamboo	3.95±0.10	3.90±0.09

4.1.10 Dislocations in bamboo fiber

Dislocations in bamboo fibers were studied for observing the dislocations. Dislocations were found in bamboo fiber, which are marked in the Figure 4.21. Some natural fiber contains dislocations i.e. region where cell structure differs from that of the surrounding cell wall. Dislocation is the irregular region within the cell wall in the living plant. It has also been called slip plane or nodes. Dislocations often affect only the inner secondary wall and not the outer primary wall. The exact structure and composition of dislocation is still remaining unknown. They are assumed to contained cellulose, hemicelluloses and lignin like the rest of the secondary cell wall. Traditionally dislocations are considered to contain cellulose in contrast to the cell wall. But now a day dislocation it has been proof that cellulose micro fibrils continue through the dislocation i.e. dislocation may have a less 'ordered' and/or may 'loose' order, but they are not places where mocro fibrils are discontinuous. Dislocations are known to bind more ligand molecule better than the surrounded cell wall. Other studies have been shown that dislocations are more susceptible/ reactive than the surrounding cell wall i.e. they are in a sense the weak spots of the fiber (Thygesen 2010). For dislocations fiber are seen to break into segments at the dislocations.

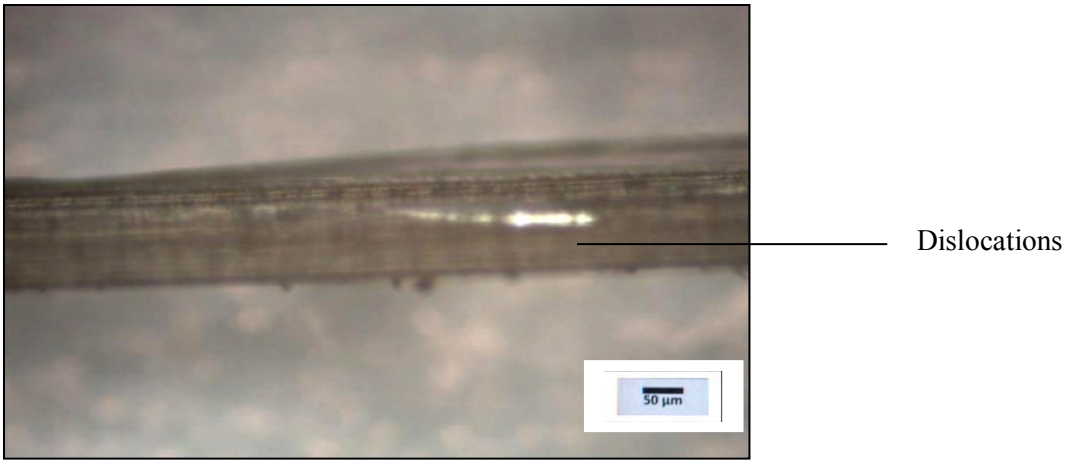

Figure 4.21 Optical image of dislocations in raw bamboo fiber.

4.1.11 Fiber length test

Bamboo fiber was delignified and fiber length was meassured and found 2.38±0.57 mm. Bambooo fiber was found to be flattened and untwisted. Bamboo fiber is medium length fiber. Cellulose is a linear, stereo-regular polysacride built from repeated D-glucopyronose units linked by 1,4-β glycoside bonds. The later size of the cellulose chains is about 0.3nm. The degree of polymerization of native cellulose from various origins can fall in the range 1000 to 30,000, which corresponds to chain lengths from 500 to 15000 nm. Cellulose is located within the fiber walls of plants. One fiber is an elongated vegetable cell. Fiber of various plants have different shapes and dimensions. fiber of cotton and blast plants are enough long, with length in the cm. while the wood are short 1-3mm in length. Cotton fiber are twisted while the wood fiber are generally untwisted and are flattening when delignified. Flex and remie are straight and round (Michel 2008). A typical optical image delignified bamboo fiber is shown in Fig 4.22.

Figure 4.22 Optical image of delignified raw bamboo sample for fiber length determination.

4.1.12 Image analysis

Through the application of the Digital Image Analysis (IA) method the properties of bamboo was established. Appropriate calculation was developed to present the fiber distribution across the thickness of the cross-section. These calculations allow the designer to calculate the solid phase of bamboo with some degree of precision. In this experiment, 66.70% solid phase was observed and others are vacuum phase. In terms of area, it was 242166.302 sq. micron.

Increasing the application of bamboo as structural elements requires profound scientific knowledge about its behaviour in nature, considering its macro, meso and microstructures. From the structural mechanics point of view, bamboo acquired several natural geometries mainly in order to counteract wind load and the own weight. These characteristics turn it into one of the best materials/structures for the requirements of compression-deflection. A conical form alone the culm, an approximately circular transversal section, a hollow form in most species, which reduces its weight, a functionally gradient rigidity of its cross-section to deflection in the radial direction among others.

.

In this paper it has been shown that image analysis provides a reliable method for establishing the meso-structure of bamboo. Studies are underway to establish the form of the vascular bundles of different types of bamboo through which the species of bamboo can be recognized. SEM images of raw bamboo fiber and void phases are shown in Figure 4.23.

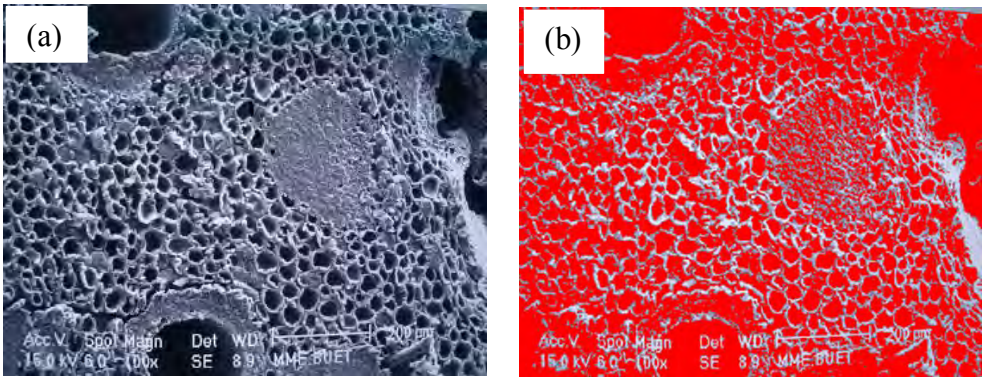

Figure 4.23 Scanning electron micrograph showing solid phase (a) raw fiber image (b) void phases are shown in red color.

4.2 Physical modification

4.2.1 Physical modification using gamma radiation

4.2.1.1 Tensile properties

The values for tensile strength, uncorrected and corrected Young's modulus and strain to failure of irradiated and raw technical bamboo fiber are shown in Figures 4.24 to 4.27. Figure 4.24 shows the tensile strength of for raw and irradiated bamboo fibers. From figure it can be concluded that with increasing the radiation, the tensile strength increased. However after 50 KGy radiation, the tensile strength was found to decrease.

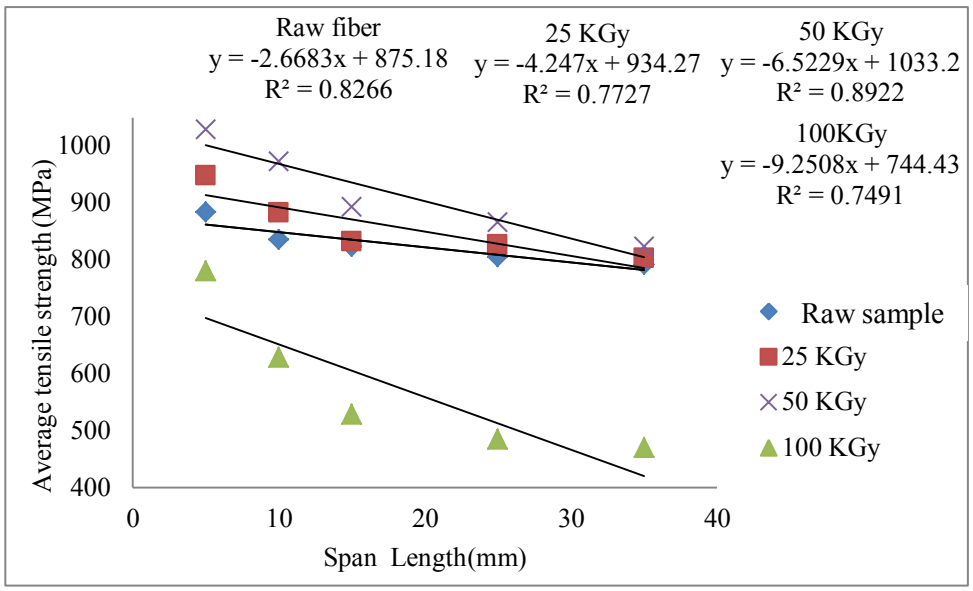

Figure 4.24 Average tensile strength of different irradiated sample vs span length.

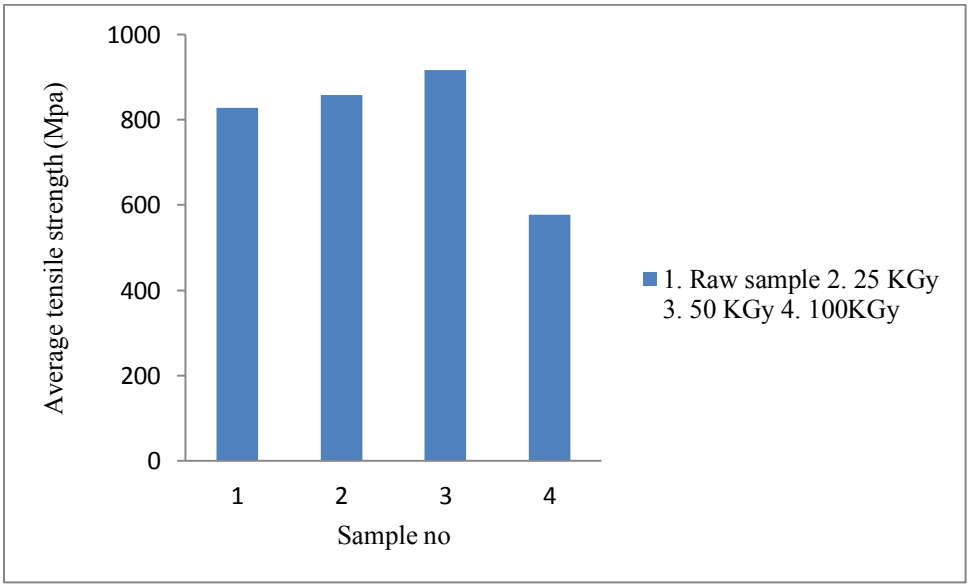

Figure 4.25 Average tensile strength of 1) raw bamboo fiber 2) 25 KGy 3) 50 KGy and 4) 100 KGy irradiated sample.

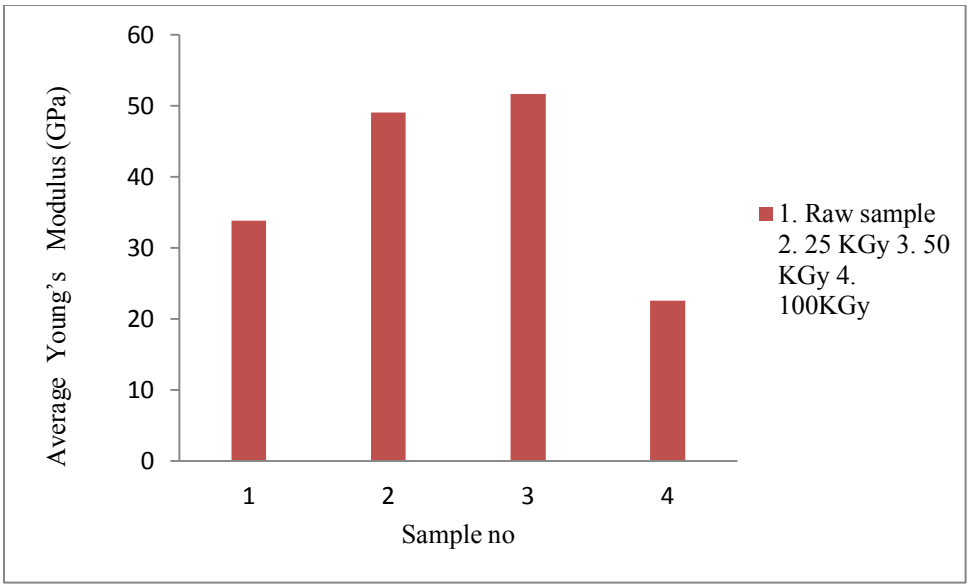

Figure 4.26 Average corrected Young's modulus 1) raw bamboo fiber 2) 25 KGy 3) 50 KGy and 4) 100 KGy irradiated bamboo fiber sample.

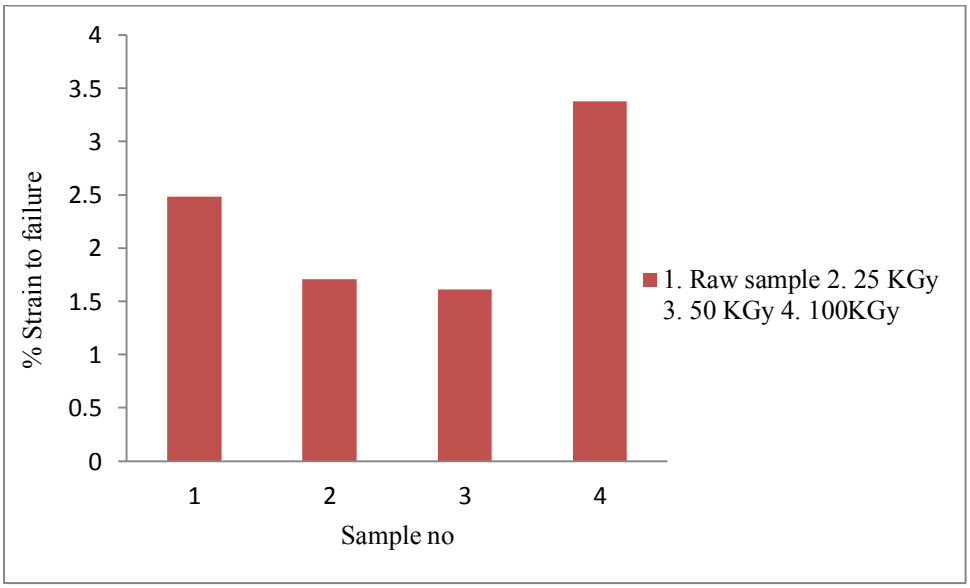

Figure 4.27 Average strain to failure vs 1) raw bamboo fiber 2) 25 KGy 3) 50 KGy and 4) 100 KGy irradiated bamboo fiber sample.

The effects of gamma radiation on the mechanical properties (Young's modulus and strain to failure) of bamboo fiber were also monitored. The results are shown graphically in Figures 4.26

and 4.27. Gamma radiation has influenced the polymeric chain of cellulose in natural fiber. This has been extensively studied over the past few decades. Gamma radiation is an ionizing radiation. As a result it deposits energy in solid surface of cellulose by Compton scattering. Gamma radiation also localizes energy within molecules produced, which trapped macrocellulosic radicals. For that reason radicals were generated that is responsible for changing the physical, chemical and biological properties of cellulose fiber. Tensile strength was found to increase from raw sample to 25 KGy irradiated sample. 50 KGy irradiated sample was found to have highest tensile strength and in 100 KGy irradiated sample found to decrease the tensile strength than the raw sample. This is may be due to gamma irradiation in the bamboo fiber. Up to 50 KGy radiation may be the surface energy on the bamboo fiber has increased and produced radicals which gave rise of reactive sides. As a result crosslinking occurred and increased up to certain level of radiation doses. The possible reaction mechanism may be explained that radical are produced by gamma radiation on the cellulose chains by hydrogen and hydroxyl abstraction as explained in Figure 3.14. This property can be attributed by occurrence of irradiation-induced crosslinking which is explained by several authors (Haydaruzzaman 2009; Sarawut 2012; Mokhtar 2002; Ratnam 2002).

From Figure 4.25, it is clear that increase of total gamma radiation dose, the TS of bamboo fiber increased from 827 MPa (indicated as raw sample) to 915 MPa and then decreased to 577 MPa at 100 KGy. Young's modulus has increased to 45% and 54% at 25KGy and 50KGy respectively, and then decreased 29% at 100 KGy due to irradiation on cellulose. Better tensile strength and Young's modulus was observed because of increase of surface energy. Bamboo culm comprises about 50% fiber. Fiber percentage is higher, which contributed to its superior slenderness and strength. Most fiber has a thick poly-lamellate secondary wall. In bamboo, fiber is either grouped in bundles or sheaths around the vascular bundle. This gives the high tensile strength to the bamboo fiber. When fiber was irradiated then poly-lamellate secondary walls of cellulose became closer and bear the tensile load with more fiber. As a result the strength and Young's modulus increased. At higher radiation dose, the main chain may be broken and polymer may degrade into fragments. During irradiation strength was lost due to primary bond breakage in the cellulose constituents. It results reduce in degree of polymerization. For that

tensile properties decreased with higher radiation (Hassan 2003). From present study it can be concluded that gamma radiation and anatomy are correlated to tensile properties.

The cross sectional view of technical bamboo fiber and irradiated fiber are shown in Fig 4.28. Lumens and porosity was found to be more compact compared to the raw sample. Similar observation was found in xylem and protoxylem vessels and phloem. As fiber possesses high strength and strain to failure, radiation made positive effect on the strength. The anatomy and physical properties of bamboo culms have been known to have significant effects on their durability and strength. The fibers constitute the sclerenchymatous tissue and occur in the internodes as caps of vascular bundles or isolated strands.

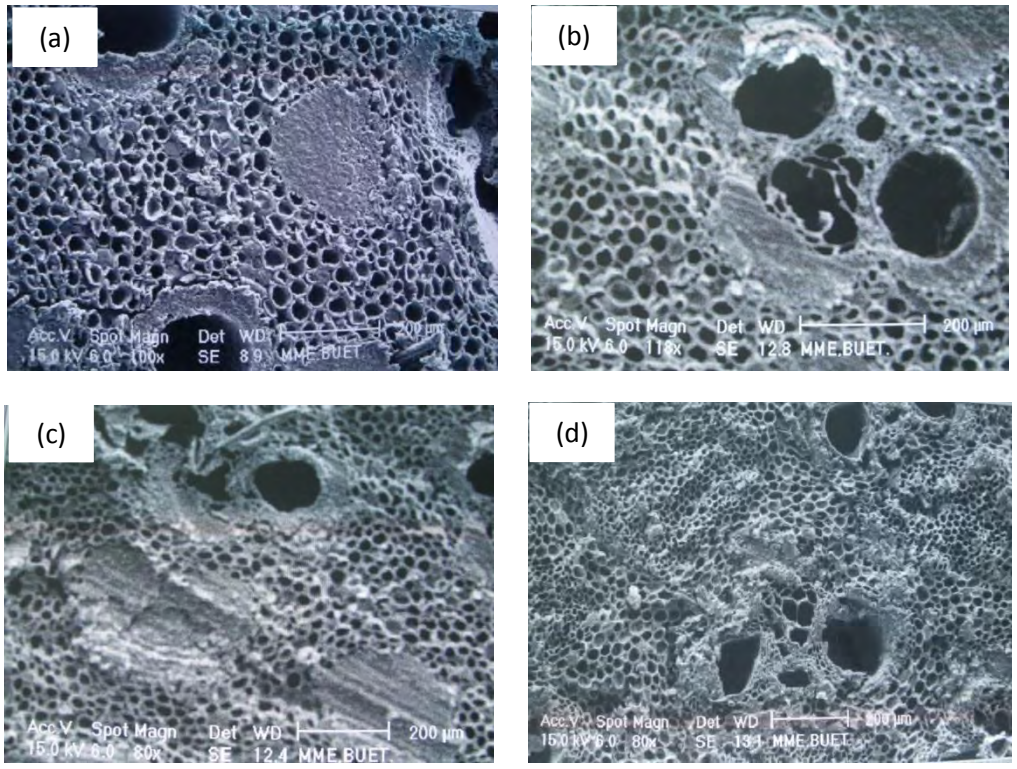

Figure 4.28 Scanning electron micrograph of cross-sectional views of (a) raw, (b) 25 KGy irradiated, (c) 50 KGy irradiated and (d) 100 KGy irradiated bamboo samples showing the more impact on radiation in schlerenchyma and parenchyma cell.

Due to irradiation, the sclerenchymatous tissue became more compact bearing load with increasing radiation. However due to chain scissoring at higher radiation, the tensile strength

became lower. Cellulose has become small fragments and strength is lower. In Fig 4.27 the strain to failure has shown as a function of raw and irradiated sample. Lower strain to failure was observed at higher radiation. But at higher radiation strain to failure was low. This can be explained that at higher radiation due to breaking of cellulose chain the total load is transfer to the matrix. Here lignin acted as matrix. Lignin is phenyl propane and organic substance with covalent bond. As a result, when force was applied, sharing of electron before going to plastic deformation lignin occurred. As a result strain rate was very high. Again from the cross-sectional morphology of raw and irradiated bamboo fiber observed under SEM, It is clearly observed that bamboo fiber is a technical fiber.

During primary wall formation, most fiber was bi-nucleate or multi-nucleate contributing to their elongation, which might be related to amitosis. During secondary wall formation, fiber wall undergo dominant thickening during the first 4 years and then the degree of wall thickening decreased gradually with the thickening of secondary wall. During primary wall formation, a fiber successively exhibits co-growth with vascular elements and intrusive growth. At this stage, fiber maintained its cylinder form and partly elongated coupled with radial extension and elongation of vessel elements (Walter, 1992). Bi-nuclei or multinuclei cells were observed with a dense protoplast and smaller vacuole. Following that fiber with bi-nuclei or multinuclei was gradually vacuolated and in parallel way arranged which is shown in Figure 4.29 in surface morphology of bamboo fiber.

Normally, sclerenchyma fiber have high strength and modulus of elasticity (MOE), while parenchymatous ground tissue has low strength and MOE and high capability of deformation. Therefore, in view of mechanical behaviour, the bamboo can be simplified as a composite of parallel connection model composed of two elements that are fiber and parenchymatous ground

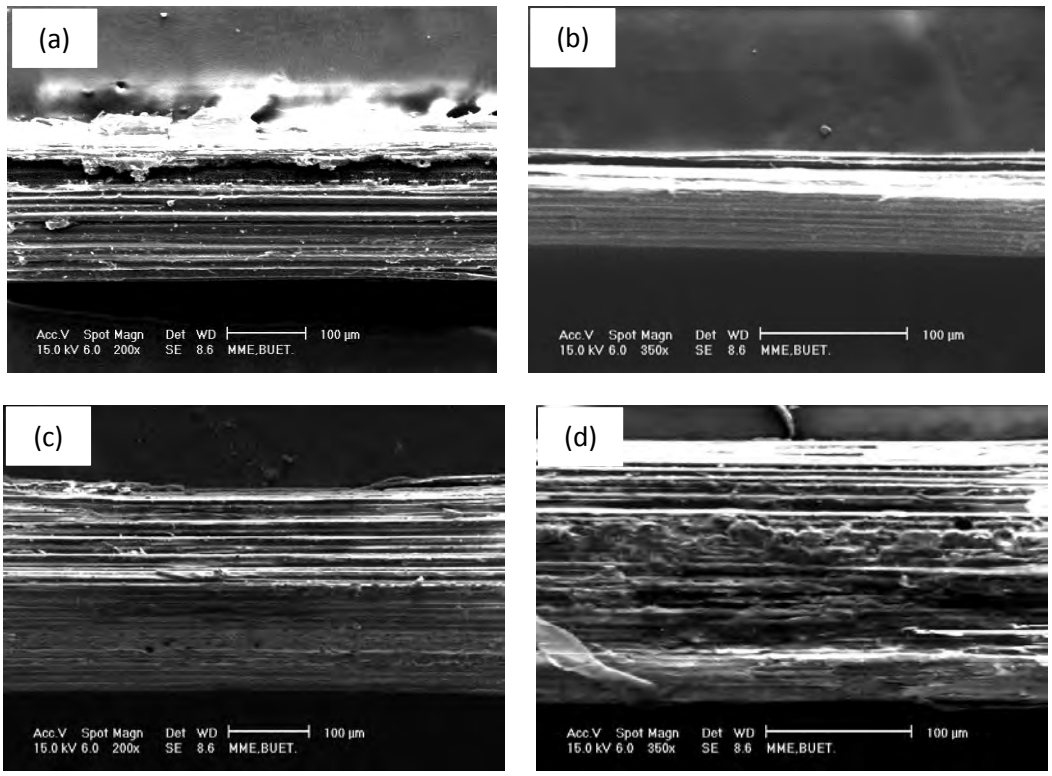

Figure 4.29 Scanning electron micrograph of (a) raw, (b)25 KGy irradiated, (c)50 KGy irradiated and (d) 100 KGy irradiated bamboo samples surface were smoother up to certain doses.

tissue, as shown in Figure 4.3 (Zhuo et al. 2010). When bamboo fiber was irradiated, amorphous region in the cellulose chain tried to become more aligned with the crystalline region as shown in Figure 4.30.

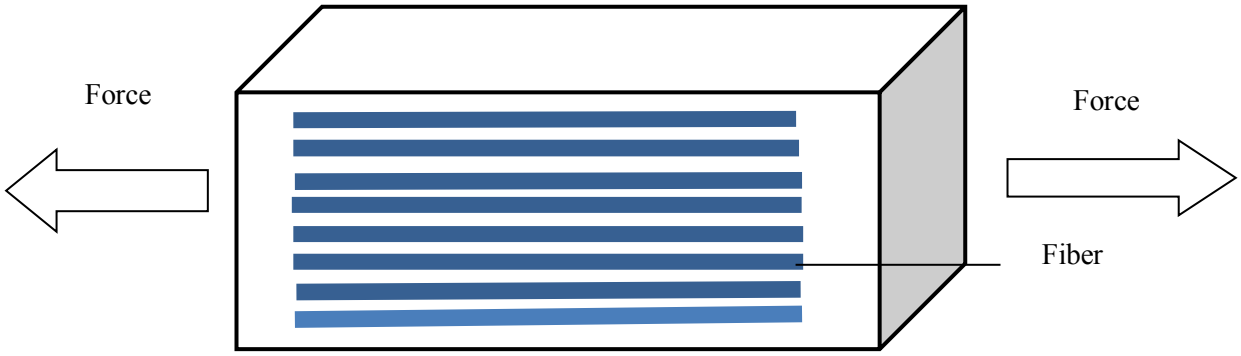

Figure 4.30 Schematic representation of a simplified parallel connection model of bamboo fiber and parenchymatous ground tissue (Zhuo et al. 2010).

When load was applied, it was carried by aligned cellulose. With increase in the radiation, chain opening took place. As a result crystalline phase decreased. For that reason at higher radiation dose (100 KGy), the mechanical strength decreased. But for strain to failure, at lower radiation dose crystallinity of fiber increased and as result rigidity developed and lower strain to failure was observed. In the case of higher radiation the chain opening broke the crystalline chain. As a result, amorphous region of cellulose bear the load. When load was applied the amorphous regions, they became more elastic and showed high strain to failure.

4.2.1.2 Chemical analysis of physically irradiated technical bamboo fiber

Chemical analysis was conducted for various raw and irradiated technical bamboo fiber samples. No significant change was observed in chemical analysis results for raw and radiated samples. However changes in mechanical properties were observed with increase in irradiation. This may be attributed to a change in interatomic spacing within the amorphous and crystalline regions, which is evidence of the interaction of disorder results in mechanical properties (Zaher 2001). The ash (%) was found to be decreased with increasing the dose of radiation. Table 4.7 is showing the chemical analysis results of raw and irradiated bamboo fiber samples.

Table 4.7 Chemical analysis resulta of raw and irradiated bamboo fiber samples.

Sample		Hot Water Soluble (%)	Moisture (%)	Lignin (%)	Holocellulose (%)	α-cellulose (%)	Hemicellulose (%)	Ash (%)
Raw Sample		5.07±0.06	12.33±0.56	23.91±0.58	67.08±0.17	50.23±0.18	16.85±0.09	1.38±0.05
Irradiated	25 KGy	4.13±0.06	12.33±0.56	23.91±0.58	67.45±0.43	50.93±0.21	16.52±0.09	1.15±0.03
	50 KGy	5.00±0.06	13.52±0.56	23.77±0.78	66.58±0.40	51.11±0.27	14.47±0.09	0.45±0.03
	100 KGy	5.21±0.06	12.33±0.56	23.91±0.58	66.76±0.17	50.07±0.35	16.69±0.09	0.93±0.05

4.2.1.3 Thermal analysis of irradiated technical bamboo single fiber

In order to observe the thermal stability, Thermogravimetry analysis (TGA) was conducted for raw and irradiated bamboo fiber. TGA can help in understanding the degradation mechanism and must assist any effort to enhance the thermal stability of a polymeric material. The threshold decomposition temperature of composite indicates the fabrication temperature. The thermal degradation of natural fiber has received considerable attention in the past years. This is due to the effects of crystallinity, orientation and crosslinking on the pyrolytic behavior of cellulose fiber (Shehrzade 2003; Kazuhiro et al. 2000).

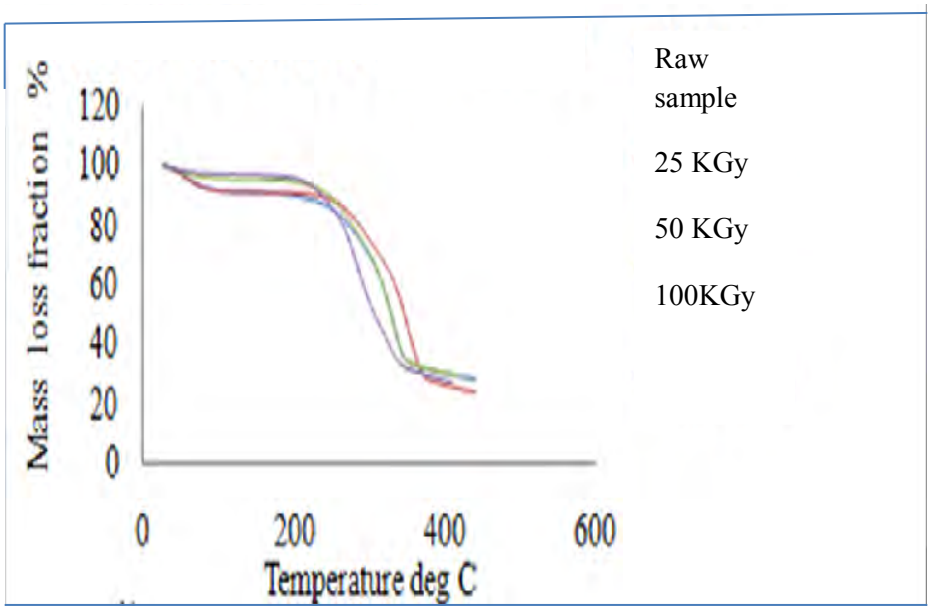

Figure 4.31 TGA results of raw and irradiated bamboo fiber.

From Figure 4.31 it can be seen that, in the irradiated sample, a decomposition step is observed between $(230\text{-}300)^0$C. This decomposition at $(230\text{-}300)^0$C temperature range was not observed in raw bamboo fiber sample. The decomposition is due to the hemicellulose. In the irradiated sample, radiation affected the hemicellulose by making it crystallize chain. When the sample was heated then energy required to break down the chain of hemicellulose. But in the case of raw sample hemicellulose was almost merged with α- cellulose.

Almost 50% weight loss occurred at 331^{0}C, 350^{0}C, 350^{0}C and 341^{0}C for raw, 25 KGy, 50 KGy and 100 KGy radiated bamboo samples. Such weight loss is mainly due to the thermal decomposition involving discharge of CO_2, CO and H_2O from hemicelluloses. Hemicellulose is containing C, O, H which are forming CO_2, CO and H_2O. Lignin soften at (230-300)^{0}C, but unlike cellulose, the softening temperatures of these amorphous components undergo a marked fall with moisture content due to the cleavage of ester bond between lignin and hemicellulose during heat treatment, in addition to the cleavage of inter monomer linkage (b-O-4 linkage) (Shunliu et al. 2009). Table 4.8 is showing the derivative weight change measurement from TGA for raw and irradiated bamboo fiber.

Table 4.8 Derivative weight change measurement from TGA for raw and irradiated bamboo fiber.

Sample		Wt. change between 50-150^{0}C (%)	Wt. change between 150-300^{0}C (%)	Wt. change between 300-450^{0}C (%)	Derivative wt. change temp(%/^{0}C)	Residual wt. (%)	50%wt. loss temp (^{0}C)
	Raw sample	9.31	30.77	71.66	331.54	28.34	329.15
Irradiated	25 KGy	10.12	24.66	75.67	350.77	24.33	346.26
	50 KGy	5.01	20.90	80.98	354.51	29.02	347.74
	100 KGy	8.34	28.97	78.56	341.66	25.78	339.01

4.2.1.4 XRD of physically irradiated technical bamboo fiber

Irradiated bamboo fiber was subjected to XRD experiment in order to observe crystallinity index, degree of crystallinity and microfibril angle. Figure 4.32 shows XRD representation of raw and irradiated bamboo fiber. From the Figure it can be seen that in the irradiated samples, a clear increase of intensity peak height is observed compared to raw sample. The increasing intensity of peak height was observed due to effect of radiation. Crystallinity index, degree of crystallinity, microfibril angle of fibrils and crystallite size were measured form the intensity of peak height of XRD and calculated values are given in Table 4.9.

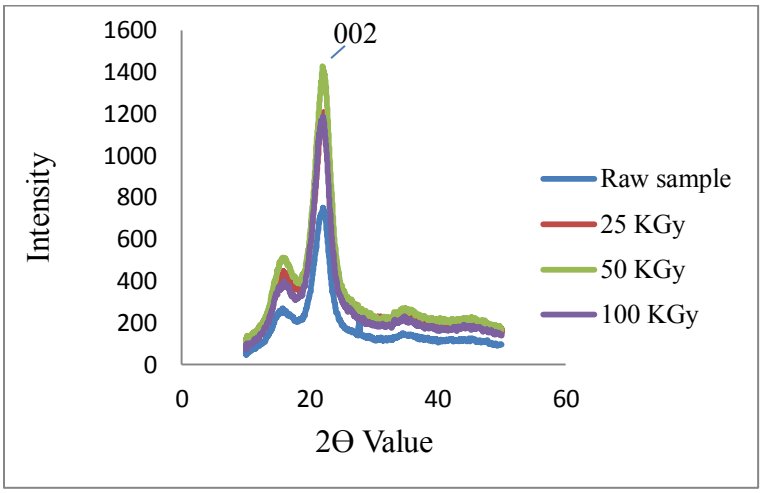

Figure 4.32 XRD representation of raw and irradiated bamboo fiber in which crystallinity 002 plane was increasing.

The effect of gamma radiation on the structure, properties and processing of polymers are of considerable scientific and commercial significance and have been reported elsewhere (Zhishen et al. 1995; Bhateja et al. 1995; Akpalu et al. 2010; Stribeck et al. 2010; Burger et al. 2010).

Table 4.9 Microfibril angle, crystallite size, crystallinity index, degree of crystallinity obtained from XRD for raw and irradiated bamboo fiber.

Sample No		MFA	C.S (nm)	C.I %	D.C%
Raw sample		3.90	2.44	69.75	75.69
Irradiated	25 KGy	3.67	2.20	71.42	79.62
	50 KGy	3.45	2.05	72.65	81.32
	100 KGy	3.99	2.28	68.59	74.93

The degree of crystallinity is an important parameter for crystalline polymers. The physical and mechanical properties of polymers are profoundly dependent on the degree of crystallinity. As the amount of irradiation is increased, XRD of irradiated fiber showed an overall increase in crystallinity index, degree of crystallinity but after attaining higher properties it was found to decrease again. This is due to an overall increase of formation of bond by forming H radical. In this research, bamboo fiber are classifies as “crosslinking type” or “chain-scission type”. Bamboo fibers were not fully crystallized. Crystalline parts remained surrounded by amorphous part of cellulose of bamboo fiber. H radicals combined together forming stronger bond and increased the amount of crystallinity. But with increasing the radiation, the chain scissoring took place. As a result the amount of crystallinity decreased and the values were found to be lower compared to the other irradiated samples. The increase in crystallinity obtained in the raw fiber and irradiated fiber is thought to be the main contributing factor for the increase in fiber strength as well as better tensile properties of the fiber. In the case of MFA and C.S. it was found to increase up to 50 KGy and then decrease again with increase in radiation.

4.2.1.5 FTIR analysis of physically irradiated technical bamboo fiber

Fourier transform infrared spectroscopy (FT-IR) is a useful technique for studying bamboo chemistry, as well as to characterize the chemistry of bamboo. The specific objectives of the

present work were to modify bamboo and its cellulosic polymer components through physical modification using gamma radiation as the radical initiating agents. A second objective was to characterize the modified bamboo technical fiber and cellulosic polymers. FT-IR analysis was performed to investigate the reaction.

The spectrum of raw technical bamboo fiber shows the basic structure as all bamboo samples: strong broad OH stretching (3300–4000 cm^{-1}), C–H stretches in methyl and methylene groups (2800–3000 cm^{-1}) and a strong broad superposition with sharp and discrete absorptions in the region from 1000 to 1750 cm^{-1}. Comparing the spectra of holocellulose and lignin reveals that the absorptions situated at 1510 cm^{-1} and 1600 cm^{-1} (aromatic skeletal vibrations) are caused by lignin and the absorption located at 1730 cm^{-1} is caused by holocellulose; this indicates the C=O stretch in non-conjugated ketones, carbonyls and in ester groups. Appearance of the band near 1600 cm^{-1} is a relative pure ring stretching mode strongly associated with the aromatic C–O–CH_3 stretching mode, The C=O stretch of conjugated or aromatic ketones absorbs below 1700 cm^{-1} and can be seen as shoulders in the spectra (Bruce et al. 2002; Sunkyu et al. 2010).

Figure 4.33 shows the FT-IR spectra of unmodified raw bamboo fiber and physically modified bamboo fiber represented only in the fingerprint region between 1800 and 1100 cm^{-1}. This region comprises bands assigned to the main components from bamboo: cellulose, hemicelluloses and lignin (Table 4.6), which is very complex. Clear differences can be detected in the infrared spectra, both in the different absorbance values and shapes of the bands and in their location.

A decrease in the intensity of the O–H absorption band at 3456 cm^{-1} was observed (data not represented here) indicating that the hydroxyl group content in bamboo was reduced after radiation. After 50 KGy radiation the decreasing trend was found to increase again. This may be due to the chain scissoring of cellulosic chain polymer. As a result H radicals were produced and it easily formed –OH groups with the air. The higher xylan content in bamboo is evidenced by a stronger carbonyl band at 1740 cm^{-1}, for physically modified bamboo this being shifted to a lower wavenumber value (1735 cm^{-1}). The enhanced carbonyl absorption peak at 1735 cm^{-1} (C=O ester), C–H absorption at 1381 cm^{-1} (– C– CH_3) and –C– O– stretching band at 1242 cm^{-1} confirmed the formation of ester bonds. This bond was found to have increasing rate upto 50

KGy radiation. With increasing the radiation doses the increasing trend of peak was found to decrease. This indicated the breaking of bond the cellulosic chain.

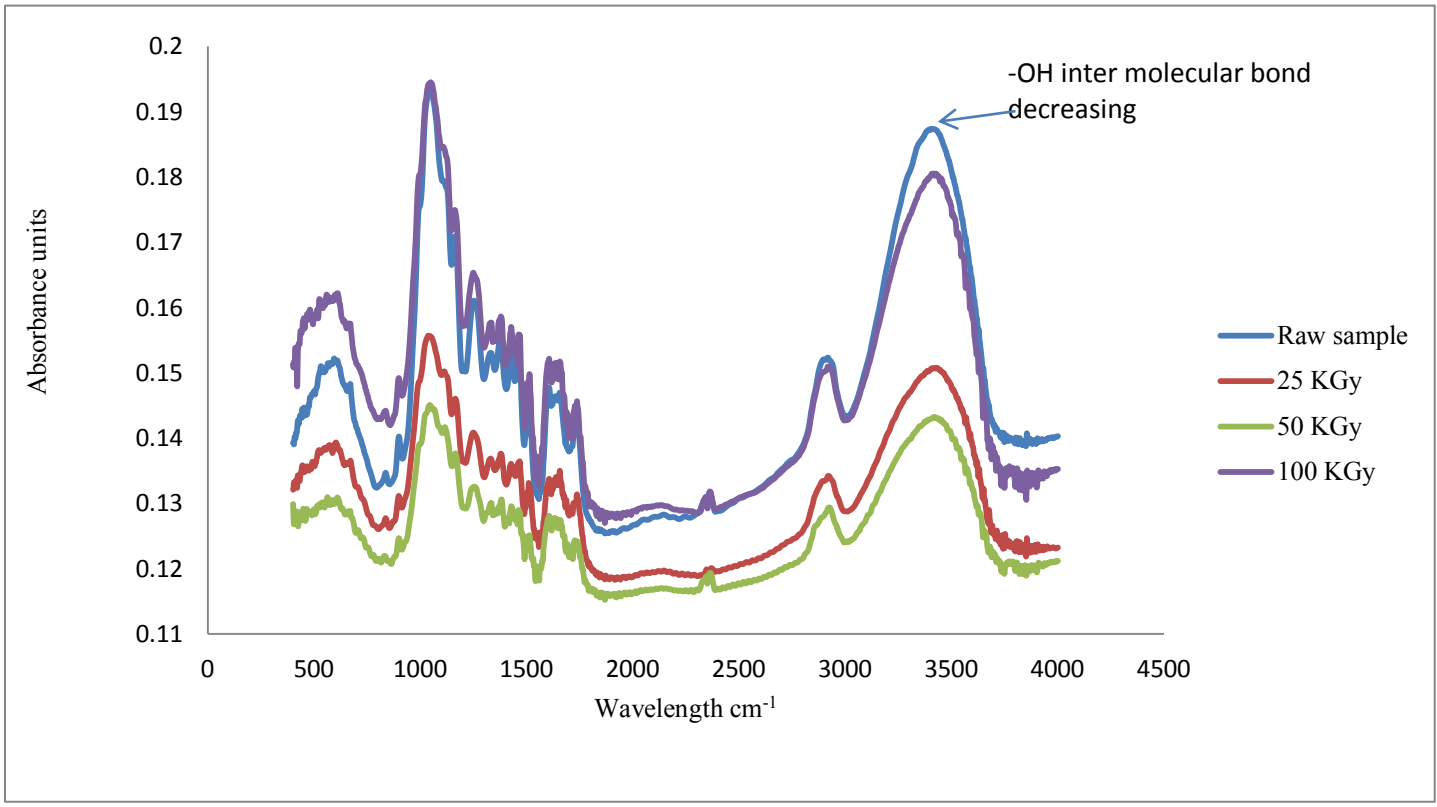

Figure 4.33 FTIR representation of raw and irradiated bamboo fiber showing the change in peak height.

Clearly, the cellulose chains were present in amorphous and crystalline regions. Hence, a spectral intensity decreased in the 1050–1000 cm^{-1} region might be associated with the functional groups in amorphous regions and spectral intensity increase in the 1000–950 cm^{-1} region could arise from crystalline regions (Yongliang 2013; Bodirlau et al. 2009). Figure 4.33 was obtained from raw bamboo fiber and might provide information on the compositional and structural changes during the radiation in the fiber. With respect to radiation, cellulose concentrating induces fiber density augmentation and cellulose chain rearrangement through the formation of effective inter- and intra-molecular hydrogen bonding and also inter-chain van der Waals interactions. This has

revealed in the mechanical properties of single bamboo fiber. Mechanical strength was found to increase upto 50KGy radiation and with increasing the dose it is found to decrease again.

4.2.1.6 Water absorption test of physically irradiated technical bamboo single fiber

Water uptake by the physically treated and raw samples was monitored at 25^0C. The results are shown in Figure 4.34. The water absorption by both treated and raw bamboo fiber was very fast within the initial 30 minutes. Then the soaking rate decreased in the treated samples, whereas the raw samples still continued to soak water slowly.

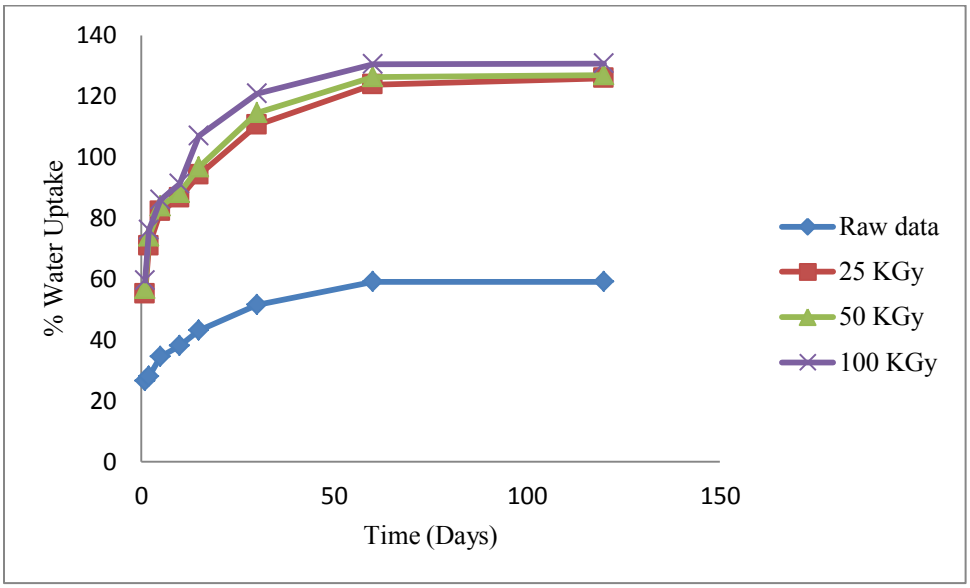

Figure 4.34 Variation of water uptake tests with time of raw and irradiated bamboo fiber after 180 mins where the water uptake was higher in irradiated sample.

The raw sample gained water up to about 33%, whereas that for the treated samples was about 88-90%, which is expected. The reason for increase water uptake by the treated sample may be a polymer chains were open and formed H radical, which was hydrophilic in the presence of water. In the case of jute fiber the water uptake was found to be 67% (Khan et al. 2009).

4.2.1.7 Biodegradation test of physically irradiated technical bamboo single fiber

Biodegradability test for physically treated and raw samples was monitored at 25^{0}C with dipping the bamboo fiber into the water for 180 days. After different interval of time the weight was measured and the percent of degradability was calculated. At the initial stage the rate of degradability was very low as the cellulosic polymer chain was reinforced in the lignin matrix. Lignin is an aromatic compound and hydrophobic. For that reason it persist the degradability of bamboo fiber. The results are shown in Figure 4.35. The degradability by both treated and raw bamboo fiber was very low within the initial 30 days. Then the degrading rate increased in the treated samples, whereas the raw samples still continued to degrade very slowly in water. The untreated and treated samples degraded almost entirely all. The reason for increase degradability in the treated sample may be the polymer chains. The chains were open and formed H radical, which was hydrophilic in the presence of water. This leads the bamboo fiber to degrade faster than the raw sample.

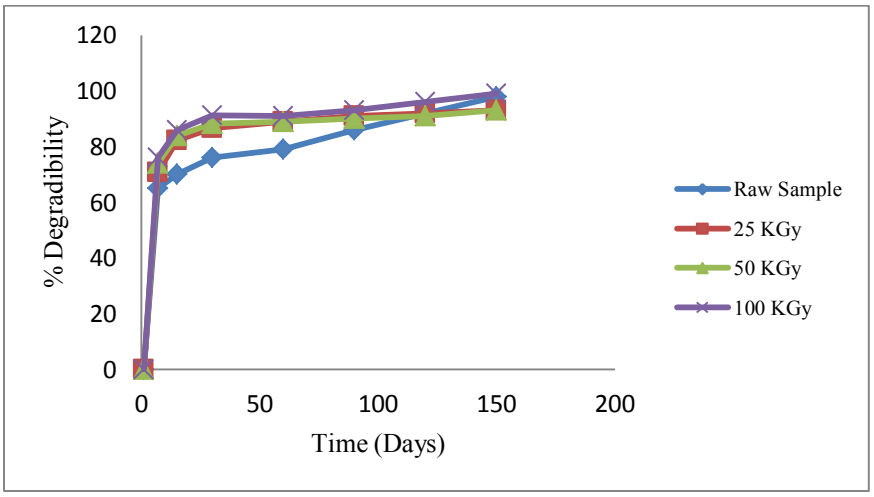

Figure 4.35 Biodegradation test results of raw and irradiated bamboo fiber after 180 minutes.

4.2.1.8 Soil degradation test of physically irradiated technical bamboo single fiber

Soil degradation test for raw and physically treated sample was monitored at 25^{0}C with dipping the bamboo fiber into the water for 180 days. After different interval of time the weight was measured and the percent of soil degradability was calculated. At the initial stage the rate of

degradability was very low as the cellulosic polymer chain was reinforced in the lignin matrix. Lignin is an aromatic compound and hydrophobic. For that reason it persist the degradability of bamboo fiber. The results of the soil degradation test are shown in Figure 4.36. The degradability by both treated and raw bamboo fiber was very low within the initial 30 days. Then the degrading rate increased in the treated samples, whereas the untreated samples still continued to degrade slowly in the soil. The raw and treated samples degraded almost entirely all bamboo fiber for 180 days. The reason for increase degradability by the treated sample may be the polymer chains. Those chains were open and formed H radical, which was hydrophilic in the presence of microorganism in the soil. This leads the bamboo fiber to degrade faster compared to the untreated samples.

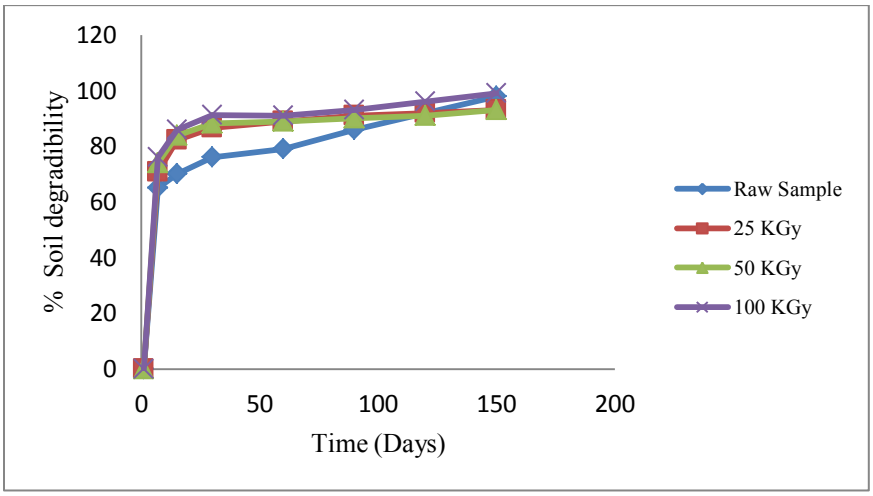

Figure 4.36 Soil degradation results of raw and irradiated bamboo fiber after 180 minutes in which degradation trend is almost similar.

4.2.1.9 Optical microscopic dislocation test of physically irradiated technical bamboo single fiber

Raw and irradiated bamboo fiber was observed under optical microscope to observe any dislocation due to irregular cell wall in the natural fiber. The exact composition of dislocation is still unknown (Thygesen 2010). They are assuming to contain cellulose, lignin and hemicellulose like the rest of the secondary wall. Traditionally dislocations are considered to contain

amorphous cellulose in contrast to the surrounding cell wall. When dislocations are observed under the optical microscope they are birefringence in the bulk cell wall which indicates that structure is not amorphous. Figure 4.37 shows the optical microscope micrograph for the raw and irradiated sample. In the raw sample, the dislocations are observed very clearly. But in the case of irradiated sample, the dislocations are not dominant. This may be due to the fact that after radiation the cellulosic chains became aligned and the dislocations were compressed. For that reason the birefringence was not observed. For that reason the mechanical properties was found to be better compared the raw sample. When the load was applied in the longitudinal direction, the dislocations were stretched and thus aligned with the cellulose microfibrils of the surrounding bulk cell. When the fiber is irradiated, then the dislocations were aligned with the microfibril and had a less orderly and more loosely structure. On the molecular level the intra-fibril and inter-fibril are much stronger than the inter-fibril and intra-fibril.

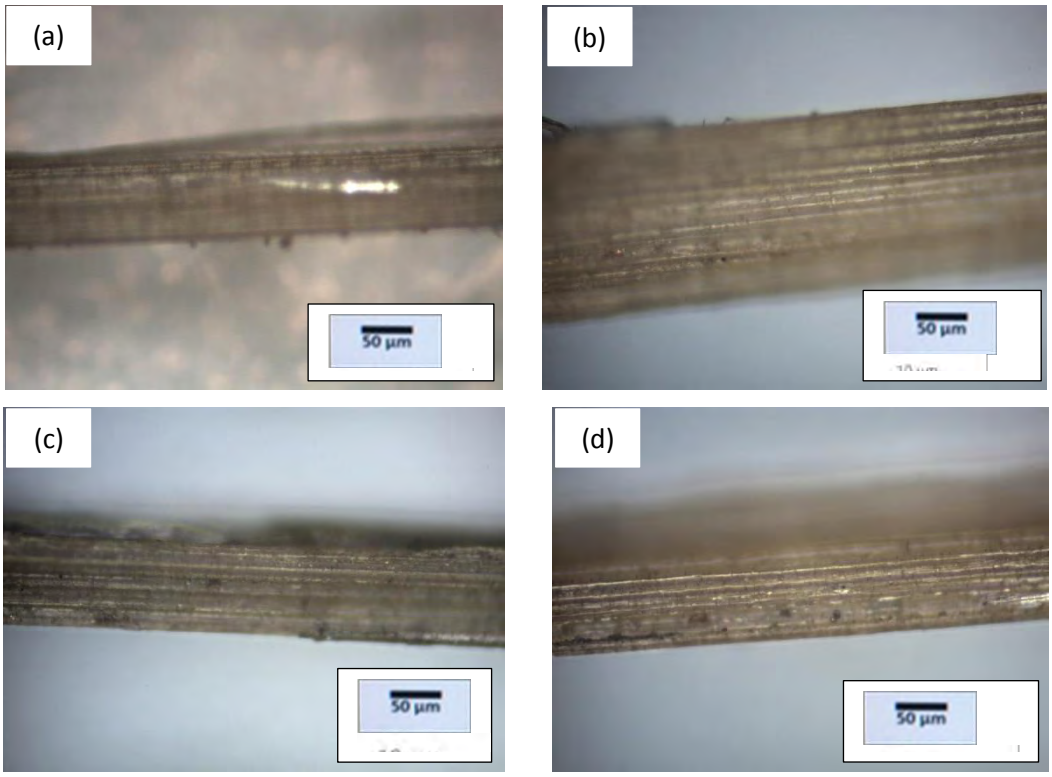

Figure 4.37 Optical microscopic micrograph of (a) raw (b) 25 KGy (c) 50 KGy (d) 100 KGy irradiated bamboo fiber indicating the dislocations.

Table 4.23 Chemical analysis of raw, BCS and BCS+$NaHCO_3$ grafted bamboo fiber sample.

Sample	Hot Water Soluble %	Moisture %	Lignin %	Holocellulose %	α-cellulose %	Hemicellulose %	Ash %
Raw Sample	5.07±0.06	12.33±0.56	23.91±0.58	67.08±0.17	50.23±0.18	16.85±0.09	1.38±0.05
BCS grafted fiber	4.07±0.06	11.15±0.34	22.41±0.32	67.78±0.24	51.52±0.18	15.56±0.09	1.25±0.05
BCS+$NaHCO_3$ grafted sample	4.06±0.06	11.33±0.21	22.54±0.60	67.08±0.51	50.41±0.18	16.67±0.09	0.91±0.02

4.4.1.3 TGA analysis

Raw bamboo fiber, BCS and BCS + $NaHCO_3$ grafted sample was subjected to TGA experiment. The results are shown in Figure 4.77. It is observed that the weight change temperature was 340^0C for BCS grafted sample and 357^0C for BCS + $NaHCO_3$ grafted sample. The % derivative weight change was higher in double treated sample compared to the raw sample. As Cr formed bond with the cellulose, it shifted the derivative temperature to higher value.

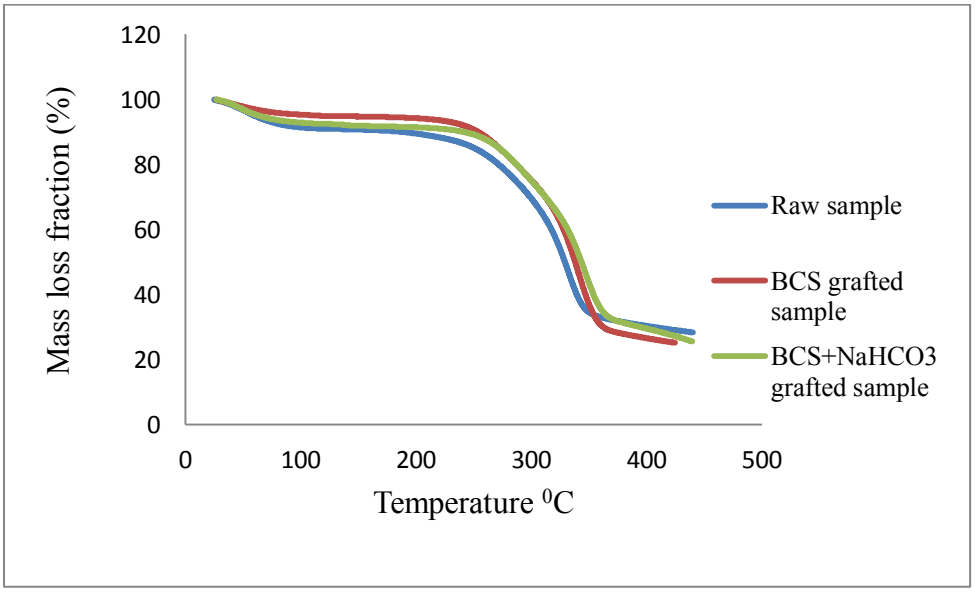

Figure 4.77 TGA curve of raw, BCS and BCS + $NaHCO_3$ grafted sample with increasing rate of weight change temperature.

It can be seen from the Table 4.24 that for 10% and 50% weight loss temperature was much higher in the BCS grafted fiber compared the raw fiber. Cellulose consists of long and linear homopolymeric chains of β-1,4 - **D(**+)-glucopyranose units linked together by 1,4-glucosidic bonds. The cellulose molecule is not planar but has a screw axis, each glucose unit being at right angles to the previous one. Grafted BCS and BCS+$NaHCO_3$ formed octahedral complexes with cellulose reducing free rotation about the anhydro glucopyranose C-0-C link, which did not occur due to steric effects in the solid state. In the case of BCS+$NaHCO_3$, Cr is surrounded by $NaHCO_3$. As a result masked Cr having high molecular weight formed intermolecular hydrogen bond. The naturally polymerized molecules are thus rigid. The adjacent long chains were held together in the main chain by hydrogen bonds in addition to certain dispersion intermolecular forces. So the otherwise two-dimensional molecules of cellulose "having an average molecular weight of about existed in a three dimensional ordered network as larger microfibrillar ordered domains". The pyrolytic reaction became complicated and required high energy. For that reason BCS+$NaHCO_3$ complex structure of cellulose and chromium need much higher energy to breaking the bond of molecules (Kandola 1996).

Table 4.24 Derivative weight change data of raw and BCS grafted bamboo fiber.

Sample	Wt. change between 50-150^{0}C (%)	Wt. change between 150-300^{0}C (%)	Wt. change between 300-450^{0}C (%)	Derivative wt. change temp (%/^{0}C)	Residual wt. (%)	50%wt. loss temp (^{0}C)	10%wt.loss temp (^{0}C)
Bamboo	9.31	30.77	71.66	331.54	28.34	329.15	188.15
BCS grafted	5.18	19.22	74.82	340.07	25.18	353.28	235.86
BCS+$NaHCO_3$ grafted sample	8.12	24.71	74.47	357.17	25.53	344.10	240.88

4.4.1.4 XRD analysis

Technical single raw bamboo fiber was subjected to XRD to observe the change in cellulose polymer crystallinity. XRD results shown in 4.78 indicate the increasing trend of cellulosic polymer crystallinity. Change of crystallinity in BCS grafted sample was not significant compared to the raw sample. But in the case of BCS+$NaHCO_3$ grafted sample, the change in the crystallinity was significant.

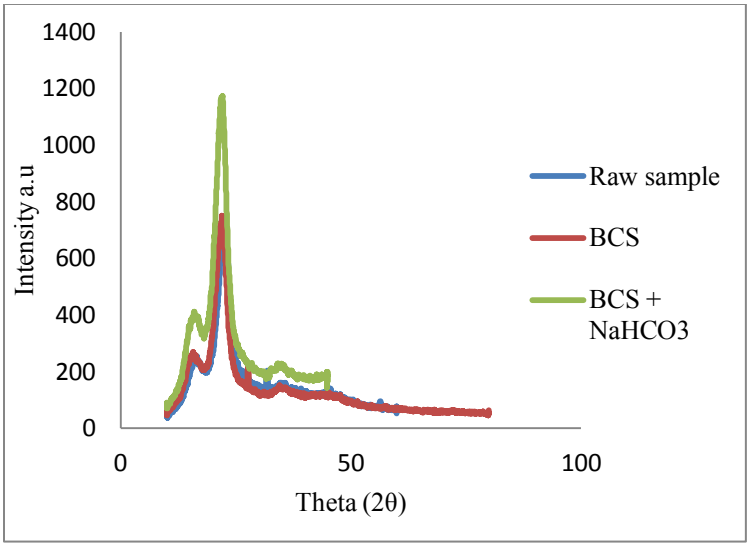

Figure 4.78 XRD data of raw, BCS and BCS + $NaHCO_3$ grafted sample showing increasing rate with modification on 002 plane.

Table 4.25 Measurement of MFA and crystalinity data of raw, BCS and BCS+$NaHCO_3$ grafted bamboo fiber.

Sample No	MFA	C.S (nm)	C.I %	D.C
Raw sample	3.90	2.44	69.75	75.69
BCS grafted sample	2.63	1.57	72.62	78.29
BCS+$NaHCO_3$ grafted sample	2.50	1.49	73.15	81.98

The MFA and crystallite size decreased win the BCS grafted sample (Table 4.25). However, the value of % C.I and D.C increased indicating that the crystallinity also increased. When the load was applied, cellulosic fibril in the secondary wall (having lower MFA) tried to align with more force and energy. It is revealed in the mechanical properties of the BCS grafted fiber as compared with the raw fiber.

4.4.1.5 FTIR analysis

FTIR is an effective tool to explain the bond formation and bond breaking. From the spectrum of FTIR for raw and treated bamboo fiber (Figure 4.9) it is observed that the –OH group spectrum was reduced. So in Cr solution OH was replaced and Cr formed bond with the negatively charged carboxylate ion. For that reason the broad peak around 3400cm^{-1} is in decreasing trend. The peak at 1026^{-1} due to carbonyl radical was also found to have decreasing trend. Amorphous cellulosic chains formed crystalline chain showing the decreasing trend. A remarkable change was also observed in the finger print region.

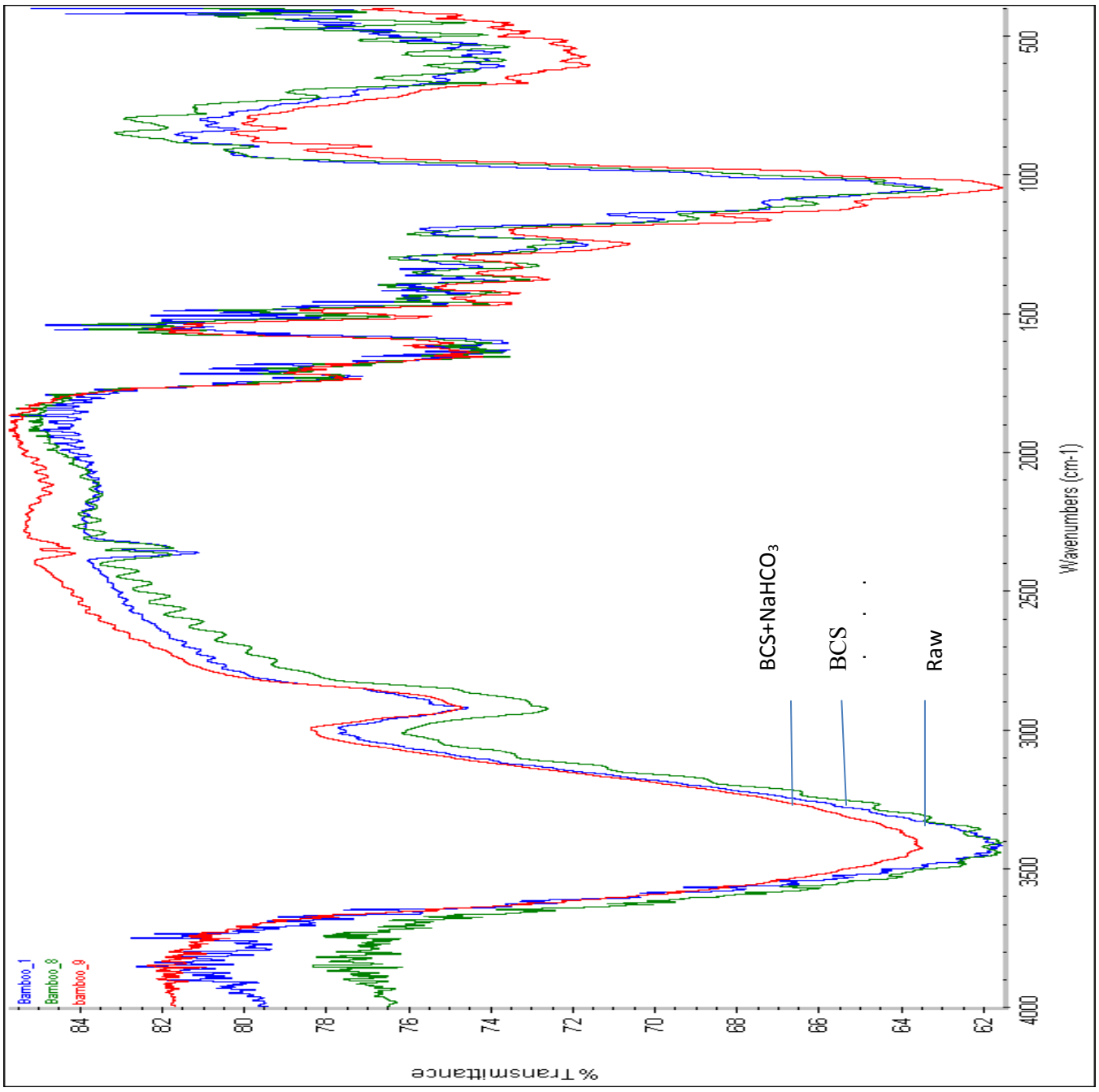

Figure 4.79 FTIR spectrum of raw, BCS and BCS + $NaHCO_3$ grafted bamboo fiber sample showing the change in bonding in grafted fiber.

4.4.1.6 Water uptake, biodegradability and soil degradation test results

Water uptake, biodegradability and soil degradation test results are shown in Figures 4.80 to 4.82. In all of these tests, it was found that degradation rate of BCS and BCS + $NaHCO_3$ grafted fiber were lower compared to the raw sample.

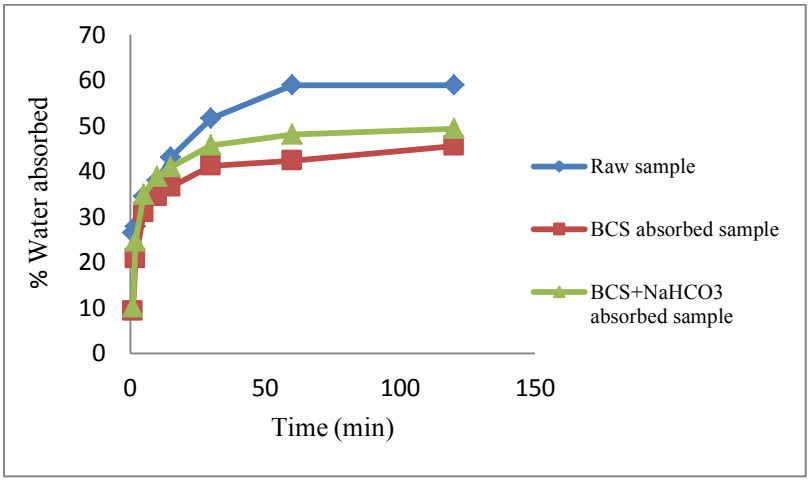

Figure 4.80 Water uptake test results for raw, BCS and BCS + $NaHCO_3$ grafted bamboo fiber sample showing lower rate of water absorption in grafted sample compared to the raw sample.

It may be stated that chromium formed bond with cellulose, thus positively charged chromium was surrounded by –OH ions. These polymers generally contain carboxylic groups that are in equilibrium with their dissociated form in the presence of water or carboxylate groups. The polymer coils extend themselves and widen in consequence of the electrostatic repulsion of negative charges. Carboxylate groups are also able to interact through hydrogen bonding with additional quantities of water. The presence of crosslinking allows swelling of the three-dimensional network and gel formation without polymer dissolution (Pó 1994). In the case of soil degradation, the growth of micro-organism was hindered and degradation rate was slow.

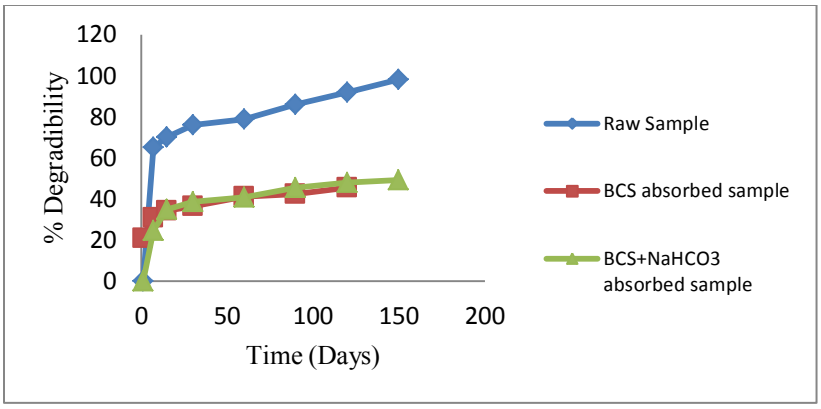

Figure 4.81 Biodegradability test for raw, BCS and BCS + $NaHCO_3$ grafted bamboo fiber sample showing lower rate of biodegradation in grafted bamboo fiber compared the raw bamboo fiber.

Moisture absorption into the polymeric materials is considered by three major mechanisms; (i) diffusion of water molecules inside the micro gaps between polymer chains; (ii) capillary transport of water molecules into the gaps and flaws at the interface between fiber and the polymer due to the incomplete wettability and impregnation; and (iii) transport of water molecules by micro cracks in the matrix formed during the biodegradable process. Though all three mechanisms are active, the overall effect can be modeled conveniently considering the diffusion mechanism (Kushwaha 2010).

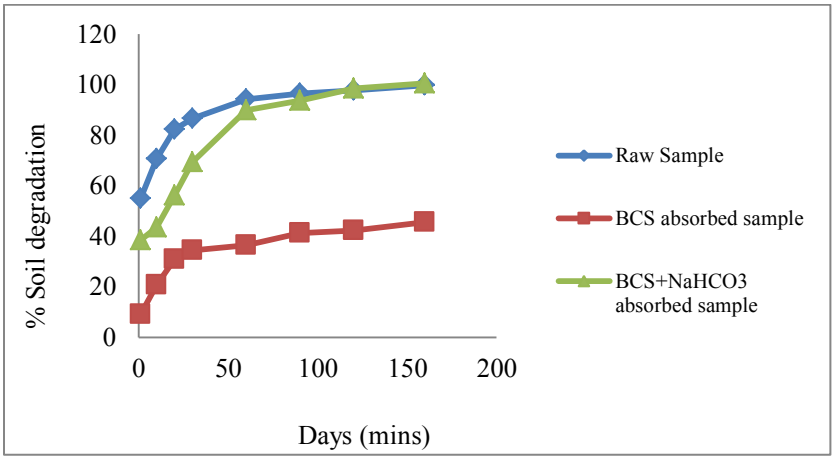

Figure 4.82 Soil degradation test for raw, BCS and BCS + $NaHCO_3$ grafted bamboo fiber sample showing lower rate of soil degradation in grafted sample compared the raw sample.

4.4.1.7 Optical micrograph (dislocation), MFA and fiber length test results

Bamboo fiber was grafted with BCS and BCS + $NaHCO_3$ with the cellulose polymer consist with a suitably reactive end group, which then reacted with another backbone polymer allowing much greater the properties over the raw polymer. In single treatment, BCS formed bond with cellulose polymer. Cellulose fiber with double treatment made masking of BCS with $NaHCO_3$. BCS + $NaHCO_3$ became larger and trapped in the cellulose chain. As a result the dislocations tried to align with the crystalline polymer (Budi et al. 2012). For that reason, the dislocations were not visible in the BCS and BCS+$NaHCO_3$ grafted fiber. From fig 4.83, it is observed that in raw fiber the bifringerence was visible, however in the BCS and BCS+$NaHCO_3$ grafted fiber, no bifringerence was observed. The dislocations decreased the strength of natural fiber. The decrease in strength is often severe enough to cause fiber breakage under moderate mechanical treatments although on the other hand they make fiber more flexible with an accompanying

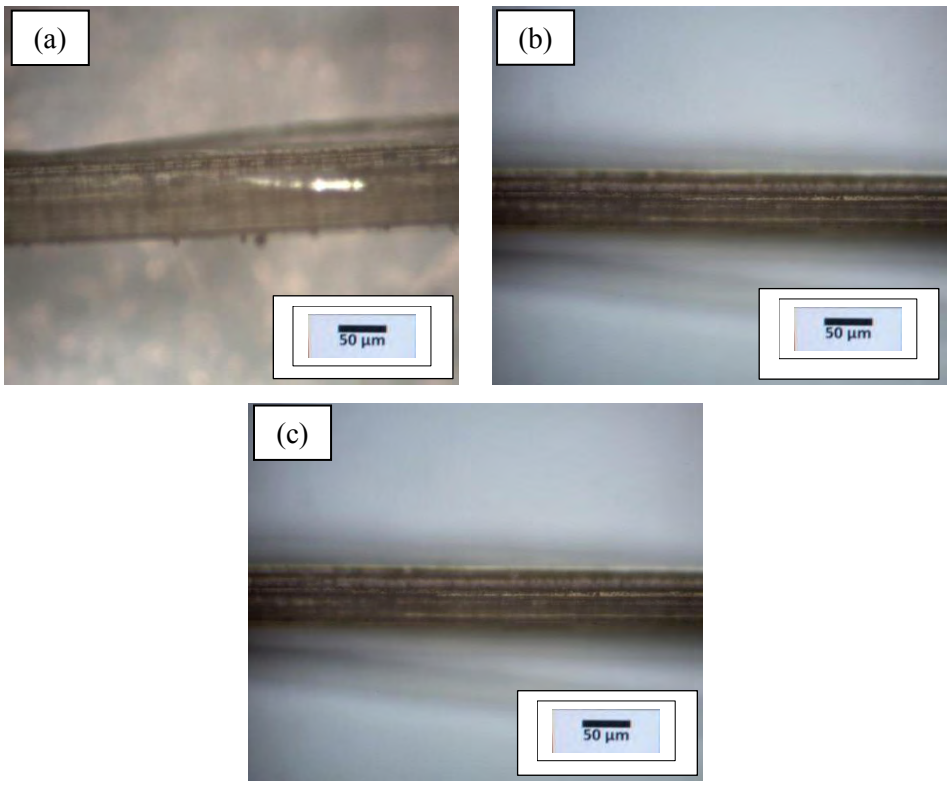

Figure 4.83 Optical micrograph of (a) raw, (b) BCS grafted and (c) BCS + $NaHCO_3$ grafted bamboo fiber in which grafter surface was smoother and more compact compared to the raw fiber.

improvement in binding potential. The damages include buckling of the cell wall, indentations in the lumen side of the cell wall and development of splits in the middle lamellae regions. The resulting ‘‘loosening’’ of the tissue intuitively renders the regions more accessible to chemical agents and enzymes. When cellulose fiber is grafted with BCS then chromium join the cellulose chain, recovered the damage of cell wall and caused indentation in lumen.

From the optical micrograph, the MFA was measured and compared with results from XRD. The results are given in Table 4.26. There was also a similarity in two methods. It was observed that due to grafting of Cr the crystalline portion became more crystalline in the secondary wall, which turns the MFA to lower value. In the raw sample it was found to be 3.98^0, but in the BCS grafted sample it was around 2.55^0. From this table it is also observed that the MFA decreased after treatment. BCS grafted fiber had lower MFA compared to raw bamboo fiber. However the BCS+ $NaHCO_3$ grafted fiber had lower MFA compared to other raw and BCS grafted fiber. As BCS+ $NaHCO_3$ grafter fiber had lowered MFA, it showed the best set of mechanical properties among all bamboo fiber.

Table 4.26 MFA data of raw, BCS and BCS+ $NaHCO_3$ grafted bamboo fiber.

Sample name	Microfibril angle (MFA deg) (Optical)	MFA (XRD)
Bamboo Fiber	3.98±0.10	3.90±0.09
BCS grafted fiber	2.55±0.07	2.63±0.06
BCS+ $NaHCO_3$ grafted fiber	2.45±0.07	2.50±0.05

Table 4.27 is indicating the fiber length of raw, BCS grafted and BCS+ $NaHCO_3$ grafted sample. Due to crystallization between cellulose and BCS, BCS+ $NaHCO_3$ the cellulosic chain ried to align forming large chain of cellulose polymer. For that reason in Table 4.27 the highest fiber length was found in BCS+ $NaHCO_3$ modified sample. Cellulosic chains are held in the lignin matrix. BCS and double treated samples tried to crystallize in the presence of chromium. Sodium also masked the Cr inside the cellulose. These phenomena made more bonding in the cellulose

chain. The inter and intra molecular bonding became closer in the chain. For that reason, fiber length determining solution was not able to break the bonding between the lignin and cellulose. This effect was prominent in the mechanical properties.

Table 4.27 Measurement results of fiber length of raw and BCS grafted bamboo fiber.

Sample No	Fiber length (mm)
Raw sample	2.38±0.57
BCS grafted fiber	2.63±0.59
BCS+ $NaHCO_3$ grafted fiber	3.11±0.81

4.4.1.8 Image analysis test results

Chromium in BCS sample formed octahedral complexes with cellulose chain after treatment. This complex increased the crystallinity of the cellulose and the cellulose became more compact in S2 level of secondary wall. Ground tissue cell was also very close to each other. As result solid surface was found higher in BCS grafted samples. The double treatment $NaHCO_3$ masked the chromium and filled the void in the surface and cross section of the cellulose fiber. For that reason solid phase was higher in the treated sample. The measurement results are also mentioned in Table 4.28. Figure 4.84 is showing the solid phase (ash colour) in raw sample, BCS grafted sample and BCS+ $NaHCO_3$ grafted sample.

Table 4.28 Amount of solid phases of raw and BCS grafted bamboo fiber.

Sample No	Solid phase (area sq μm)	Solid phase (area %)
Raw sample	242166.302 ± 51	66.70
BCS grafted	364026.244 ± 57	69.38
BCS+$NaHCO_3$ grafted sample	857101.373 ± 71	72.56

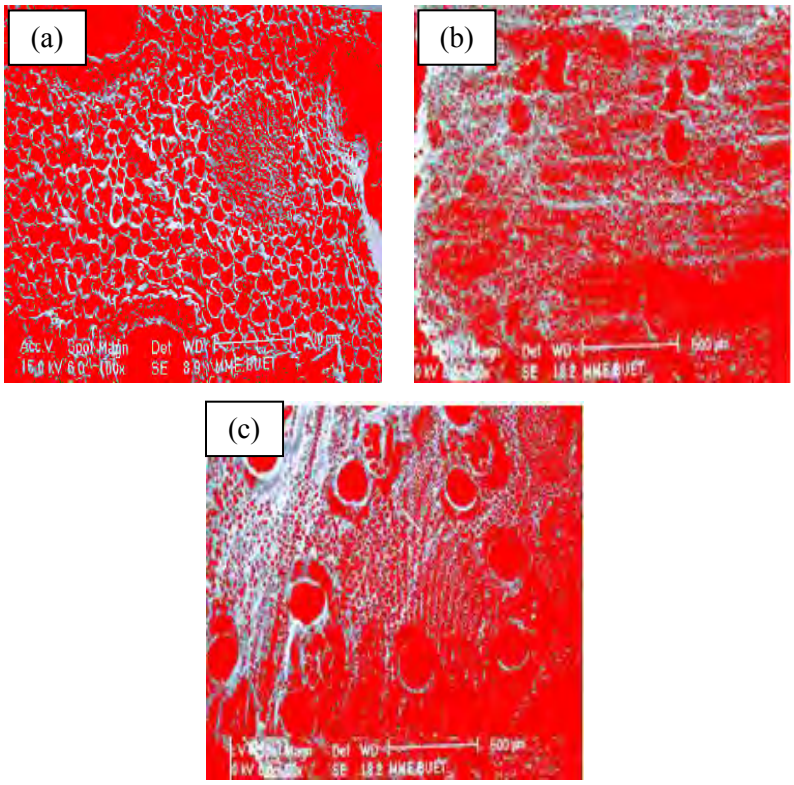

Figure 4.84 Image analysis of (a) raw, (b) BCS grafted and (c) BCS + $NaHCO_3$ grafted sample in which treated fiber surface was smoother and more compact compared to the raw fiber.

4.5 Comparison of properties of raw and modified bamboo fiber

Average tensile strength of raw and modified sample is shown in Figure 4.85. In the case of physically treated sample the tensile strength increased up to 50KGy. With increase in radiation, the tensile strength was found to be decreased than the raw and irradiated sample. In the mimosa and mimosa+$NaHCO_3$ treated sample, the tensile strength was higher than the raw sample. In the case of basic chromium sulfate grafted sample, the tensile strength was found to be increased compared to the raw sample. In the case of syntan treated sample, tensile strength was found to increase than the raw sample. In the case syntan+$NaHCO_3$, tensile strength was found to increase as compared to the raw sample. However, the highest tensile strength was found in the case in basic chromium sulfate + $NaHCO_3$ i.e. in the inorganic double treatment.

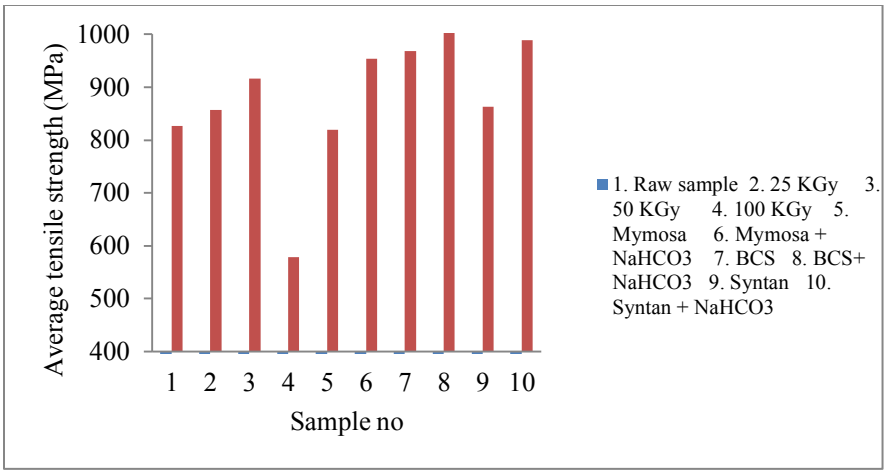

Figure 4.85 Average tensile strength of raw and modified samples.

Average Young's modulus of raw and modified sample is shown in Figure 4.86. In the case of physically treated sample, the Young's modulus increased up to 50KGy. With increase in radiation, the Young's modulus decreased compared to the raw and irradiated samples. In the case of basic chromium sulfate, mimosa, mimosa+$NaHCO_3$, syntan and syntan+$NaHCO_3$ treated samples, the Young's modulus increased as compared the raw sample. However it can be seen from Figure 4.86 that the highest Young's modulus was found in the case in basic chromium sulfate + $NaHCO_3$ i.e. in the inorganic double treatment.

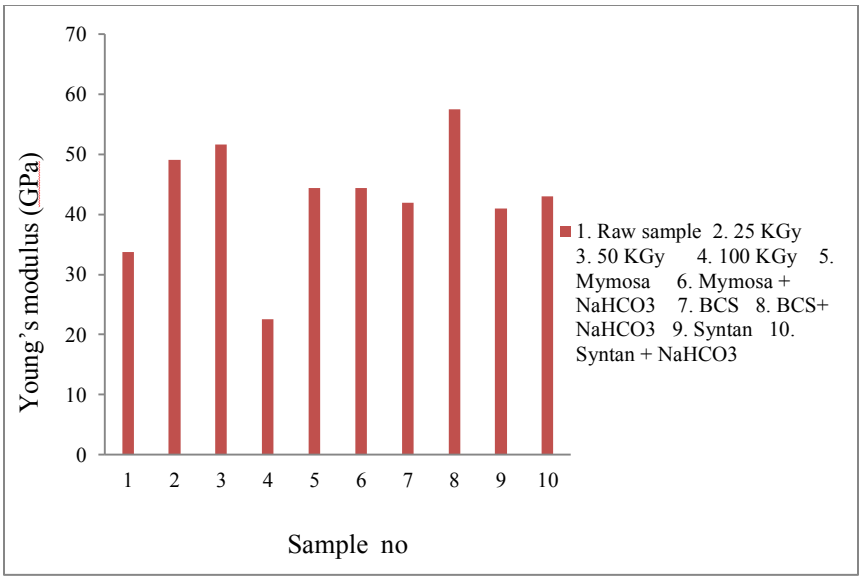

Figure 4.86 Average Young's modulus of raw and modified samples.

Average strain to failure of raw and modified sample is shown in Figure 4.87. In case of the physically treated sample, the strain to failure decreased up to 50KGy. With increase in radiation, the strain to failure was found to be increased as compared to the raw and irradiated samples. In the case of basic chromium sulfate, mimosa, mimosa+$NaHCO_3$, syntan and syntan+$NaHCO_3$ treated samples, the strain to failure decreased as compared the raw sample. However it can be seen from Figure 4.87 that the lowest strain to failure was found in the case in basic chromium sulfate + $NaHCO_3$ i.e. in the inorganic double treatment.

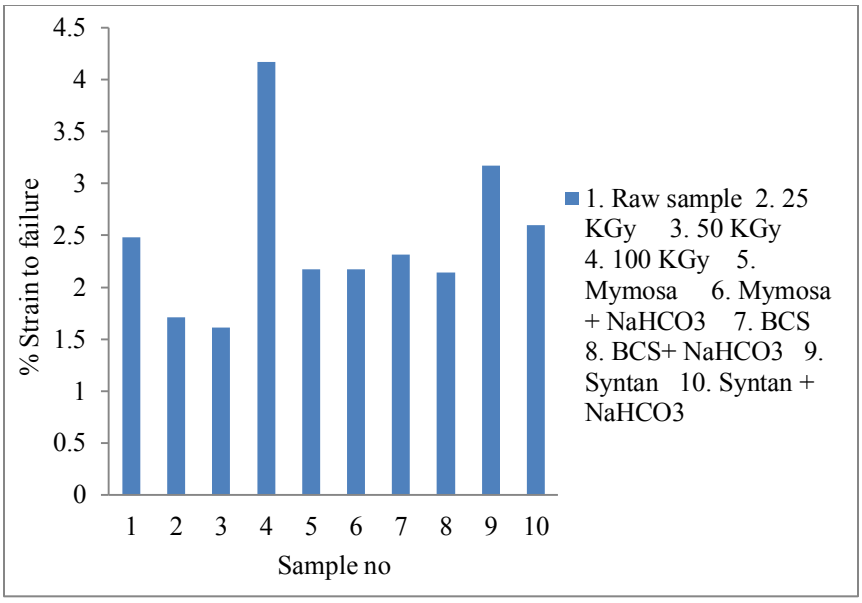

Figure 4.87 Average strain to failure of raw and modified samples.

Average microfibril angle of raw and modified sample is shown in Figure 4.88. In case of the physically treated sample, the microfibril angle decreased up to 50KGy. With increase in radiation, the microfibril angle was found to be increased than the raw and irradiated sample. In the case of basic chromium sulfate, mimosa, mimosa+$NaHCO_3$, syntan and syntan+$NaHCO_3$ treated samples, the microfibril angle decreased as compared the raw sample. From Figure 4.88 it can be seen that the lowest microfibril angle was found in the case in basic chromium sulfate + $NaHCO_3$ i.e. in the inorganic double treatment.

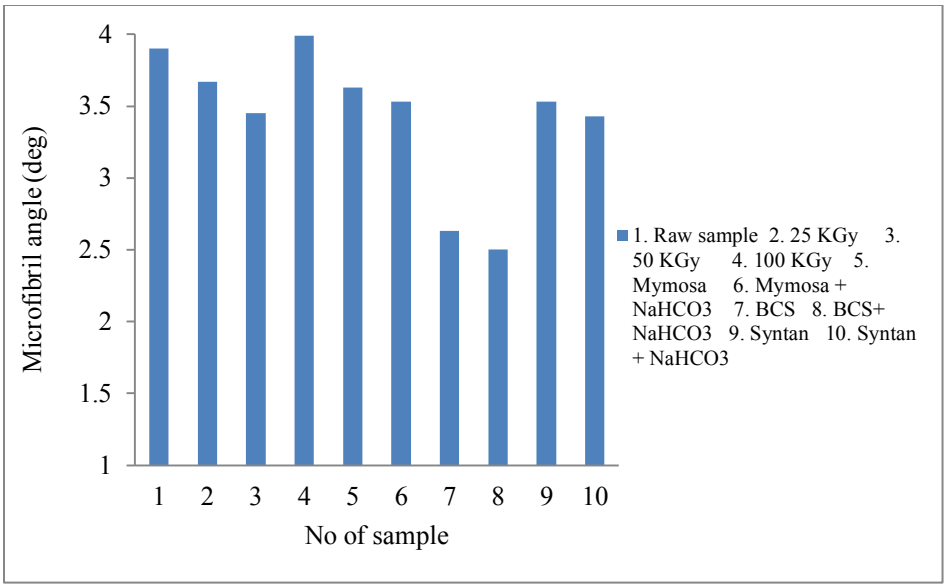

Figure 4.88 Average microfibril angle of raw and modified samples.

Average crystallite size of raw and modified sample is shown in Figure 4.89. In the case of physically treated sample, the crystallite size decreased up to 50KGy. With increase in the radiation, the crystallite size was found to increase as compared to the raw and irradiated samples. In the case of basic chromium sulfate, mimosa, mimosa+$NaHCO_3$, syntan and syntan+$NaHCO_3$ treated samples, the crystallite size decreased as compared the raw sample. It can be seen from Figure 4.89 that the lowest crystallite size was found in the case in basic chromium sulfate + $NaHCO_3$ i.e. in the inorganic double treatment.

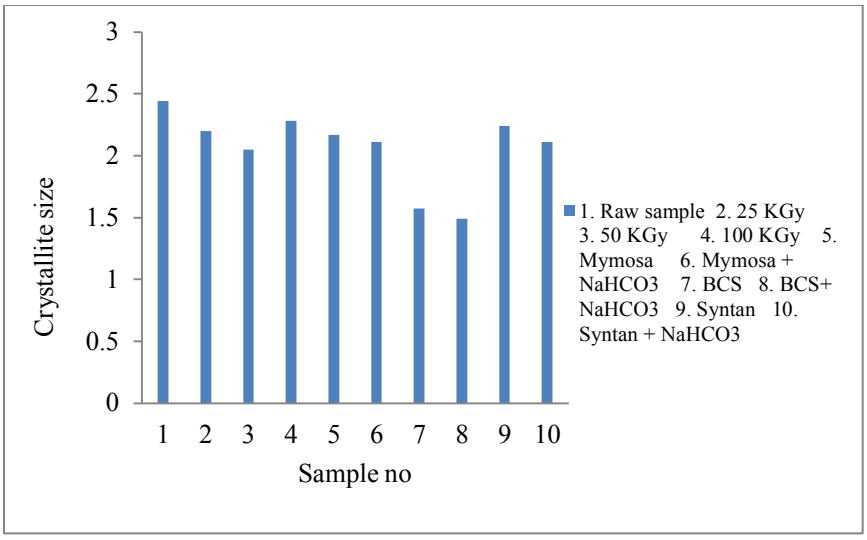

Figure 4.89 Average crystallite size of raw and modified samples.

Average crystalline index of raw and modified sample is showing in shown in Figure 4.90. In the case of physically treated sample, the crystalline index increased up to 50KGy. With increase in radiation, the crystalline index was found to decrease compared to the raw and irradiated samples. In the case of basic chromium sulfate, mimosa, mimosa+$NaHCO_3$, syntan and syntan+$NaHCO_3$ treated samples, the crystalline index increased as compared the raw sample. It can be seen from Figure 4.90 that the highest crystalline index was found in the case in basic chromium sulfate + $NaHCO_3$ i.e. in the inorganic double treatment.

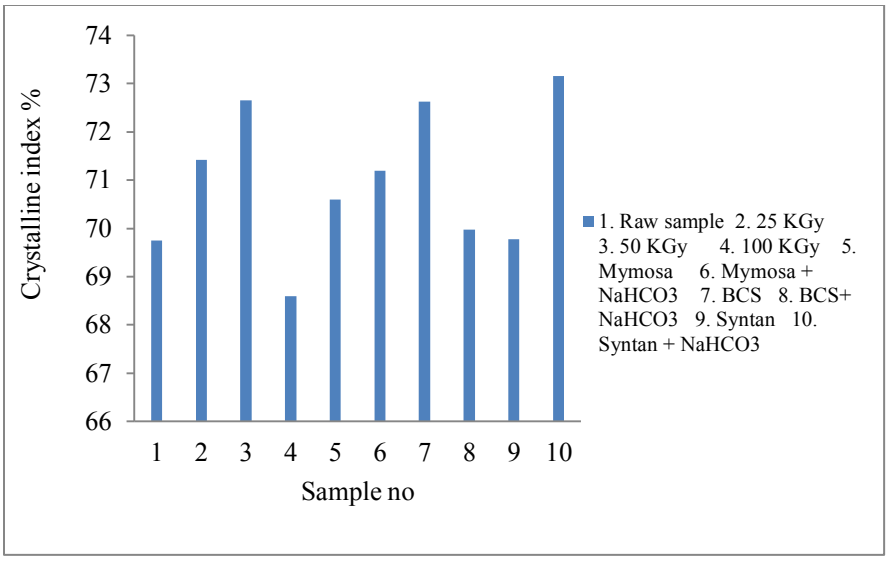

Figure 4.90 Average crystalline index of raw and modified samples.

Average degree of crystallinity of raw and modified sample is shown in Figure 4.91. In case of the physically treated sample, the degree of crystallinity increased up to 50KGy. With further increase in radiation, the degree of crystallinity was found to decrease than the raw and irradiated sample. In the case of basic chromium sulfate, mimosa, mimosa+$NaHCO_3$, syntan and syntan+$NaHCO_3$ treated samples, the degree of crystalinity increased as compared the raw sample. From Figure 4.91, it can be said that the highest degree of crystallinity was found in the case in basic chromium sulfate + $NaHCO_3$ i.e. in the inorganic double treatment.

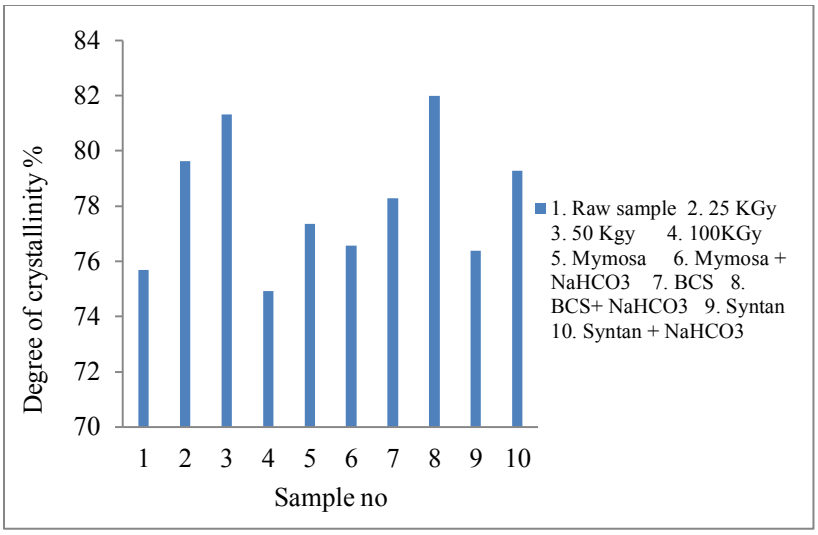

Figure 4.91 Average degree of crystallinity of raw and modified samples.

Table 4.29 is showing the length fiber of raw and modified bamboo fiber. In case of the physically treated sample, the fiber length increased up to 50KGy. With increase in the radiation, the fiber length was found to decrease as compared to the raw and irradiated sample. In the case of basic chromium sulfate, mimosa, mimosa+$NaHCO_3$, syntan and syntan+$NaHCO_3$ treated samples, the fiber length increased as compared the raw sample. It is seen in Table 4.29 that the highest fiber length was found in the case in basic chromium sulfate + $NaHCO_3$ i.e. in the inorganic double treatment.

Table 4.29 Average fiber length of raw and modified bamboo fiber.

Sample No	Fiber length (mm)
Raw Sample	2.38±0.57
25 KGy	2.57±0.51
50 KGy	2.68±0.98
100 KGy	1.43±0.41
Mimosa	2.63±0.64
Basic chromium sulfate	2.63±0.59
Syntan	1.87±0.52
Mimosa+ $NaHCO_3$	2.08±0.52
BCS+ $NaHCO_3$	3.11±0.81
Syntan + $NaHCO_3$	2.05±0.67

Depending on the mechanical and physical properties described above, raw and BCS+$NaHCO_3$ treated samples were selected for composite fabrication.

4.6 Properties of composites

4.6.1 Mechanical properties

Tensile properties

After characterizing raw and modified bamboo fiber, they were incorporated into polypropylene for composite fabrication. Among all modified fibers, the BCS+$NaHCO_3$ treated fiber was selected for this purpose. Thus composite was fabricated with polypropylene along with raw and BCS+$NaHCO_3$ modified bamboo fiber. During composite processing, the fiber trend to orient along the flow direction of matrix causing the mechanical properties to vary in different directions. As a result mechanical properties of the composite become different in the different

portion of the composite (Ismail et al. 2000). To eliminate this effect, three samples from each type of composite were tested and the average values were calculated.

The variation of tensile strength against different raw and modified bamboo fiber weight percentage is shown in the Figure 4.92. The tensile strength increased up to 50 wt% bamboo fiber and then it decreased. The Young's modulus increased and the strain at maximum force decreased with fiber weight fraction in the raw and treated samples (Mubarak et al. 2009), as shown in the Figures 4.93 and 4.94 respectively. The Young's modulus and tensile strength of raw and modified bamboo fiber composite were higher as compared to PP. The Young's modulus increased by 126% and 266% for raw and modified bamboo fiber composites with fiber loading (Paul et al. 2008). However, the Young's modulus increased up to certain weight fraction, after that it decreased. During tensile loading partially separated micro space are created, which obstructs stress propagation between the fiber and matrix. As the fiber loading increases, the degree of the obstruction increased, which consequently increases the stiffness. Again, with increase in fiber weight, the matrix weight was decreased. This in turn, increased debonding. This reveals that there might be some mechanical interlocking or chemical bond that was formed. Obviously the shrinkage of the matrix will always impose a compressive load that insists the mechanical interlocking in between the fibers and matrix. For this reason, the mechanical inter locking decreased with increase in fiber weight fraction.

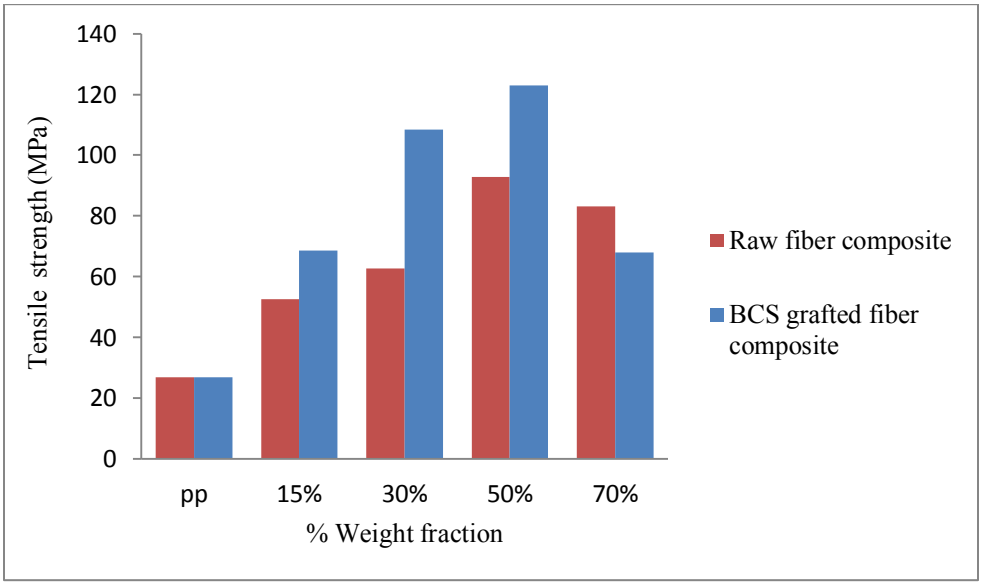

Figure 4.92 Tensile strength vs weight fraction graphs for raw and BCS+$NaHCO_3$ grafted fiber composite where BCS+$NaHCO_3$ grafted composite had better tensile strength.

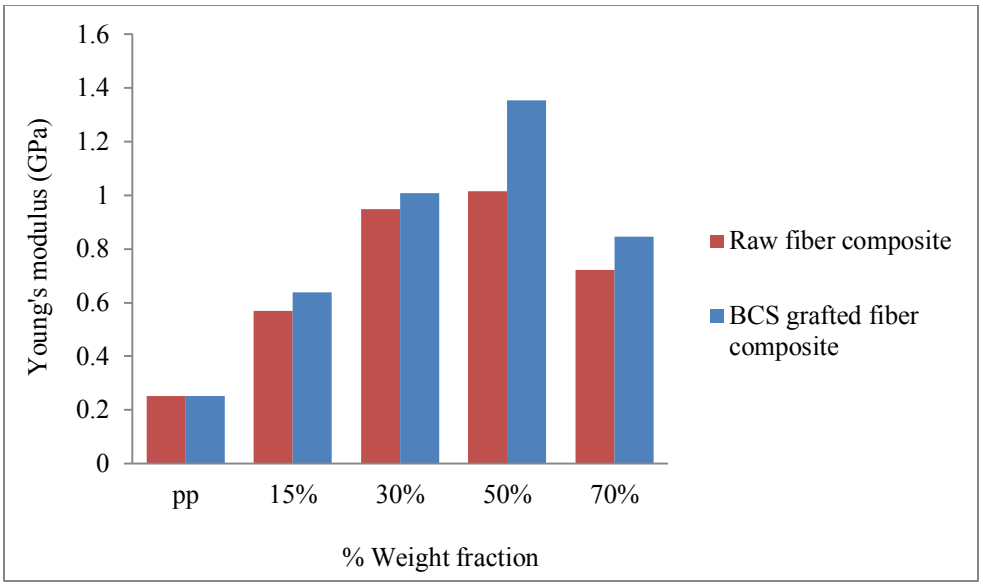

Figure 4.93 Young's modulus vs weight fraction graph for raw and BCS grafted fiber composite where the Young's modulus increased with increase in weight fraction of fiber.

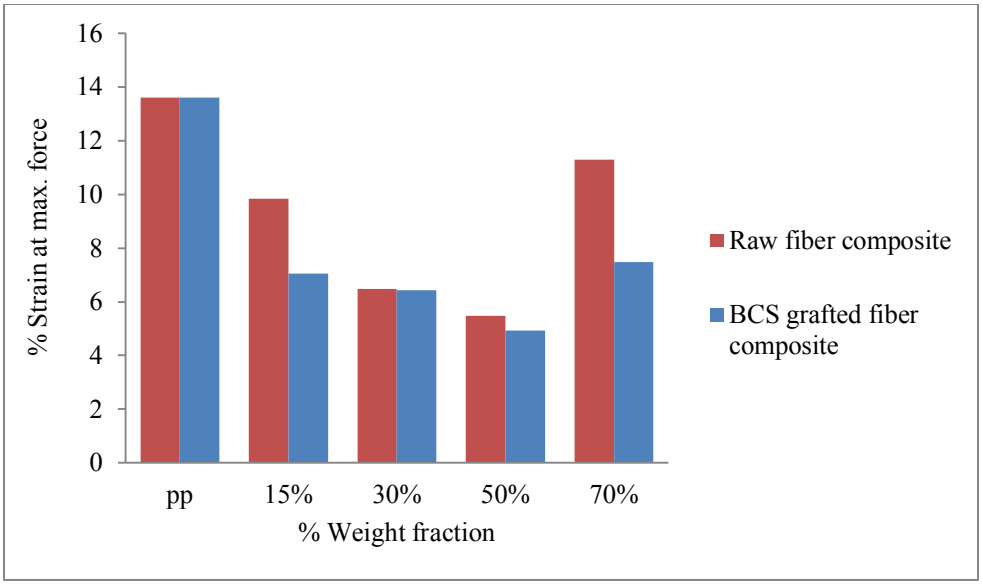

Figure 4.94 Strain to failure vs weight fraction graph for raw and modified fiber composite where the strain to failure decreased with increase in weight fraction of fiber.

The Young's modulus of the BCS+$NaHCO_3$ treated composites was higher as compared to the raw sample composite. Similar trend was observer in the tensile strength and strain to failure.

After certain fiber loading, the tensile strength and Young's modulus decreased. This trend may due to the poor adhesion between the fiber and the matrix. However, the value obtained is considerable for medium load bearing situation. For poor fiber matrix adhesion, results a loose bundle, embracing a lower aspect ratio with less reinforcing potential than a single fiber. In addition the bundle itself may be low in strength due to poor adhesion (Ping et al. 2011).

The graft copolymerization reaction of BCS+$NaHCO_3$ on to cellulose backbone is affected by the diffusion of monomer into the fiber, the swelling of trunk polymer and the effect of solvent on graft polymer radicals. Swelling of the fiber on bulk monomer increase the cross section of the fiber at the same time the fiber surface become luster. As a result monomer can easily diffuse in the fiber and react with cellulose in lower swelling time. In higher swelling time, the fiber become twisted, shrinkage and change its outer febrile layer (Khan et al. 2007).

In order to observe the variation of composite properties against fiber orientation, three different fiber orientations were chosen: 0^0, 45^0, and 90^0 during bamboo fiber based composite fabrication. Variations of tensile properties of bamboo composites prepared at different fiber orientation are shown in Figures 4.95 to 4.97. Specimens of unidirectional bamboo fiber based reinforced composite with PP were tested for all the four elastic constants: longitudinal modulus, transverse modulus, Poisson's ratio and shear modulus and for tensile strengths in longitudinal direction. The values of such parameters for unidirectional bamboo fiber reinforced PP composite results as summarized are: the Young's modules for UD+UD+UD was the highest (1040 MPa). When the composite was fabricated as UD+45^0+UD, the value decreased to 954 MPa and lowest value was found for UD+45^0+90^0.

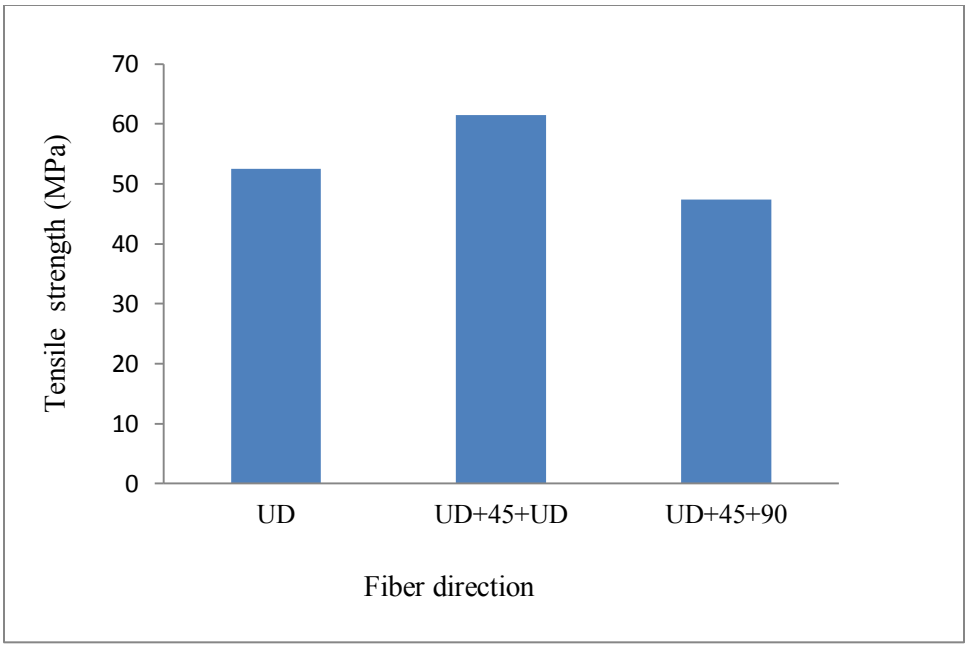

.
Figure 4.95 Variation of tensile strength at fiber orientation for raw fiber composite.

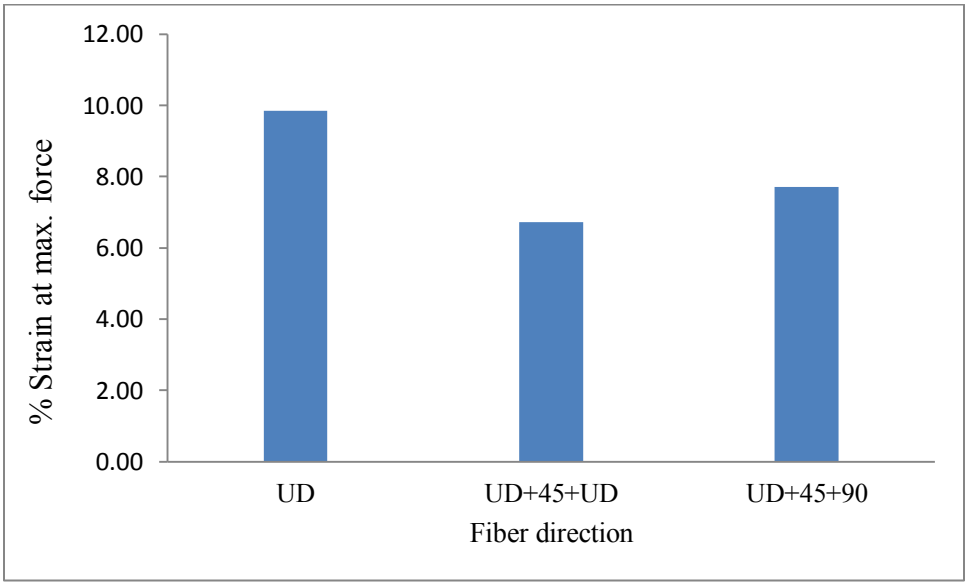

Figure 4.96 Variation of strain at maximum force with different fiber orientation for 15% raw fiber composite.

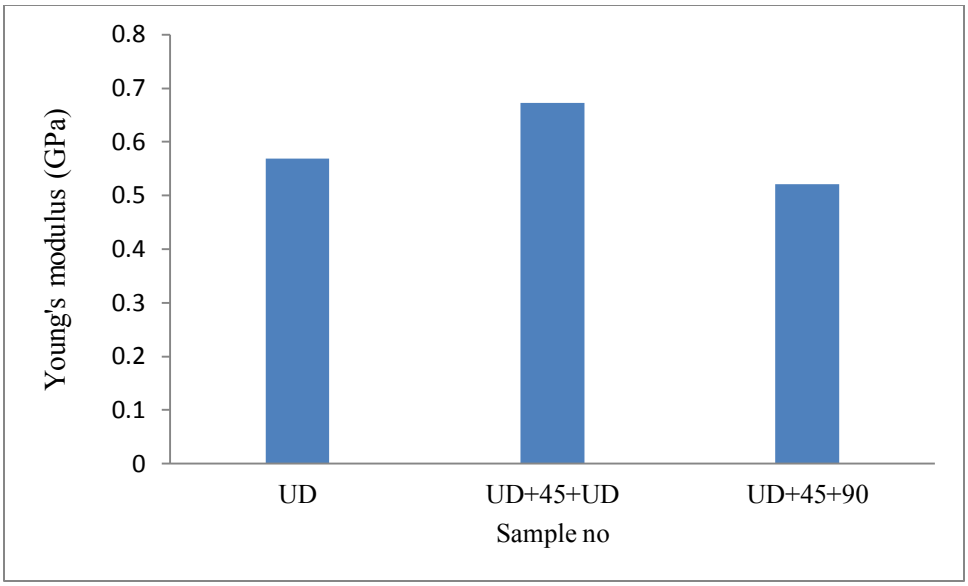

Figure 4.97 Variation of Young's modulus at different fiber orientation for 15% raw fiber composite.

Chemical modification of bamboo fiber removed the hemicellulose and lignin, as well as the internal constrain. As a result, the fibrils became more capable of rearranging themselves in a compact manner. This leads to the close packing of the cellulose chain, which caused in the improvement in the fiber strength and other mechanical properties. This is also responsible for the increase in the crystallinity of the BCS treated sample as supported by the XRD analysis (Pó et al. 1994).

Impact properties

Variation of the impact strength of raw and modified bamboo fiber reinforced PP composites against fiber wt% is shown in Figure 4.98. The impact strength of the composite increased with fiber loading (Hydar et el. 2009). After treatment, the strength increased compared to the PP and raw fiber based composite. As far as the void content in the natural fiber composite is concern, the fabrication technique is not fully developed and natural origin of the fiber component necessary reduces an element of the variation to the composite; both factors contributes in creation of voids affecting to the overall properties of the composites. In the cross section of the fiber under SEM and image analysis, it is seen that in the treated sample are more compact

compared to the raw sample. The treated fiber also had more solid content phase compared the raw fiber. May be for this reason the impact strength was higher in treated fiber composite compared to in the raw fiber composite (Rodrlguez et al. 1995).

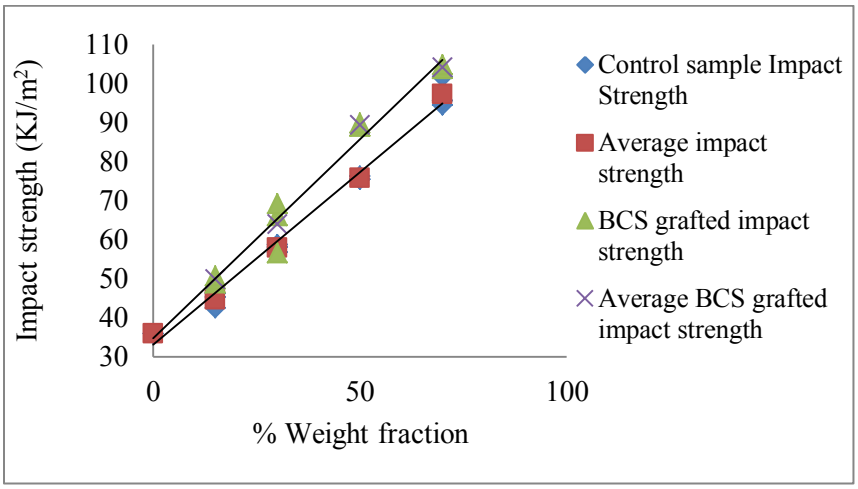

Figure 4.98 Variation of impact strength vs weight fraction graphs for raw and treated fiber composite.

The impact strength of the fiber reinforced composite depend on the nature of the fiber, polymer and fiber-matrix interfacial bonding. It has been reported that higher fiber content increases the probability of fiber agglomeration, which results in region of stress concentration require less energy for crack propagation. As presented in the Figure 4.98 impact strength of all composites increased with fiber loading. These results suggested that the fiber was capable of absorbing load because of strong interfacial bonding between the fiber and the matrix (Satyanarayana et al. 1993). Another factor if impact failure of the composite is fiber pull out. With increase in the fiber loading, more force is required for fiber pull out. This consequently increases the impact strength.

4.6.2 Fracture surface

SEM micrographs of tensile fracture surface of raw and treated composites are shown in Figure 4.97. With increase in the fiber weight fraction, the fiber content in the surface of the raw fiber composite increased. Similar results were obtained in the treated bamboo fiber composites.

During processing fiber tend to orient along the flow of the matrix causing the mechanical properties to vary in different directions. Fibers were elongated and finally broke down which is shown as fiber pull out. When the fiber was positioned along the tensile test direction, the fibers as well as the matrix bear the load. SEM observation was similar with previous research (Zhidan et al. 2007; Ashish et al. 2011; Yuanyuan et al. 2011).

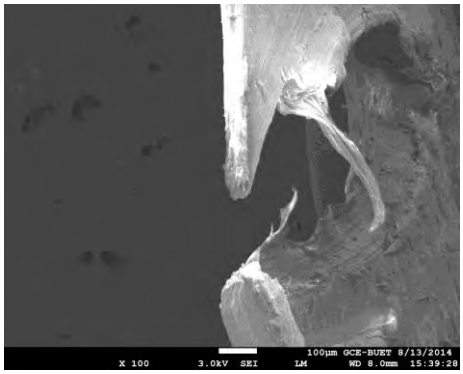

Figure 4.99 Scanning electron micrographs of tensile fracture surface of PP.

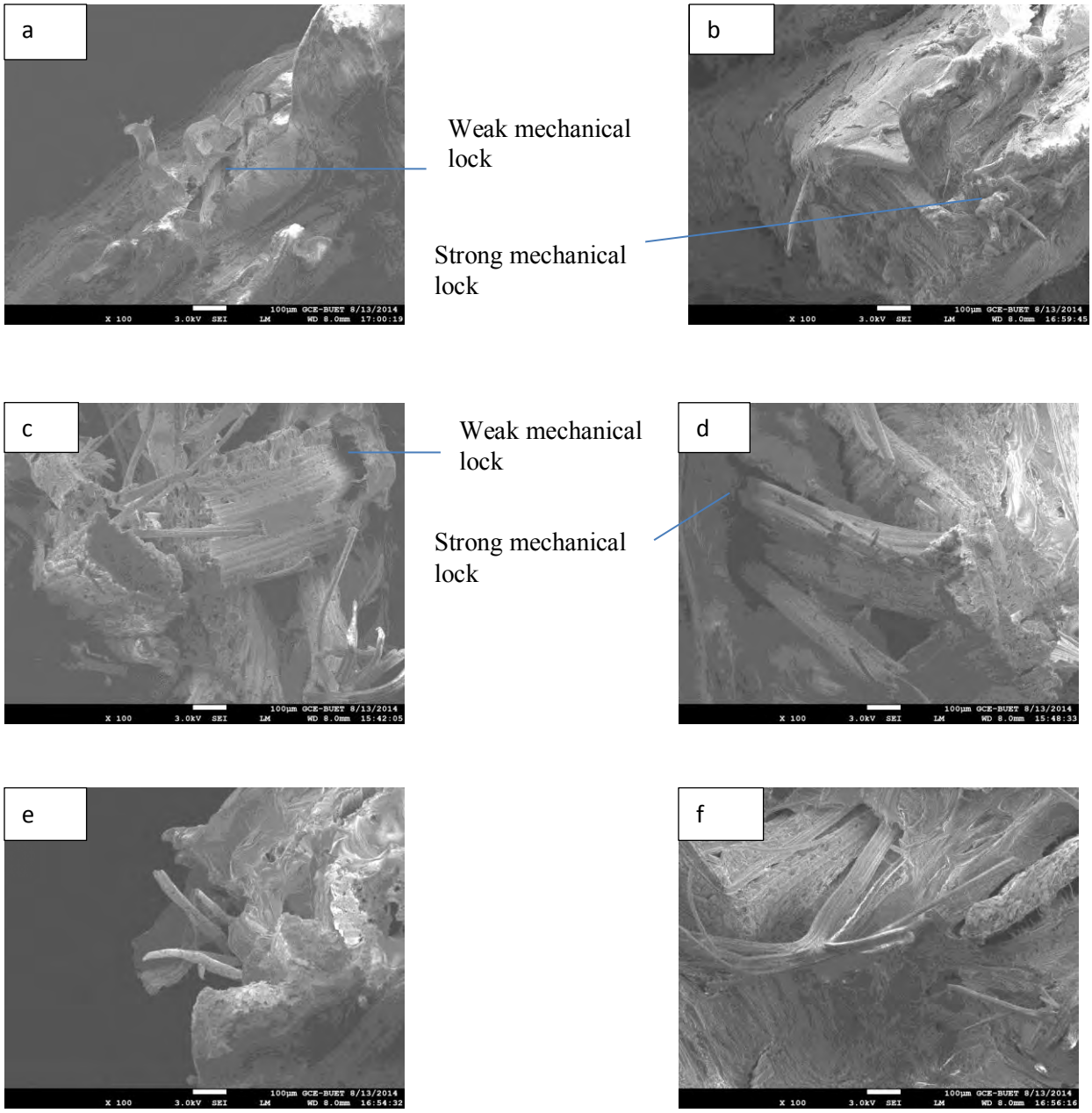

Figure 4.100 Scanning electron micrographs of tensile fracture surface of (a) 15% raw fiber composite (b) 15% BCS grafted fiber composite (c) 30% raw fiber composite (d) 30% BCS grafted fiber composite (e) 50% raw fiber composite (f) 50% BCS grafted fiber composite.

Optical images of tensile fracture surface were taken for better understanding of fiber matrix interlocking. It is well known that, with effective bonding of fiber with matrix, strong interfacial adhesion can be achieved and interfacial interactions will result a good mechanical properties for

the composite. Therefore, the optical images studies support the tensile and impact testing results. In the unidirectional fiber oriented composite, there was enhanced interactions between the reinforcement and matrix and fiber distribution became more uniform in matrix. Better distribution of bamboo fiber in the PP matrix in horizontal position and in in fiber matrix interface surface are shown in Figures 4.100(a) and 4.100(b) respectively. The possible mechanism of interaction between the fiber and PP matrix can be explained to the formation of hydrogen bonds in the interfacial region, for instance, between the hydroxyl (-OH) groups of cellulose or its counterpart lignin in bamboo fiber with the anhydride groups in the PP matrix (Xiaoya et al. 1998). Furthermore, it was found that PP had crystallized on the bamboo surface, so that the bamboo fiber acted as both reinforcing agent and nucleator for PP.

With increase in the fiber content, the mechanical properties of the composites varied. Those findings are supported by optical micrographs shown in Figures 4.101 to 4.103 for 30, 50 and 70 fiber wt% composites. The tensile strength and the Young's modulus were found to increase upto 50% and again decreased at 70%. In Figure 4.102 for 50% fiber weight fraction, the fracture surface was more conical shear deformation of matrix than 15% and 30% weight fraction composite. This change in topography due to large plastic deformation is indicating the better interface bonding of fiber with matrix in 50% fiber fraction composite. For this reason 50% fiber fraction has the better mechanical properties.

During fabrication of composites, fiber orientation was varied at UD+45^0+UD and UD+45^0+90^0 for attaining better mechanical properties. Figures 4.95 and 4.97 show the variation of tensile strength and Young's modulus of various fiber orientated samples. Figures 4.106 to 4.109 are representing the optical micrographs of BCS grafted fiber PP composite manufactured using differently oriented fibers. In Figure 4.104 the load was bearded by UD fiber and 45 degree oriented fiber. Because of non-uniformity in the dispersion of fiber, crack propagation increased in the UD+45^0+90^0 composite. As a result, mechanical properties were also found to be decreased as compared to the UD+UD+UD and UD+45^0+UD. In UD+45^0+90^0 composite, PP was bearing the load after fracture of fiber. This in turn increased the strain at maximum force. Again from the horizontal and surface fracture, it was observed that fiber and PP interface had

formed more conical shape than the raw sample reinforced sample. For that reason better mechanical properties was observed in BCS grafted fiber reinforced composite.

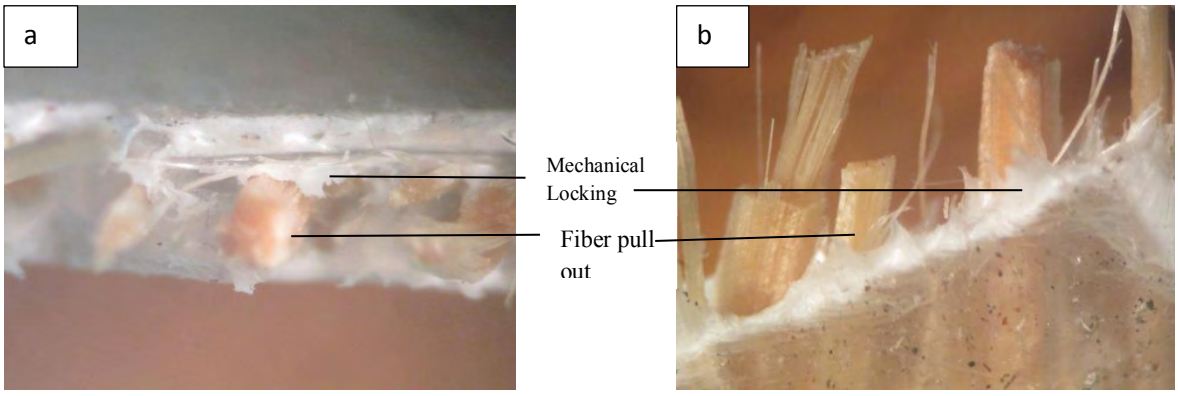

Figure 4.101 Optical micrographs of tensile fracture surface of (a) horizontal and (b) surface for 15% raw bamboo fiber containing composite.

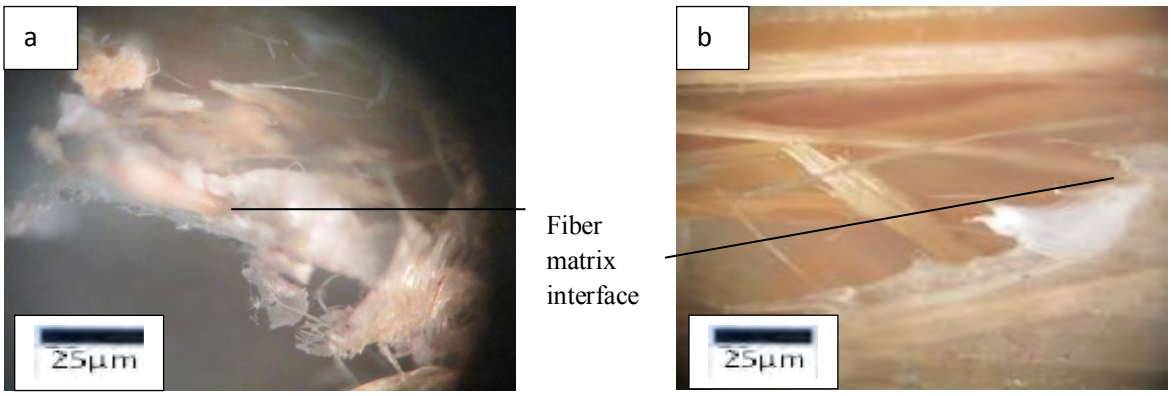

Figure 4.102 Optical micrographs of tensile fracture surface of (a) horizontal and (b) surface for 30% raw bamboo fiber containing composite.

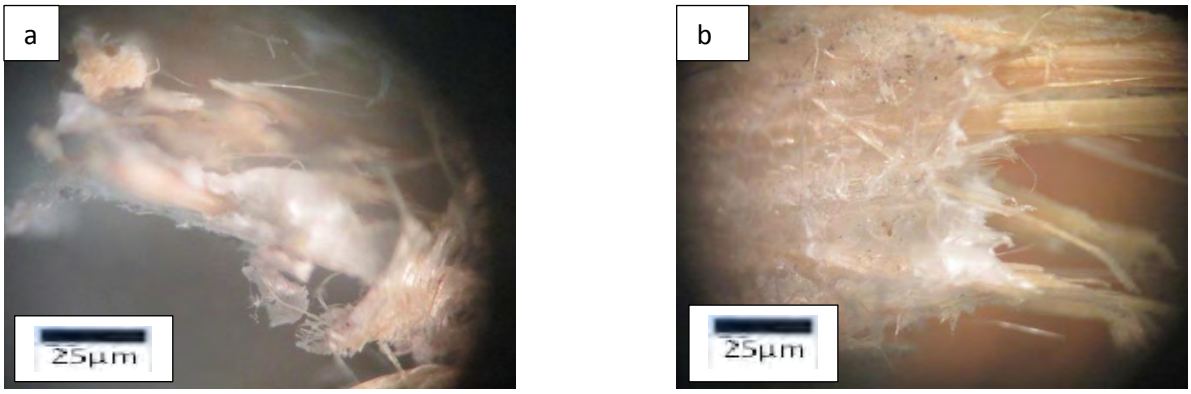

Figure 4.103 Optical micrographs of tensile fracture surface of (a) horizontal and (b) surface for 50% raw bamboo fiber containing composite.

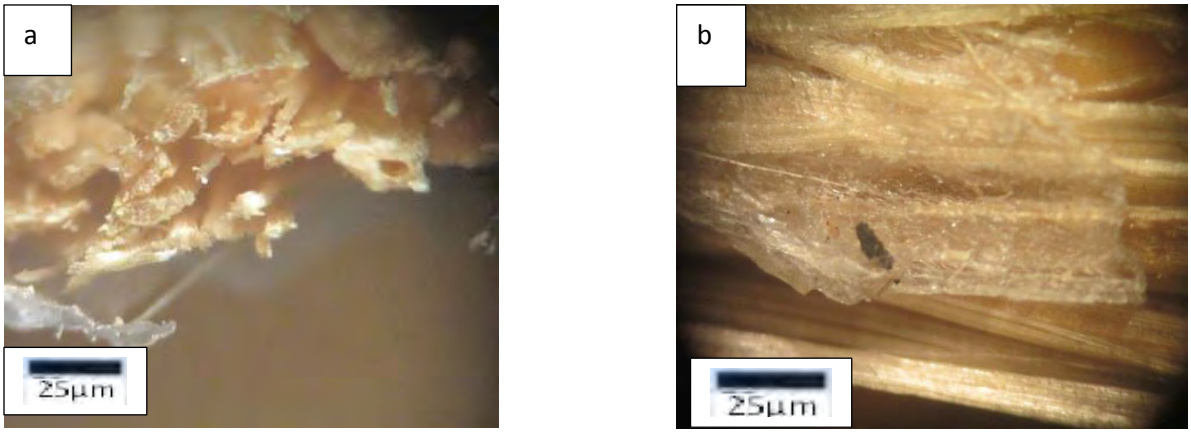

Figure 4.104 Optical micrographs of tensile fracture surface of (a) horizontal and (b) surface for 70% raw bamboo fiber containing composite.

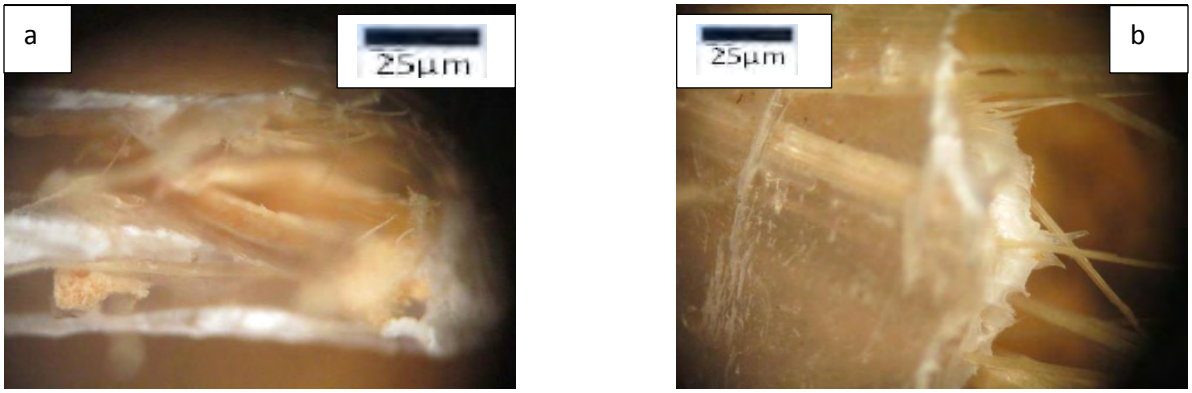

Figure 4.105 Optical micrographs of tensile fracture surface of (a) horizontal and (b) surface for UD+45^0+UD raw bamboo fiber containing composite.

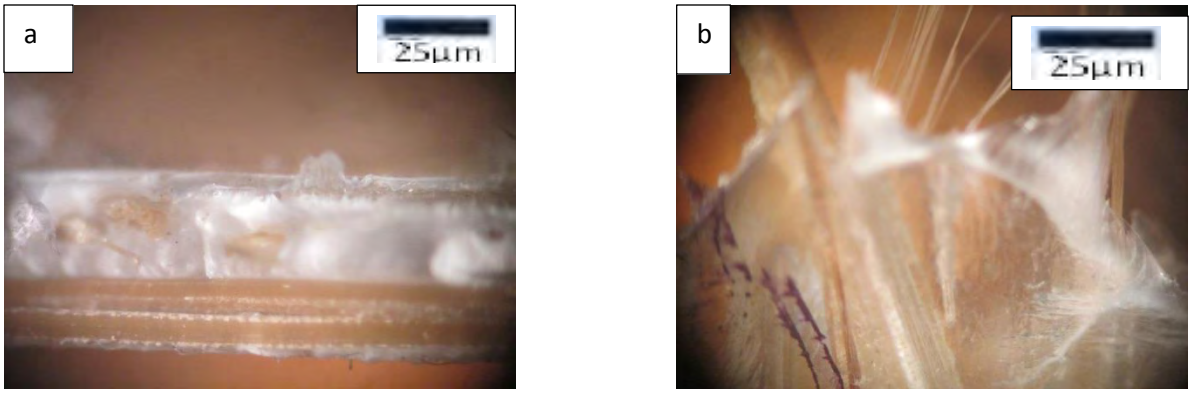

Figure 4.106 Optical micrographs of tensile fracture surface of (a) horizontal and (b) surface for UD+45^0+90^0 raw bamboo fiber containing composite.

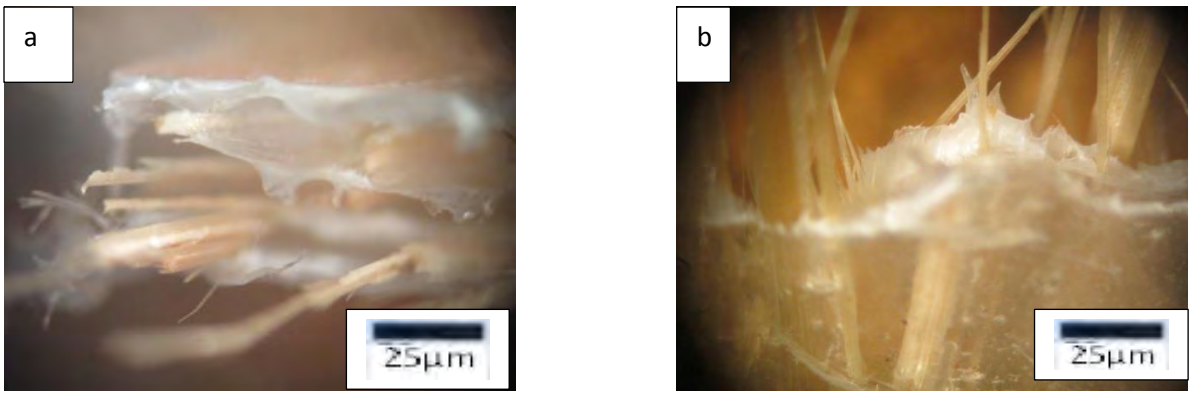

Figure 4.107 Optical micrographs of tensile fracture surface of (a) horizontal and (b) surface for 15% BCS grafted bamboo fiber containing composite.

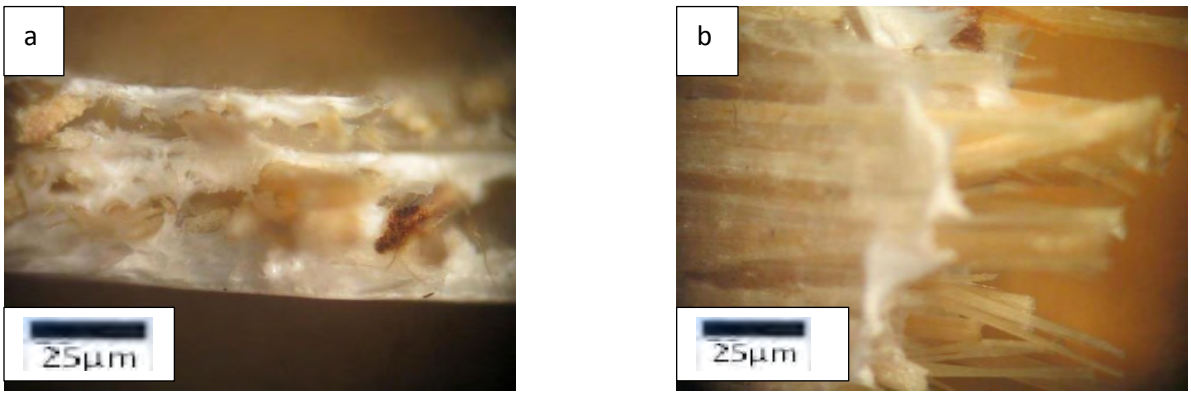

Figure 4.108 Optical micrographs of tensile fracture surface of (a) horizontal and (b) surface for 30% BCS grafted bamboo fiber containing composite.

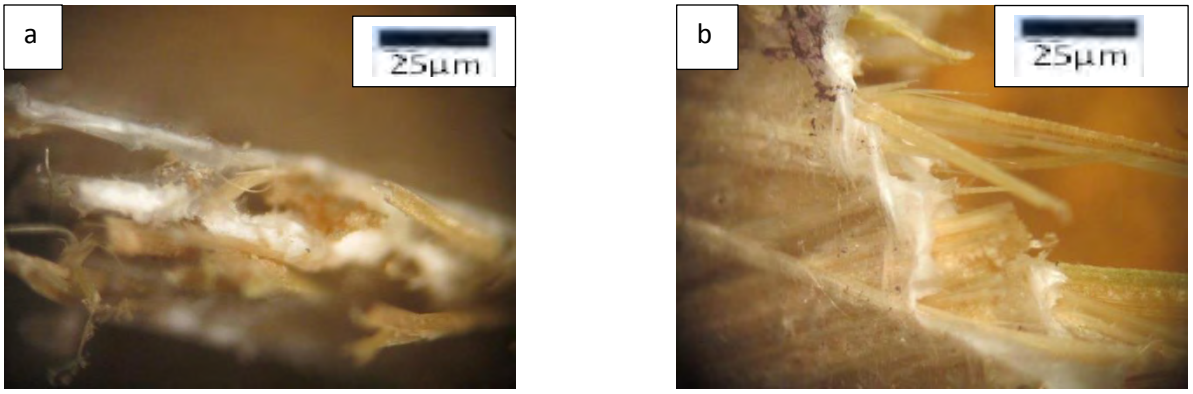

Figure 4.109 Optical micrographs of tensile fracture surface of (a) horizontal and (b) surface for 50% BCS grafted bamboo fiber containing composite.

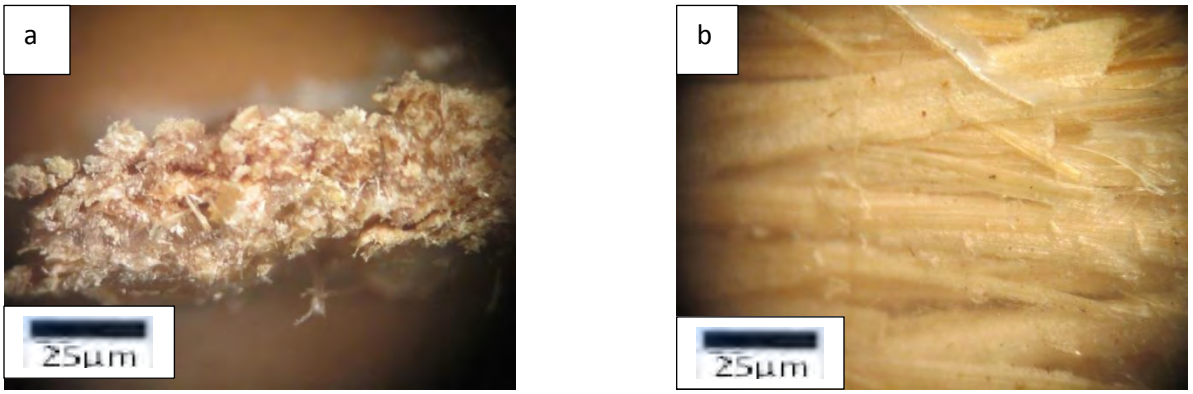

Figure 4.110 Optical micrographs of tensile fracture surface of (a) horizontal and (b) surface for 70% BCS grafted bamboo fiber containing composite.

4.6.3 Fourier Transform Infra-Red analysis results

Figure 4.110 shows the FTIR of raw fiber, PP and composite spectrum. The FTIR observation of treated sample composite reveals that the bamboo fiber and the matrix formed bond in between them. Treated bamboo fiber formed bond with carbonyl group of the matrix, which is in increasing trend. Other peaks in different wavelength were changed with composite preparation (Rumana et al. 2010). Most of the observed peaks of bamboo represent major cell wall components such as cellulose 1,154cm^{-1}, 898 cm^{-1}, hemicelluloses 1,738, 1,024, 1,057, 1,090 cm^{-1} and lignin 1,596, 1,505, 1,270 cm^{-1}. Although the bamboo fiber spectra are very similar to

composite spectra, closer inspection revealed some differences in 972 cm^{-1},1160 cm^{-1}, 1373 cm^{-1}, 1510 cm^{-1}, 2898cm^{-1} and 3340 cm^{-1} in compared to those of raw bamboo fiber peak. Peak arising at 1,626 cm^{-1} due to stretching vibration of C=O and peak at 781 cm^{-1} (unknown compounds) . The guaiacyl peaks was prominent at 1,330 (1,320) cm^{-1}, which indicates syringyl ring breathing with CO stretching was more pronounced in the spectra.

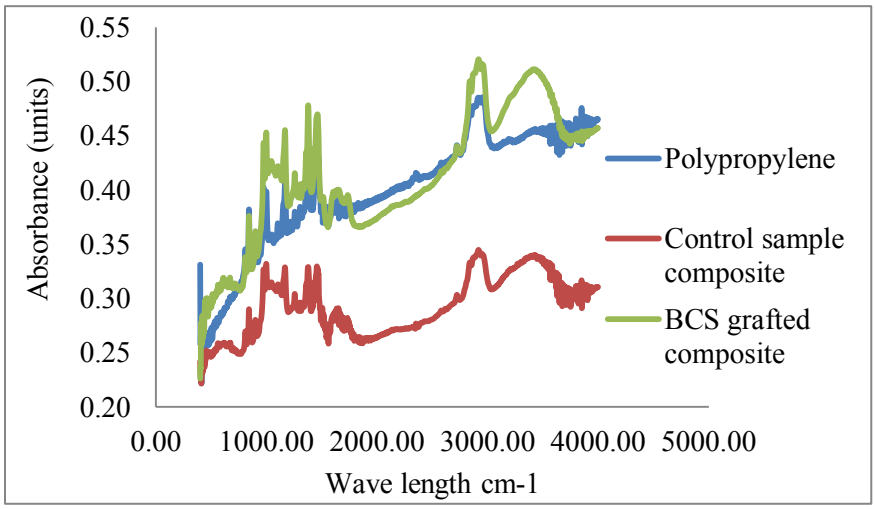

Figure 4.111 FTIR spectrum of the raw and treated bamboo fiber composite.

4.6.4 TGA study of composite

TGA study of matrix, fiber and composites were conducted under N_2 atmosphere. From the TGA curves (Figure 4.111), it can be said that thermal stability of fiber was higher compared to the PP matrix. Again thermal stability of the composite was higher compared to the fiber and matrix alone. This indicates that fiber matrix adhesion was strong and it required more energy to break the bond having more thermal energy.

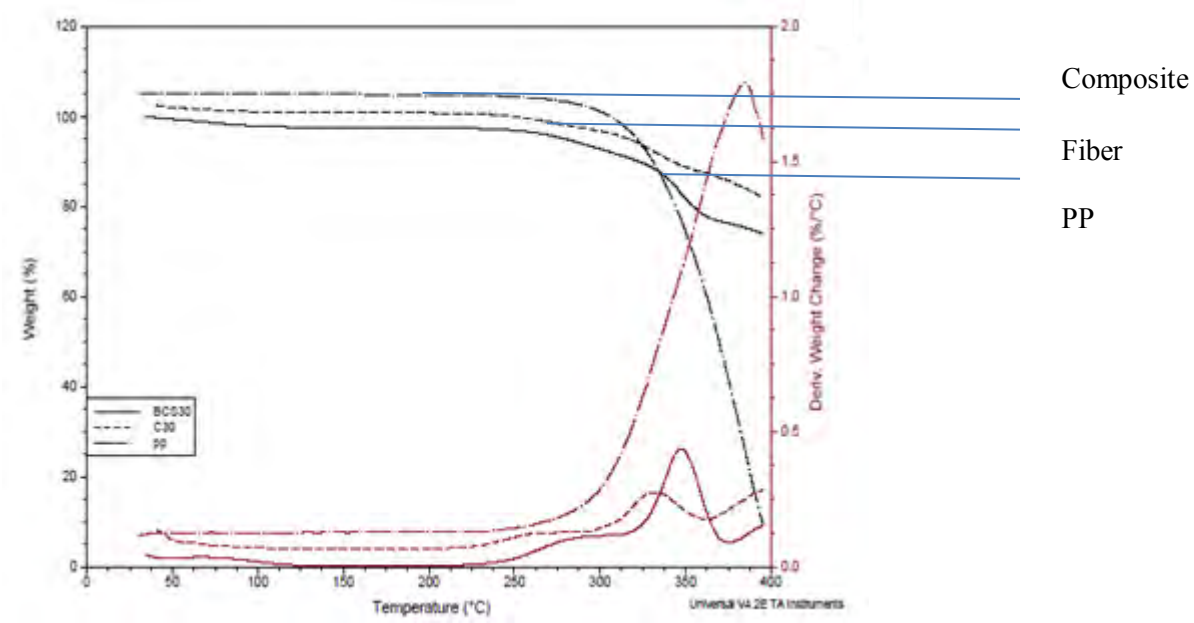

Figure 4.112 TGA spectrum of the PP, raw fiber and treated fiber composite.

When a composite is subjected to thermal testing, there is an increase in the rigidity of the fiber. During the initial stress related to structural rearrangements in the fiber, thermal activation of their visco-elastic properties occurs, over the temperature range from 30°C to 200°C. This corresponding to *in situ* relaxation of the constituent polymers (hemicelluloses and lignin) and a decrease in rigidity and endurance attributing to thermal degradation of the cellular walls at temperatures between 150°C and 180°C. Indeed, the bamboo fiber cell wall has a complex composition and organization. The polypropylene-bamboo fiber composite manufactured according to these criteria clearly demonstrates the potential for obtaining high performance materials.

Chapter 5
Conclusion and recommendation for future work

Conclusions

In the present study, tensile properties of single raw and modified bamboo fibers were carried out by varying span length. Surface morphology was observed under scanning electronic microscope (SEM). Thermal properties were measured using thermo gravimetric analysis (TGA). Structural analysis was carried out by Fourier transform infrared (FTIR) spectrophotometer. Water uptake test at different conditions was carried out for raw and modified bamboo fibers. Subsequently, bamboo fiber reinforced PP composites were manufactured by varying fiber loading and orientation. Mechanical, structural and thermal properties of manufactured composites were later determined. Based on the experimental results, the following conclusions are drawn:

- The Young's modulus increased, while the tensile strength and strain to failure decreased with increasing in span length for both raw and modified bamboo fiber. However, the Young's modulus became independent of span length after correction using newly developed equations. The basic chromium sulphate and sodium bi-carbonate doubly treated bamboo fiber was found better according to strength, modulus and strength to failure data.

- Thermogravimetric analysis (TGA) was used to monitor fiber decomposition as a function of increasing temperature. TGA result showed that the incorporation of treatment increased the thermal stability of bamboo fiber. While syntan absorbed fiber did not show any significant improvement compared to the raw fiber.

- Scanning electron microscopy (SEM) was used to show the surface morphology of raw and modified bamboo fiber. The surface roughness was found to decrease after modification. This is considered as a proof of surface coverage of the fiber with chemical layers.

- From XRD analysis, it is seen that the crystallinity index of bamboo fiber increased with modification. The increase in crystallinity obtained during double treatment with BCS in bamboo fiber is thought to be the main contributing factor of the increasing the fiber strength. Similar results were observed in the case of other modifications.

- The percentage of moisture absorption was high in the raw bamboo fiber. Moisture absorption rate was higher in the case 100 KGy radiation treatment, while the absorption rate was found to be very low in the syntan absorbed fiber.

- FTIR result showed that hydroxyl bond was found to decrease after modification. It also revealed that after each modification the peak height decreased.

- Among all, the BCS+$NaHCO_3$ double stage modified bamboo fiber had the best set of properties in terms of tensile strength, thermal stability and crystallinity. The leather waste chemicals were also reused along the way.

- Incorporation of BCS+$NaHCO_3$ modification resulted in better interfacial bond between the fiber and polypropylene matrix in composites.

Bamboo fiber reinforced PP composite showed an improvement in various properties compared to polypropylene alone

Recommendations for future work

The results documented in the current research are significant; however recommendations for further investigation are as follows:

1. The current research should be further developed using different species of technical bamboo fiber from different bamboo.

2. The current modification system should be further developed to improve the optimum condition of modification, especially for mimosa and syntan.

3. Weathering behaviour of the raw and modified technical bamboo fiber should be evaluated. The method of water retardant should be improved by chemical treatment.

4. Higher percentage of the fiber could be incorporated through modern machine during composite manufacturing. The extruder and injection moulding machine may be used in order to get better composites from chopped fiber. Hybrid approach could be adopted for enhancement of the mechanical properties and dimensional stability of the composite.

5. Lower percentage as nanofiber could be used as reinforcing agent during composites preparation.

Reference

Abd L.M., Mohd. T. M., Variation in Anatomical Properties of Three Malaysian Bamboos From Natural Stands, Journal of Tropical Forest Science, vol- 5, no-1, pp. 90-96,1992.

Abhijit P., Dehpande M., C. Bhaskar, Rao Lakshmana, Extraction of Bamboo Fibers and Their Use as Reinforcement in Polymeric Composites , Journal of Applied Polymer Science, vol-76, pp.83–92,2000.

Acid-insoluble lignin in wood and pulp, T 222 cm-98, 1998, TAPPI, USA.

Ahmad M., Kamke F.A., Analysis of Calcutta bamboo for structural composite materials: surface characteristics, Wood Science Technology, vol- 37, pp. 233–240, 2003.

Akpalu, Yvonne A., Scattering from Polymers, Polymer Reviews, vol-50, no-1, pp.1-13, 2010.

Alam M.M., Akhtar F., Mina M.F., Dafader N.C., Mustafa A.I., Studies of γ-Ray Induced Polymerization of Aqueous Acrylamide, Polymer-Plastics Technology and Engineering, vol-42, no- 2, pp.285-296, 2003.

Alpha cellulose in paper, T 429 cm-84, 1984, TAPPI, USA.

Alves, N.M. , Ribelles, J L. Gómez and Mano, J.F., Study of the Molecular Mobility in Polymers with the Thermally Stimulated Recovery Technique—A Review, Polymer Reviews, vol-45, no.2, pp.99-124, 2005.

Anna C., Emma L., Eva M., Grafting of cellulose by ring-opening polymerisation – A review, European Polymer Journal, vol- 48, pp.1646–1659, 2012.

Anuar H. and Zuraida A., Thermal Properties of Injection Moulded Polylactic Acid – Kenaf Fibre, Biocomposite, Malaysian Polymer Journal, vol-6, no-1, pp. 51-57, 2011.

Ash in wood, pulp, paper and paperboard: combustion at 525°C, T 211 cm-93, 1993,TAPPI, USA.

Ash in wood, pulp, paper and paperboard: combustion at 900°C, T 413 cm-93, 1993, TAPPI, USA.

Atanassov A., Genieva S., Vlaev L., Study on the Thermo-oxidative Degradation Kinetics of Tetrafluoroethylene-Ethylene Copolymer Filled with Rice Husks Ash, Polymer-Plastics Technology and Engineering, vol-49, no- 6, pp.541-554, 2010.

Athawale V.D., Rathi S.C., Graft Polymerization: Starch as a Model Substrate, Polymer Reviews, vol-39, no- 3, pp.445-480, 1999.

Barzin J., Azizi H., Morshedian J., Preparation of Silane-Grafted and Moisture Crosslinked Low Density Polyethylene. Part II: Electrical, Thermal and Mechanical Properties, Polymer-Plastics Technology and Engineering, vol-46, no- 3, pp.305 -310, 2007.

Basfar A.A., Ali K.M.I., Vaidya M.M., Bahamdan A.A., Alam M.A., Improved Ultraviolet (UV) Radiation Stability of the Polypropylene (PP) Films of Woven Jumbo Bags for Outdoor Applications, Polymer-Plastics Technology and Engineering, vol-49, no-8, pp.841-847, 2010.

Beckermann G., Performance of Hemp-Fiber Reinforced Polypropylene Composite Materials, Thesis Doctor of Philosophy, Materials and Process Engineering University of Waikato, 2007.

Bicerano J., Prediction of the Properties of Polymers from Their Structures, Polymer Reviews, vol-36, no-1, pp.161-196, 1996.

Bodirlau R., Teaca C.A., Fourier Transform Infrared Spectroscopy and Thermal Analysis of Lignocellulose Fillers Treated with Organic Anhydrides, Rom. Journ. Phys., vol. 54, No. 1–2, P. pp.93–104, 2009

Bruce F.X., Benjamin S., Gavin C., Zhou J., Koyfman I., Jamiolkowski D.D., Dormier E., Structure and Property Studies of Bioabsorbable Poly(glycolide-co-lactide) Fiber during Processing and in Vitro Degradation, Polymer, vol- 43, pp. 5527–5534, 2002.

Burger C., Hsia B., Chu B., Preferred Orientation in Polymer Fiber Scattering, Journal of Macromolecular Science, Polymer Reviews, Part C, vol-50, pp.91-111, 2010.

Cai Y., Yuan H., Junfeng X., Lei S., Weicheng F., Huaxia D., Xinglong G.,Zuyao Chen, Morphology, Thermal and Mechanical Properties of Poly (Styrene-Acrylonitrile) (SAN)/Clay Nanocomposites from Organic-Modified Montmorillonite, Polymer-Plastics Technology and Engineering, vol-46, no-5, pp.541 -548, 2007.

Carlmark A., Larsson E., Malmstrom E., Grafting of cellulose by ring-opening polymerization – A review, European Polymer Journal, vol- 48, pp.1646–1659, 2012.

Chattopadhyay S.K., Khandal R.K., Uppaluri R., Ghoshal A.K., Bamboo fiber reinforced polypropylene composites and their mechanical, thermal, and morphological properties, Journal of Applied Polymer Science, vol-119, pp.1619-1626, 2011.

Chauhan A., Kaith B., Synthesis, Characterization and Evaluation of the Novel Regenerated *Hibiscus Sabdariffa* –graft-(Acrylonitrile-co-Vinyl Monomer), Malaysian Polymer Journal, vol. 6, no. 1, pp 14-26, 2011.

Chen Q., Hanyu Xue H.,1 Lin J., Preparation of Polypropylene-graft-Cardanol by Reactive Extrusion and Its Composite Material with Bamboo Powder, Journal of Applied Polymer Science, vol. 115, pp.1160–1167, 2010.

Covington T., Vegetable Tanning, Tanning Chemistry-The Science of Leather, The Royal Society of Chemistry, Cambridge, UK , RSC Publishing, ,Ch.13, sec.13.2, pp.281-284, 2011.

Dai D., Fan M., Characteristic and Performance of Elementary Hemp Fibre Materials Sciences and Applications, vol- 1, pp. 336-342, 2010.

Effen berger F., Schweizer M., and Mohamed,W.S., Effect of Montmorillonite Clay Nanoparticles on the Properties of Polypropylene Fibres, Polymer-Plastics Technology and Engineering, vol-49, no-6, pp.525-530, 2010.

El-Zaher N.A., Study of the Effect of Ultraviolet Radiation on Some Physical Properties of Dralon Fabric, Polymer-Plastics Technology and Engineering, vol-40, no-5, pp.689-702, 2001.

en.silvateam.com/Products-Services/Leather/.../Mimosa-extracts date on issue 14.8.2010.

en.wikipedia.org/wiki/Tannin date on issue 14.7.12

en.wikipedia.org/wiki/Tannin issue date 25.6.2012

Fu B. X., Hsiao B.S., Chen G., Zhoub J., Koyfman I., Jamiolkowski D.D., Dormier E., Structure and Property Studies of Bioabsorbable Poly(glycolide-co-lactide) Fiber During Processing and in vitro Degradation, Polymer, vol-43, pp.5527–5534, 2002.

Ghavami C.S., Rodrigues S., Paciornik, Asian Journal of Civil Engineering (Building and housing) Bamboo: Functionally Graded Composite, Materia K, vol- 4, no-1, pp.1-10, 2003.

Ghavami K., Rodrigues C.S. and Paciornik S., Bamboo; Functionally Graded Composite Material, Asian Journal of Civil Engineer (Building and Housing), vol- 4, no-1, pp.1-10, 2003

Ghoshal A.K., Chattopadhyay S.K., Khandal R.K., Uppaluri R., Bamboo fiber reinforced polypropylene composites and their mechanical, thermal, and morphological properties, J. of App. P. Sci., vol-119, pp.1619-1626, 2011.

Goettler L.A., Lee K.Y., and Thakkar H., Layered Silicate Reinforced Polymer Nanocomposites: Development and Applications, Polymer Reviews, vol-47, no-2, pp.291-317, 2007.

Gustavson K.H., The vegetables tannages, The chemistry of tanning process, Academic press Inc, New York, USA, Ch.5, sec.1,2, pp. 142-147, 1956.

Han G., Lei Y., Wu Q., Kojima Y., Suzuki S., Bamboo–Fiber Filled High Density Polyethylene Composites: Effect of Coupling Treatment and Nanoclay, Journal of Polymer Environment, vol-16, pp.123–130, 2008.

Haque M.A., M.U. Ahmad, M. A. Khan, S. M. A. Raihan, N. C. Dafader, Studies on the Physicochemical Properties of Natural Rubber/Polyethylene Blends and the Impact of Radiation on Their Properties, Polymer-Plastics Technology and Engineering, vol- 49, pp. 1010–1015, 2010.

Hassan M.M., M. Rabiul Islam, Mubarak A. Khan, Surface Modification of Cellulose by Radiation Pretreatments with Organo-Silicone Monomer, Polymer-Plastics Technology and Engineering, vol-44, no- 5, pp.833-846, 2005.

Hassan M.M., M. Rabiul Islam, S. Shehrzade, Mubarak A. Khan, Influence of Mercerization Along with Ultraviolet (UV) and Gamma Radiation on Physical and Mechanical Properties of Jute Yarn by Grafting with 3-(Trimethoxysilyl) Propylmethacrylate (Silane) and Acrylamide Under UV Radiation, Polymer-Plastics Technology and Engineering, vol-42, no- 4, pp.515-531, 2003.

Haydar U.Z., Ruhul A.K., Mubarak A.K., and Shamim P., Comparative Studies of Mechanical and Interfacial Properties Between Jute and E-glass Fiber-reinforced Polypropylene Composites, Journal of Reinforced Plastic and composites, vol. 29, No.7, pp. 1078-1088, 2009.

Haydaruzzaman, Khan A.H., Hossain M.A., Khan M.A., Khan R.A., Hakim M.A., Effect of Ultraviolet Radiation on the Mechanical and Dielectric Properties of Hessian Cloth/PP Composites with Starch, Polymer-Plastics Technology and Engineering, vol-49, no- 8, pp. 757-765, 2010.

Haydaruzzaman, Khan R.A., Khan M.A., Khan A.H., Hossain M.A., Effect of gamma radiation on the performance of jute fabrics-reinforced polypropylene composites, Radiation Physics and Chemistry, vol-78, pp. 986–993, 2009.

Hazrat M.A., Organic Spectroscopy, Science view publication, pp.140-170, 2013.

Hidayat B.J., Felby C., Johansen K.S., Thygesen L.G., Cellulose is not Just Cellulose: A Review of Dislocations as Reactive Sites in the Enzymatic Hydrolysis of Cellulose Microfibrils, Cellulose, vol-19, pp.1481–1493, 2012.

Higuchi A., Tamai M., An K.Y., Ichi T., Hsuan W., Benny D.F., Tang B.J., Yung C. and Dong L.C., Polymeric Membranes for Chiral Separation of Pharmaceuticals and Chemicals', Polymer Reviews, vol-50, no-2, pp.113-143, 2010.

Hocking, Philippa J., The Classification, Preparation, and Utility of Degradable Polymers, Polymer Reviews, vol-32, no-1, pp.35-54, 1992.

Hsiao B.C., Benjamin S. and Benjamin C., Preferred Orientation in Polymer Fiber Scattering, Polymer Reviews, vol-50, no- 1, pp. 91-111, 2010.

http://ncatlab.org/nlab/show/fiber+bundle#vector_bundles date issued on 15.01.2014

http://www.google.com/search?q=chemical+structure+of+syntan&start date on issue 06.08.2012

Huq T., Avik K., Nazia N., Saha M., Ruhul A.K., Mubarak A.K., Mushfequr R., Mustafizur R., Fabrication and Characterization of Jute Fiber-Reinforced PET Composite: Effect of LLDPE Incorporation, Polymer-Plastics Technology and Engineering, vol-49,no- 4,pp. 407- 413, 2010.

Hydaruzzaman, Performance of Photocured Jute Yarn with 1,6-Hexanediol Diacrylate (HDDA), Polymer-Plastics Technology and Engineering, vol-42, no-5, pp.795-810, 2003.

Ismail M.N., Turky G.M., and Nada, A.M.A., Electrochemical Behavior of Natural Rubber-Lignocelluloic Material Composite, Polymer-Plastics Technology and Engineering, vol-39, no- 2, pp.249-263, 2000.

Jian S.X., Zahang Q.S., Shen Q., Jian S.H., On structure, production and market of bamboo based panels in China, Journal of Forestry Research, vol-13, no-2, pp.151-156, 2002.

John C.K., Nadguada R.S., Review In *vitro*-induce Flowering in Bamboos, In vitro cell div.,Book_plant, vol-95, pp.309 -3151999.

Jue J.S., Shen Z.Q., Shi J., On Structure, Production, market of Bamboo Based Panel, Journal of Forestry Research , vol-13, no-2, pp.151-156, 2002.

Julien R., Hiroyuke Y., Bernard T., Growth Stress and Cellulose Structural Parameters in Tension and Normal Wood From Three Tropical Rainfrost Angiosperm Species, Bioresources, vol-2, no-2, pp.235-251, 2007.

Kandola B.K., Horrocks A.R., Price D., and Coleman G.V., Flame-Retardant Treatments of Cellulose and Their Influence on the Mechanism of Cellulose Pyrolysis, Polymer Reviews, vol-36, no-4, pp.721-794, 1996.

Kazuhiro M., Akiyoshi S., Motoyuki S., Measurement of the Hydrothermal Reaction Rate of Cellulose Using Novel Liquid-Phase Thermogravimetry, Thermochimica Acta ,vol-348, pp.69-76, 2000.

Kazuya O., Toru F.T, Yamamoto Y., Development of Bamboo-Based Polymer Composites and Their Mechanical Properties, Composites: Part A, vol-35, pp. 377–383, 2004.

Khan M.A. , Islam T., Rahman M., Arifur J.M.M. , Khan, R.A. , Gafur, M.A. , Mollah, M.Z.I. and Alam, A.K.M., Thermal, Mechanical and Morphological Characterization of Jute/Gelatin Composites, Polymer-Plastics Technology and Engineering, vol-49, no-7, pp.742-747, 2010.

Khan M.A., Hassan M.M. , Ara J. and Mustafa A.I., Surface Modification of Sisal (Agavae sisalana) Fiber by Photocuring: Effect of Additives, Polymer-Plastics Technology and Engineering, vol-46, no-5, pp. 447-453, 2007.

Khan M.A., Khan R. A., Haydaruzzaman, Ghoshal S., Siddiky M. N. A. and Saha, M., Study on the Physico-Mechanical Properties of Starch-Treated Jute Yarn-Reinforced Polypropylene Composites: Effect of Gamma Radiation, Polymer-Plastics Technology and Engineering, vol-48, no-5, pp.542-548, 2009.

Khan R.A., Mubarak A.K. , Haque N., Abdullah A.K., , M. N. Alam, M. Z.Abedin, Jute Reinforced Polymer Composite by Gamma Radiation: Effect of Surface Treatment with UV Radiation, Polymer-Plastics Technology and Engineering, vol-45, no- 5, pp. 607-613, 2006.

Khan R.A., Mubarak A.K., Hassan M.M., Jasmin A., Mustafa A.I., Surface Modification of Sisal (Agavaesisalana) Fiber by Photocuring: Effect of Additives, Polymer-Plastics Technology and Engineering, vol-46, no- 5, pp.447- 453, 2007.

Krause J.Q., Ghavami K., Transversal Reinforcement in bamboo Culms, Proceedings of the 11th International Conference on Non-conventional Materials and Technologies (NOCMAT 2009) 6-9 September 2009, Bath, *UK*

Kumaraswamy, Guruswamy, Crystallization of Polymers from Stressed Melts, Polymer Reviews, vol-45, no-4, pp.375-397, 2005.

Kushwaha, Pradeep K. and Kumar, Rakesh, Studies on Water Absorption of Bamboo-Polyester Composites: Effect of Silane Treatment of Mercerized Bamboo, Polymer-Plastics Technology and Engineering, vol-49, no-1, pp.45-52, 2010.

Li N.P, Long J.B, Lin, Wang L. , Zhong S. , Experimental and Theoretical Study on Thermal and Moisture Characteristics of New-Type Bamboo Structure Wall, J. Central South University,vol-19, pp.600-608, 2012.

Lohse, David J., The Influence of Chemical Structure on Polyolefin Melt Rheology and Miscibility, Polymer Reviews, vol-45, no-4, pp.289-308, 2005.

Mahuya D., Debabrata C., Influence of Alkali Treatment on the Fine Structure and Morphology of Bamboo Fibers, Journal of Applied Polymer Science, vol-102, pp.5050–5056, 2006.

Mahuya D., Debabrata C., The Effect of Alkalization and Fiber Loading on the Mechanical Properties of Bamboo Fiber Composites, Part 1: – Polyester Resin Matrix , Journal of Applied Polymer Science, vol. 112, pp.489–495, 2009.

Mahuya D., Debabrata C., Thermogravimmetric Analysis and Weather Study by Water Immersion of Alkali Treated Bamboo Strips, Bioresources, vol-3, no-4, pp. 1051-1061, 2009.

Mangesh D.T., Javed S., Graft Copolymerization of Acrylamide onto Bamboo Rayon and Fiber Dyeing with Acid Dyes, Iran Polymer Journal, vol-21,pp. 43–49, 2012.

Mari G., Cellulose Derivatives: Synthesis, Properties and Applications, Laboratory of Organic Chemistry, Department of Chemistry, Faculty of Science, University of Helsinki Finland, Helsinki, 2009.

Martin, J.R., Johnson J.F. and Anthony R.C., Mechanical Properties of Polymers: The Influence of Molecular Weight and Molecular Weight Distribution, Polymer Reviews, vol-8, no-1, pp.157-199, 1972.

Michael L., Celllulose a nanostructured polymer- a short review, Bioresoure, vol-3, no-4, pp.1403-1418, 2008.

Mishra M.K., Graft Copolymerization of Vinyl Monomers onto Cellulose and Cellulosic Materials, Polymer Reviews, vol-22, no-3, pp.471-513, 1982.

Mizi F., Dasong D., Biao H., Fourier Transform Infrared Spectroscopy for Natural Fibers , Vibration Spectroscopy, vol-55, no-2 , pp.300-306, 2011.

Mo Z. and Zhang H., The Degree of Crystallinity in Polymers by Wide-Angle X-Ray Diffraction (WAXD), Polymer Reviews, vol-35, no- 4, pp.555-580, 1995.

Moe M.T., Kin L., Durability of Bamboo-Glass Fiber Reinforced Polymer Matrix Hybrid Composites, Composites Science and Technology. vol-63, pp. 375–387, 2003.

Mohanty A.K. and Misra, M., Studies on Jute Composites—A Literature Review, Polymer- Plastics Technology and Engineering, vol-34, no-5, pp.729-792, 1995.

Moisture in pulp, paper and paperboard, T 412 cm-94, 1994, TAPPI, USA .

Mokhtar S.M., Mostapha T.B., Sabaa M.W., γ-Radiation induced Graft Copolymerization of N-phenyl- and N-p-hydroxyphenylmaleimide onto Cotton Fabrics, Polymer-Plastics Technology and Engineering, vol-41, no- 1, pp.183-197, 2002.

Mubarak A.K., Jahid M. M.I., Arifur M.R., Ruhul A.K and Tuhidul I. Study on the Effect of Urea on the Mechanical and Morphological Properties of Jute/Gelatin Composites, Polymer- Plastics Technology and Engineering, vol-49, no-9, pp.885-891, 2010.

Mubarak A.K., Ruhul A.K., Aliya B.S., Nasreen Z., Effect of the Pretreatment with UV and Gamma Radiations on the Modification of Plywood Surface by Photocuring with Epoxy Acrylate, Journal of Polymers and the Environment, vol-14, no-1, pp. 123-145, 2006.

Mubarak A.K., Ruhul A.K., Effect of Gamma Radiation on the Physico-Mechanical and Electrical Properties of Jute Fiber-Reinforced Polypropylene Composites Journal of Reinforced Plastics and Composites, vol- 28, no- 13, pp.1651-1660, 2009.

Mubarak A.K., Surface Modification of Sisal (Agavaesisalana) Fiber by Photocuring: Effect of Additives Polymer-Plastics Technology and Engineering, vol-46, pp- 447–453, 2007.

Muller G., Schopper C., Boss H., Kharazipour A., Polle A., FTIR-ATR Spectroscopy changes in wood properties during particle and fiber board production of hard and soft wood properties, Bioresource, vol-4, no-1, pp. 49-71, 2009.

Nada A.A.M.A., Kady M.Y.E., Sayed E.S.A., Amine F.M., Preparation and Characterization of Microcrystaline Cellulose, Bioresource, vol-4. no-4, pp.1359-1371, 2009.

Nele D., Subhankar B., Linde D.V., Le quan N.T., Assessment of the Properties of Coir, Bamboo and Jute Fiber, Composite Part A, vol-41, pp-588-595, 2010.

Paul A., Lars H., Geoffrey D., Cleavage of soft craft pulp fibers by HCL and Celluloses, vol-3, no-2, pp.477-490, 2008.

Ping X., Huawu L., Lloyd A.D., Yi Z.J, Mechanical Performance and Cellulose Microfibrils in Wood with High S2 Microfibril Angles, Mater Sci., vol-46, pp.534–540, 2011

Pradeep K.K., Rakesh K., Studies on Water Absorption of Bamboo-Epoxy Composites: Effect of Silane Treatment of Mercerized Bamboo, Journal of Applied Polymer Science, vol-115, pp.1846–1852, 2010.

Rajalaxmi D., Thomas E., Arthur J.R., Grafting of Model Primary Amine Compounds to Cellulose Oxidation, Cellulose DOI 10.1007/s10570-012-9769-2

Ratnam C.T., Irradiation modification of PVC/ENR blend: effect of TBLS content, Polymer-Plastics Technology and Engineering, vol-41, no- 3, pp. 407- 418, 2002.

Razzak W., Mohd T.M., Othman S., Aminuddin M., Affendy H., Izyan K., Anatomical and Physical Properties of Cultivated Two- and Four-year-old Bambusa vulgaris, Sains Malaysiana, vol- 39, no-4, pp. 571–579, 2010.

Riccardo P., Water-Absorbent Polymers: A Patent Survey, Polymer Reviews, vol-34, no-4, pp.607-662, 1994.

Rodrlguez A., Jonahira B., Zhengzheng C., Stephen Z.D., Crystal Structure, Morphology, and Phase Transitions in Syndiotactic Polypropylene, Polymer Reviews, vol-35, no-1, pp.117-154, 1995.

Ruhul A.K., , Parsons A.J. , Jones I.A. , Walker G.S. and Rudd C. D., Degradation and Interfacial Properties of Iron Phosphate Glass Fiber-Reinforced PCL-Based Composite for Synthetic Bone Replacement Materials, Polymer-Plastics Technology and Engineering, vol-49, no-12, pp.1265-1274, 2010.

Ruhul A.K., Mubarak A.K., Haydaruzzaman, Sushanta G., Siddiky M N.A., and Saha M., Study on the Physico-Mechanical Properties of Starch-Treated Jute Yarn-Reinforced Polypropylene Composites: Effect of Gamma Radiation, Polymer-Plastics Technology and Engineering, vol-48, no-5, pp.542 -548, 2009.

Rumana R., Rosemarie L.H., Reiner F., Andrea P., FTIR spectroscopy, Chemical and Histochemical Characterisation of Wood and Lignin of Five Tropical Timber Wood Species of the Family of Dipterocarpaceae, Wood Science Technology, vol-44, pp.225–242, 2010.

Rumana R., Gu¨nter M., Annette N., Andrea P., FTIR spectroscopy in combination with principal component analysis or cluster analysis as a tool to distinguish beech (*Fagus sylvatica* L.) trees grown at different sites, Holzforschung, vol- 62, pp. 530–538, 2008.

Saied E., Houssni , Altaf H.B. and Riad G.H., Research Progress in Friendly Environmental Technology for the Production of Cellulose Products (Bacterial Cellulose and Its Application), Polymer-Plastics Technology and Engineering, vol-43, no-3, pp.797-820, 2004.

Samia S.M., Syed M.N.H., Hossain Md.J., Hasan M., Chemical Modification Effect on the Mechanical Properties of Coir Fiber, Engineering Journal, vol- 16, no- 2, pp.73-83, 2011.

Sanjay K.C., Khandal R.K., Uppaluri R., Ghoshal A.K., Bamboo Fiber Reinforced Polypropylene Composites and Their Mechanical, Thermal, and Morphological Properties , Journal of Applied Polymer Science, vol- 119, pp.1619–1626, 2011.

Sarawut R., Korapat S., Prartana K., Chanchira J., Sunan T. ,Chemical Crosslinking on Properties of Methylcellulose Hydrogel, Engineering Journal Volume 16 Issue 4, 2012.

Satyanarayana D. and Chatterji P.R., Biodegradable Polymers: Challenges and Strategies, Polymer Reviews, vol-33, no-3, pp.349-368, 1993.

Shehrzade S., Mubarak A.K., Effect of Pretreatment with Gamma Radiation on the Performance of Photocured Jute Yarn with 1,6-Hexanediol Diacrylate (HDDA), Polymer-Plastics Technology and Engineering, vol-42,no- 5, pp.795-810,2003.

Shi F.F., Developments in Plasma-Polymerized Organic Thin Films with Novel Mechanical, Electrical, and Optical Properties, Polymer Reviews, vol-36, no-4, pp.795-826, 1996.

Shukla R., Sumit G., Sajal S., Dwivedi P.K., Ashutosh M., Medicinal importance of Bamboo, International Journal of Biopharm & Phytochemical Research,vol-1, no-1, pp-9-159, Jan 2012.

Shunliu S., Zhenfu J., Guifeng W., Changes in chemical characteristics of bamboo (Phyllostachys pubescens) components during steam Explosion, Wood Science Technology, vol- 42, pp.439–451, 2008.

Shuvunkor B., Quamrul A., Verpost I. Mahbub H., Effect of span length on the tensile properties of natural fibers, Paper ID 116 accepted to be publish to the international conference on advance materials processing technology by International University, Malaysia (IIUM),2009.

Singha A.S. and Rana R.K., Microwave Induced Graft Copolymerization of Methyl Methacrylate onto Lignocellulosic Fibers, International Journal of Polymer Analysis & Characterization, vol-15, pp. 370–386, 2010.

Siqueira G., Bras J. and Dufresne A., Cellulosic bionano composite a review of Preparation, Properties and Application, Polymer , vol-2, pp- 728-765, 2010.

Smith S., Chemical Modification of Cellulose fibers and Their Orientation in magnetic Field, Doctor of Philosophy Thesis, University of Toronto, 2011.

Sreekumar J., Mohini S., Stribeck N., X-ray Scattering for the Monitoring of Processes in Polymer Materials withTargeted Disruption of Hydroxyl Chemistry and Crystallinity in Natural Fiber for the Isolation of NanoFibers via Enzymatic Treatment, Bioresource, vol-6, no-2, pp.1242-5, 2011.

Srebrenkoska V., Gordana B.G., Dimko D., Preparation and Recycling of Polymer Eco-composite I. Comparison of the Conventional Modeling Technique for Preparation of Polymer Eco-composites. Macedonian Journal of Chemistry and Chemical Engineering, vol. 28, no. 1, pp. 99–109, 2009.

Subhankar B., Characterization and Performance Analysis of Natural Fibers as Reinforcement in Polymeric Composite, M. Phill Thesis, Bangladesh University of Engineering and Engineering, 2010.

Sunkyu P., John O.B. , Michael E.H., Philip A.P., David K.J., Cellulose crystallinity index: measurement techniques and their impact on interpreting cellulose performance, Biotechnology for Biofuels, vol-3, no-10, 2010.

Suwat S., Siripong S., Patcharin J., Banyat C., Nirundorn M., Buhnnum K., Macroscopic and Microscopic Gradient Structures of Bamboo Culms, Walailak Journal Science Technology, vol- 2, no-1, pp.81-97,2005.

Sweety S., Characterization of Chemically Modified Jute Fiber for Polymeric Composite, M. Phill Thesis, Bangladesh University of Engineering and Engineering, 2011.

Tamikazu K., Application of Radiation in Agriculture, Proceedings of International Workshop on Biotechnology in Agriculture, October 20-21, 2006.

Tanzina H., Avik K., Nazia N., Khan S.M., Khan R.A., Mubarak A.K., Mushfiqur R.M. and Mustafizur R.K., Fabrication and Characterization of Jute Fiber-Reinforced PET Composite: Effect of LLDPE Incorporation, Polymer-Plastics Technology and Engineering, vol-49, no- 4, pp.407-413, 2010.

Thygesen L.G., Dislocation in plant fibers and in Turin shroud fibers, Proceeding in the international workshop on the scientific approach to the Archeiropoietos ENEA Frascati, Italy, 4-6 March, 2010.

Trujillo E., Osorio L., Van A.W.,Vuure, Ivens J., Verpoest I., Characterization of Polymer Composite Materials Based on Bamboo Fibers,14th European Conference on Composite Materials, June 2010, Hungary Paper ID: 344-ECCM14

Tuhidul I., Ruhul A.K., Mubarak A.K., Arifur M. R., Marcelo F.L., Q. M. I. Huque and R. Islam, Physico-Mechanical and Degradation Properties of Gamma-Irradiated Biocomposites of Jute Fabric-Reinforced Poly (caprolactone), Polymer-Plastics Technology and Engineering, vol-48, pp.1203–1210, 2009.

Vilay V., Mariatti M., Taib M.M., Todo M., Effect of Fiber Surface Treatment and Fiber Loading on the Properties of Bagasse Fiber-Reinforced Unsaturated Polyester Composites, Composite Science and Technology, vol-68, pp.631-638, 2008.

Visco A.M., Campo N., Vagliasindi L.I., and Tabb G., Study of the Radical Species Induced by Electron-Beam Irradiation in Vacuum on Biomedical UHMWPE, International Journal of Polymer Analysis Characterisation, vol-15, pp. 424–437, 2010.

Walter L., The structure of Bamboo in Relational to its Properties and Utilization, Bamboo and its use , International Symposium on Industrial use of Bamboo, International Tropical Timber organisation, Chinese Aem of Forestry, Beijing, China 7-11 Dec, 1992.

Water Solubility of Wood and Pulp, T 207 cm-99, 1999,TAPPI, USA.

www.aaqtic.org.ar/congresos/china2009/oralPresentation/1-28.pdf date on issue 05.8.2012

www.bio.miami.edudate on issue 06.08.2012

www.bondtite.com date on issue 24.07.2010

www.chem.boun.edu.tr/webpages/courses/.../deri22.htm date on issue 20.7.2011

www.cool.conservation-us.org/don/dt/dt3419.htm date on issue 12.5.2011

www.en.wikipedia.org/wiki/Gamma_ray, date on issue 06.08.2012

www.en.wikipedia.org?wiki/lignin, date on issue 06.08.2012

www.ensilateam.com, date issued on12.7.2012.

www.kaisersheepskin.com/apps/webstore/products/show/2693051date on issue 14.5.2011

www.lib.tkk.fi/Diss/2005/isbn9512276909, date on issue 06.08.2012

www.mimosa-pudica.de, date issued on12.8.2011.

www.mimosa-sa.com/frame.htmdate on issue 24.4.2012

www.missionscience.nasa.gov/ems/12_gamma*rays.html*, date on issue 06.08.2012

www.ndt-ed.org/EducationResources/.../Radiography/.../gamma.htm, date on issue 06.08.2012

www.orise.orau.gov/reacts/guide/gamma.*ht*, date on issue 06.08.2012

www.physics.isu.edu/radinf/gamma.htm, date on issue 06.08.2012

www.radiation_pentration.gif gsseser.com date on issue 06.08.2012.

www.wikipeida.tanis.com date on issue *09.08.2012*

Xiaobo L., Physical, chemical and mechanical properties of bamboo and its utilization

potential for bamboo boa manufacturing, Master of Science thesis, Louisiana State University, 2004.

Xiaoya C., Qipeng G., Yongli M., Bamboo Fiber-Reinforced Polypropylene Composites: A Study of the Mechanical Properties, Journal of Applied Polymer Science, vol-69, pp.1891–1899, 1998.

Ximena L., Gloria C.C., Néstor M. R., and Yamel L. Characterization of the anatomy of *Guaduaangustifolia*(Poaceae: Bambusoideae) culms Bamboo Science and Culture: The Journal of the American Bamboo Society, vol- 16,no-1,pp.18-31, 2010.

Xiong L., Hong-BoLiang, Ru-Min W., Yu P., The Effect of Surface Modification of TiO_2 with Di-block Copolymers on the Properties of Epoxy Nano-composites, Polymer-Plastics Technology and Engineering, vol-49, no-14, pp.1483-1488, 2010.

Yan Y., Benhua F., Bo Z.X.Y., Cell-Wall Mechanical Properties of Bamboo Investigated by in Situ Imaging Nano indentation, Wood and Fiber Science, vol-39, no-4, pp. 527 – 535, 2007.

Yasuyuki K., Kazuo K., Hiroyuki H., Crystallization Behaviour and Viscoelasticity of Bamboo- Fiber Composites, Journal of Applied Polymer Science, vol. 98, pp.603–612, 2005.

Yiying Y., A Comparative study of Cellulose I and II fibers and Nanoclays, Graduate Faculty of the Louisiana State University and Agricultural and Mechanical College Master of Science The School of Renewable Natural Resources, B.S., Heilongjiang Institute of Science and Technology, 2007, 2011.

Yongliang L., Recent Progress in Fourier Transform Infrared (FTIR) Spectroscopy Study of Compositional, Structural and Physical Attributes of Developmental Cotton Fibers, Materials, vol-6, pp.299-313, 2013.

Yuanyuan H., Huaxi L., Pingsheng H., Liang Y., Hanguo X., Youming X., Yan Y., Nonisothermal Crystallization Kinetics of Modified Bamboo Fiber/PCL Composites, Journal of Applied Polymer Science, vol. 116, pp.2119–2125, 2010.

Zaher N.A.E., Study of the effect of ultraviolet radiation on some physical properties of dralon fabric, Polymer-Plastics Technology and Engineering, vol-40, no-5, pp.689-702, 2001.

Zaman H.U., Khan A., Khan R.A., Huq T., Khan M.A., Shahruzzaman M., Rahman M.M., Mamun M.A., and Poddar P., Preparation and Characterization of Jute Fabrics Reinforced Urethane Based Thermoset Composites: Effect of UV Radiation, Fibers and Polymers, vol-11, no-2, pp.258-265, 2010.

Zaman H.U., Khan A.H., Hossain M. A., Khan M.A., Khan R.A., Mechanical and Electrical Properties of Jute Fabrics Reinforced Polyethylene/Polypropylene Composites: Role of Gamma Radiation, Polymer-Plastics Technology and Engineering,vol-48, no-7, pp.760 -766, 2009.

Zaman H.U., Khan M.A., Khan R.A., Mollah M.Z.I., Pervin S.and Mamun M.A., A Comparative Study between Gamma and UV Radiation of Jute fabrics / Polypropylene Composites: Effect of Starch, Journal of reinforced plastics and composites, vol. 29, no.13, 2010.

Zhang F. and Ilasvsky J., Ultra-Small-Angle X-ray Scattering of Polymers, Journal of Macromolecular Science, Polymer Reviews, Part C, vol-50,pp.59–90, 2010.

Zhidan and Mai K., Effect of Inorganic Filler on the Crystallization, Mechanical Properties and Rheological Behavior of Poly(trimethylene terephthalate), Polymer-Plastics Technology and Engineering, vol-46, no-4, pp.417-420, 2007.

Zhishen M. and Hongfang Z., The Degree of Crystallinity in Polymers by Wide-Angle X-Ray Diffraction (WAXD) J.M.S.-Rev. Macromolecular Chemistry Physics, vol-C35, no-4, pp. 555-580, 1995.

Zhuo-P.S., Chang-H.F., Sheng-X.H., Gen-L. T., Tensile properties of Moso bamboo (Phyllostachys pubescens) and its components with respect to its fiber-reinforced composite structure, Wood Science Technology, vol-44, pp.655–666, 2010.